Non-equilibrium statistical mechanics: from a paradigmatic model to biological transport

2011 Rep. Prog. Phys. 74 116601

(http://iopscience.iop.org/0034-4885/74/11/116601)

Rep. Prog. Phys. **74** (2011) 116601 (41pp) doi:10.1088/0034-4885/74/11/116601

Non-equilibrium statistical mechanics: from a paradigmatic model to biological transport

T Chou[1], **K Mallick**[2] **and R K P Zia**[3]

[1] Departments of Biomathematics and Mathematics, UCLA, Los Angeles, CA 90095-1766, USA
[2] Institut de Physique Théorique, CEA Saclay, 91191 Gif-sur-Yvette Cedex, France
[3] Department of Physics, Virginia Tech, Blacksburg, VA 24061, USA

Received 30 June 2011, in final form 16 August 2011
Published 24 October 2011
Online at stacks.iop.org/RoPP/74/116601

Abstract
Unlike equilibrium statistical mechanics, with its well-established foundations, a similar widely accepted framework for non-equilibrium statistical mechanics (NESM) remains elusive. Here, we review some of the many recent activities on NESM, focusing on some of the fundamental issues and general aspects. Using the language of stochastic Markov processes, we emphasize general properties of the evolution of configurational probabilities, as described by master equations. Of particular interest are systems in which the dynamics violates detailed balance, since such systems serve to model a wide variety of phenomena in nature. We next review two distinct approaches for investigating such problems. One approach focuses on models sufficiently simple to allow us to find exact, analytic, non-trivial results. We provide detailed mathematical analyses of a one-dimensional continuous-time lattice gas, the totally asymmetric exclusion process. It is regarded as a paradigmatic model for NESM, much like the role the Ising model played for equilibrium statistical mechanics. It is also the starting point for the second approach, which attempts to include more realistic ingredients in order to be more applicable to systems in nature. Restricting ourselves to the area of biophysics and cellular biology, we review a number of models that are relevant for transport phenomena. Successes and limitations of these simple models are also highlighted.

(Some figures may appear in colour only in the online journal)

This article was invited by E Frey.

Contents

1. Introduction

What can we expect of a system which consists of a large number of simple constituents and evolves according to relatively simple rules? To answer this question and bridge the micro–macro connection is the central goal of statistical mechanics. About a century ago, Boltzmann made considerable progress by proposing a bold hypothesis: when an *isolated* system eventually settles into a state of equilibrium, all its microstates are equally likely to occur over long periods of time. Known as the microcanonical ensemble, it provides the basis for computing averages of macroscopic observables: (a) by assuming (time independent) ensemble averages can replace time averages in such an equilibrium state, (b) by labelling each microstate $\mathcal{C}$, (a configuration of the constituents which can be reached via the rules of evolution) as a member of this ensemble, and (c) by assigning the same weight to every member ($P^*(\mathcal{C}) \propto 1$). This simple postulate forms the foundation for equilibrium statistical mechanics (EQSM), leads to other ensembles for systems in thermal equilibrium, and frames the treatment of thermodynamics in essentially all textbooks. The problem of answering the question posed above shifts, for systems in equilibrium, to computing averages with Boltzmann weights.

By contrast, there is no similar stepping stone for non-equilibrium statistical mechanics (NESM), especially ones far from equilibrium. Of course, given a set of rules of stochastic evolution, it is possible to write down equations which govern the time-dependent weights, $P(\mathcal{C}, t)$. But that is just the starting point of NESM, as little is known, in general, about the solutions of such equations. Even if we have a solution, there is an added complication: the obvious inequivalence of time- and ensemble-averages *à la* Boltzmann. Instead, since our interest is the full dynamic behavior of such a statistical system, we must imagine (a) performing the same experiment many times, (b) collecting the data to form an ensemble of trajectories through configuration space, and (c) computing *time dependent* averages of macroscopic observables from this ensemble. The results can then be compared with averages obtained from $P(\mathcal{C}, t)$. Despite these daunting tasks, there are many studies [1–3] with the goal of understanding such far-from-equilibrium phenomena.

Here, we focus on another aspect of NESM, namely systems which evolve according to rules that violate detailed balance. In general, much less is known about their behavior, though they are used to model a much wider range of natural phenomena. Examples include the topic in this review—transport in biological systems, as well as epidemic spreading, pedestrian/vehicular traffic, stock markets, and social networks. A major difficulty with such systems is that, even if such a system is known (or assumed) to settle eventually in a time-independent state, the appropriate stationary weights are not generally known. In other words, there is no overarching principle, in the spirit of Boltzmann's fundamental hypothesis, which provides the weights for such *non-equilibrium* steady states (NESSs). We should emphasize that, if the dynamics is Markovian, then these weights can be constructed formally from the rules of evolution [4]. However, this formal solution is typically far too intractable to be of practical use. As a result, such NESS distributions are explicitly known only for a handful of model systems. Indeed, developing a fundamental and comprehensive understanding of physics far from equilibrium is recognized to be one of the 'grand challenges' of our time, by both the US National Academy of Sciences [5] and the US Department of Energy [6]. Furthermore, these studies point out the importance of non-equilibrium systems and their impact far beyond physics, including areas such as computer science, biology, public health, civil infrastructure, sociology, and finance.

One of the aims of this review is to provide a framework in which issues of NESM are well-posed, so that readers can appreciate why NESM is so challenging. Another goal is to show that initial steps in this long journey have been taken in the form of a few mathematically tractable models. A good example is the totally asymmetric simple exclusion process (TASEP). Like the Ising model, TASEP also consists of binary constituents, but evolves with even simpler rules. Unlike the scorn Ising's model faced in the 1920s, the TASEP already enjoys the status of a paradigmatic model. Fortunately, it is now recognized that seemingly simplistic models can play key roles in the understanding fundamental statistical mechanics and in formulating applied models of real physical systems. In this spirit, our final aim is to provide potential applications of the TASEP, and its many relatives, to a small class of problems in biology, namely transport at molecular and cellular levels.

This paper is organized along the lines of these three goals. The phrase 'non-equilibrium statistical mechanics' has been used in many contexts, referring to very different issues, in a wide range of settings. The first part of the next section will help readers discern the many facets of NESM. A more specific objective of section 2 is to review a proposal for characterizing all stationary states by a *pair* of time-independent distributions, $\{P^*(\mathcal{C}), K^*(\mathcal{C} \to \mathcal{C}')\}$, where K^* is the probability current 'flowing' from $\mathcal{C}$ to $\mathcal{C}'$ [7]. In this scheme, ordinary equilibrium stationary states (EQSSs) appear as the restricted set $\{P^*, 0\}$, whereas states with $K^* \neq 0$ are identified as NESS. Making an analogy with electromagnetism, this distinction is comparable to that of electrostatics versus magnetostatics, as the hallmark of the latter is the presence of steady and persistent currents. Others (e.g. [8]) have also called attention to the importance of such current loops for NESS and the key role they play in the understanding of fluctuations and dissipation. Two examples of NESS phenomena, which appear in contrast to the conventional wisdom developed from EQSM, will be provided here.

Section 3 will be devoted to some details on how to 'solve' the TASEP, for readers who are interested in getting involved in this type of study. In particular, we will present two complementary techniques, with one of them exploiting the relationship between two-dimensional systems in equilibrium and one-dimensional systems in NESM. While TASEP was introduced in 1970 [9] for studying interacting Markov processes, it gained wide attention two decades later in the statistical physics community [10–12]. In a twist of history, two years before its formal introduction, Gibbs and his collaborators introduced [13, 14] a more complex version

of TASEP to model mRNA translation in protein synthesis. Since the need for modelling molecular transport in a biological setting provided the first incentives for considering such NESM systems, it is fitting that we devote the next part, section 4, to potential applications for biological transport. In contrast to the late 1960s, much more about molecular biology is known today, so that there is a large number of topics, even within this restricted class of biological systems. Although each of which deserves a full review, we will limit ourselves to a few paragraphs for each topic. The reader should regard our effort here as a bird's eye view 'tour guide', pointing to more detailed, in-depth coverages of specific avenues within this rich field. Finally, we should mention that TASEP naturally lends itself to applications in many other areas, e.g. traffic flow [15] and surface growth [16, 17], etc. All are very interesting, but clearly beyond the scope of this review, as each deserves a review of its own. In the last section, 5, we conclude with a brief summary and outlook.

2. General aspects of NESM

In any quantitative description of a system in nature, the first step is to specify the degrees of freedom on which we focus our attention, while ignoring all others. For example, in Galileo's study of the motion of balls dropped from a tower, the degrees of freedom associated with the planets are ignored. Similarly, the motion of the atoms within the balls plays no role. The importance of this simple observation is to recognize that all investigations are necessarily limited in scope and all quantitative predictions are approximations to some degree. Only by narrowing our focus to a limited window of length- and/or time scales can we make reasonable progress toward quantitative understanding of natural phenomena. Thus, we must start by specifying a set of configurations, $\{\mathcal{C}\}$, which accounts for all the relevant degrees of freedom of the system. For example, for the traditional kinetic theory of gases (N particles in d spatial dimensions), $\mathcal{C}$ is a point in a $2dN$ dimensional phase space: $\{\vec{x}_i, \vec{p}_i\}, i = 1, \ldots, N$. For an Ising model with N spins $s = \pm 1$, the set $\{\mathcal{C}\}$ is the 2^N vertices of an N dimensional cube: $\{s_i\}, i = 1, \ldots, N$. In the first example, which should be suitable for describing argon at standard temperature and pressure, the window of length scales certainly excludes Ångströms or less, since the electronic and hadronic degrees of freedom within an atom are ignored. Similarly, the window in the second example also excludes many details of solid state physics. Yet, the Ising model is remarkably successful at predicting the magnetic properties of several physical systems [18–20].

Now, as we shift our focus from microscopic to macroscopic lengths, both $\{\mathcal{C}\}$ and the description also change. Keeping detailed accounts of such changes is the key idea behind renormalization, the application of which led to the extremely successful prediction of non-analytic thermodynamic properties near second order phase transitions [21]. While certain aspects of these different levels of description change, other aspects—e.g. fundamental symmetries of the system—remain. One particular aspect of interest here is time reversal. Although physical laws at the atomic level respect this symmetry[4], 'effective Hamiltonians' and phenomenological descriptions at more macroscopic levels often do not. One hallmark of EQSM is that the dynamics, effective for whatever level of interest, retain this symmetry. Here, the concept and term 'detailed balance' is often used as well as 'time reversal.' By contrast, NESM provides a natural setting for us to appreciate the significance of this micro-macro connection and the appearance of time-irreversible dynamics. We may start with a system with many degrees of freedom evolving with dynamics obeying detailed balance. Yet, when we focus on a *subsystem* with far fewer degrees of freedom, it is often reasonable to consider a dynamics that violates detailed balance. Examples of irreversible dynamics include simple friction in elementary mechanics, resistance in electrical systems, and viscosity in fluid flows.

Before presenting the framework we will use for discussing fundamental issues of NESM, let us briefly alert readers to the many settings where this term is used. Starting a statistical system in some initial configuration, $\mathcal{C}_0$, and letting it evolve according to rules which respect detailed balance, it will eventually wind up in an EQSS (precise definitions and conditions to be given at the beginning of section 2 below). To be explicit, let us denote the probability to find the system in configuration $\mathcal{C}$ at time t by $P(\mathcal{C}, t)$ and start with $P(\mathcal{C}, 0) = \delta(\mathcal{C} - \mathcal{C}_0)$. Then, $P(\mathcal{C}, t \to \infty)$ will approach a stationary distribution, $P^*(\mathcal{C})$, which is recognized as a Boltzmann distribution in equilibrium physics. Before this 'eventuality', many scenarios are possible and all of them rightly deserve the term NESM. There are three important examples from the literature. Physical systems in which certain variables change so slowly that reaching P^* may take many times the age of the universe. For time scales relevant to us, these systems are always 'far from equilibrium'. To study the statistics associated with fast variables, these slow ones might as well be considered frozen, leading to the concept of 'quenched disorder'. The techniques used to attack this class of problems are considerably more sophisticated than computing Boltzmann weights [1, 2], and are often termed NESM. At the other extreme, there is much interest in behavior of systems near equilibrium, for which perturbation theory around the EQSS is quite adequate. Linear response is the first step in such approaches [23–26], with a large body of well established results and many textbooks devoted to them. Between these extremes are systems which evolve very slowly, yet tractably. Frequently, these studies come under the umbrella of NESM and are found with the term 'ageing' in their titles [3].

Another frequently encountered situation is the presence of time-dependent rates. Such a problem corresponds to many experimental realizations in which control parameters, e.g. pressure or temperature, are varied according to some time-dependent protocol. In the context of theoretical investigations, such changes play central roles in the study of work theorems [27–35]. In general these problems are much less tractable and will not be considered here.

[4] Strictly speaking, if we accept CPT as an exact symmetry, then time reversal is violated at the subatomic level, since CP violation has been observed. So far, there is no direct observation of T violation. For a recent overview, see, e.g., [22].

By contrast, we will focus on systems which evolve according to dynamics that *violates* detailed balance. The simplest context for such a system is the coupling to two or more reservoirs (of the same resource, e.g. energy) in such a way that, when the system reaches a stationary state, there is a steady flux *through* it. A daily example is stove-top cooking, in which water in a pot gains energy from the burner and loses it to the room. At a steady simmer, the input balances the heat loss and our system reaches an NESS. That these states differ significantly from ordinary EQSSs has been demonstrated in a variety of studies of simple model systems coupled to thermal reservoirs at two different temperatures. Another example, at the global scale, is life on Earth, the existence of which depends on a steady influx of energy from the Sun and re-radiation to outer space. Indeed, all living organisms survive (in relatively steady states) by balancing input with output—of energy and matter of some form. Labeling these reservoirs as 'the medium' in which our system finds itself, we see the following scenario emerging. Although the medium + system combination is clearly evolving in time, the system may be small enough that it has arrived at a time-independent NESS. While the much larger, combined system may well be evolving according to a time-reversal symmetric dynamics, it is quite reasonable to assume that this symmetry is violated by the effective dynamics appropriate for our smaller system with its shorter associated time scales. In other words, when we sum over the degrees of freedom associated with the medium, the dynamics describing the remaining configurations, $\mathcal{C}$s, of our system should in general violate detailed balance.

In general, it is impossible to derive such effective dynamics for systems at the mesoscopic or macroscopic scales from well-known interactions at the microscopic, atomic level. There are proposals to derive them from variational principles, based on postulating some quantity to be extremized during the evolution, in the spirit of least action in classical mechanics. The most widely known is probably 'maximum entropy production'. The major challenge is to identify the constraints appropriate for each NESM system at hand. None of these approaches has achieved the same level of acceptance as the maximum entropy principle in EQSM (where the constraints are well established, e.g. total energy, volume, particle number, etc). In particular, the NESS in the uniformly driven lattice gas is known to differ from the state predicted by this principle [36]. Readers interested in these approaches may study a variety of books and reviews which appeared over the years [37–44]. How an effective dynamics (i.e. a set of rules of evolution) arises is not the purpose of our review. Instead, our goal is to explore the nature of stationary states, starting from a *given* dynamics that violates detailed balance. Specifically, in modeling biological transport, the main theme of the applications section, it is reasonable to postulate a set of transition rates for the system of interest.

2.1. Master equation and other approaches to statistical mechanics

Since probabilities are central to statistical mechanics, our starting point for discussing NESM is $P(\mathcal{C}, t)$ and its evolution. Since much of our review will be devoted to models well suited for computer simulations, let us restrict ourselves to discrete steps ($\tau = 0, 1, \ldots$ of time δt) as well as a discrete, finite set of $\mathcal{C}$s ($\mathcal{C}_1, \mathcal{C}_2, \ldots, \mathcal{C}_{\mathcal{N}}$). Also, since we will be concerned with time reversal, we will assume, for simplicity, that all variables are even under this operation (i.e. no momenta-like variables which change sign under time reversal). To simplify notation further, let us write $P_i(\tau)$, interchangeably with $P(\mathcal{C}_i, \tau\delta t)$. Being conserved ($\sum_i P_i(\tau) = 1$ for all τ), P must obey a continuity equation, i.e. the vanishing of the time rate of change of a conserved density plus the divergence of the associated current density. Clearly, the associated currents here are *probability currents*. Since we restrict our attention to a discrete configuration space, each of these currents can be written as the flow from $\mathcal{C}_j$ to $\mathcal{C}_i$, i.e. $K_i^j(\tau)$ or $K(\mathcal{C}_j \to \mathcal{C}_i, \tau\delta t)$. As a net current, $K_j^i(\tau)$ is by definition $-K_i^j(\tau)$, while its 'divergence' associated with any $\mathcal{C}_i$ is just $\sum_j K_i^j(\tau)$. In general, K is a new variable and how it evolves must be specified. For example, in quantum mechanics, P is encoded in the amplitude of the wave function ψ only, while K contains information of the phase in ψ as well (e.g. $K \propto \psi^* \overleftrightarrow{\nabla} \psi$ for a single non-relativistic particle). In this review, as well as the models used in essentially all simulation studies, we follow a much simpler route: the master equation or the Markov chain. Here, K is assumed to be proportional to P, so that $P_i(\tau + 1)$ depends only on linear combinations of the probabilities of the previous step, $P_j(\tau)$. In a further simplification, we focus on time-homogeneous Markov chains, in which the matrix relating K to P is constant in time. Thus, we write $P_i(\tau + 1) = \sum_j w_i^j P_j(\tau)$, where w_i^j are known as the transition rates (from $\mathcal{C}_j$ to $\mathcal{C}_i$).

As emphasized above, we will assume that these rates are *given* quantities, as in a mathematical model system like TASEP or in phenomenologically motivated models for biological systems. Probability conservation imposes the constraint $\sum_i w_i^j = 1$ for all j, of course. A convenient way to incorporate this constraint is to write the master equation in terms of the changes

$$\begin{aligned}\Delta P_i(\tau) &\equiv P_i(\tau + 1) - P_i(\tau) \\ &= \sum_{j \neq i} [w_i^j P_j(\tau) - w_j^i P_i(\tau)]. \end{aligned} \tag{1}$$

This equation can be written as

$$\Delta P_i(\tau) = \sum_j L_i^j P_j(\tau) \tag{2}$$

where

$$L_i^j = \begin{cases} w_i^j & \text{if} \quad i \neq j \\ -\sum_{k \neq j} w_k^j & \quad\quad i = j \end{cases} \tag{3}$$

is a matrix (denoted by $\mathbb{L}$; sometimes referred to as the Liouvillian) that plays much the same role as the Hamiltonian in quantum mechanics. Since all transition rates are non-negative, w_i^j is a stochastic matrix and many properties of the evolution of our system follow from the Perron–Frobenius theorem [45]. In particular, $\sum_i L_i^j = 0$ for all j (probability

conservation), so that at least one of the eigenvalues must vanish. Indeed, we recognize the stationary distribution, P^*, as the associated right eigenvector, since $\mathbb{L}P^* = 0$ implies $P_i^*(\tau + 1) = P_i^*(\tau)$. Also, this P^* is unique, provided the dynamics is ergodic, i.e. every $\mathcal{C}_i$ can be reached from any $\mathcal{C}_j$ via the ws. Further, the real parts of all other eigenvalues must be negative, so that the system must decay into P^* eventually.

Since the right-hand side of equation (1) is already cast in the form of the divergence of a current, we identify

$$K_i^j(\tau) \equiv w_i^j P_j(\tau) - w_j^i P_i(\tau) \tag{4}$$

as the (net) probability current from $\mathcal{C}_j$ to $\mathcal{C}_i$. Note that the antisymmetry $K_i^j = -K_j^i$ is manifest here. When a system settles into a stationary state, these time-independent currents are given simply by

$$K_i^{*j} \equiv w_i^j P_j^* - w_j^i P_i^*. \tag{5}$$

As we will present in the next subsection, a reasonable way to distinguish EQSS from NESS is whether the K^* vanish or not. Before embarking on that topic, let us briefly remark on two other common approaches to time-dependent statistical mechanics. More detailed presentations of these and related topics are beyond the scope of this review, but can be found in many books [46–49].

Arguably the most intuitive approach to a stochastic process is the Langevin equation. Originating with the explanation of Brownian motion [50] by Einstein and Smoluchowski [51, 52], this equation consists of adding a random drive to an otherwise deterministic evolution. The deterministic evolution describes a single trajectory through configuration space: $\mathcal{C}(\tau)$ (starting with $\mathcal{C}(0) = \mathcal{C}_0$), governed by, say, an equation of the form $\Delta\mathcal{C}(\tau) = \mathcal{F}[\mathcal{C}(\tau)]$. In a Langevin approach, $\mathcal{F}$ will contain both a deterministic part and a noisy component. Of course, a trajectory (or history, or realization) will depend on the specific noise force appearing in that run. Many trajectories are therefore generated, each depending on a particular realization of the noise and the associated probability. Although each trajectory can be easily understood, the fact that many of them are possible means the system at time τ can be found at a collection of $\mathcal{C}$s. In this sense, the evolution is best described by a probability distribution, $P(\mathcal{C}, \tau)$, which is controlled by both the deterministic and the noisy components in $\mathcal{F}$. Historically, such considerations were first provided for a classical point particle, where $\Delta\mathcal{C} = \mathcal{F}$ would be Newton's equation, $\partial_t^2 \vec{x}(t) = \vec{F}/m$, with continuous time and configuration variables. How the deterministic and noisy parts of $\vec{F}$ are connected to each other for the Brownian particle is the celebrated Einstein–Smoluchowski relation. Of course, $P(\mathcal{C}, \tau)$ becomes $P(\vec{x}, t)$ in this context, while the Langevin approach can be reformulated as a PDE for $P(\vec{x}, t)$

$$\partial_t P(\vec{x}, t) = \frac{\partial^2}{\partial x_\alpha \partial x_\beta} D_{\alpha\beta}(\vec{x}) P(\vec{x}, t) - \frac{\partial}{\partial x_\alpha} V_\alpha(\vec{x}) P(\vec{x}, t). \tag{6}$$

Here, $D_{\alpha\beta}$ and V_α are the diffusion tensor and the drift vector, respectively, and are related to the noisy and deterministic components of the drive[5]. This PDE is referred to as the Fokker–Planck equation, although it was first introduced for the velocity distribution of a particle [48].

An experienced reader will note that the master equation (1) for $P(\mathcal{C}, \tau)$ and the Fokker–Planck equation (6) for $P(\vec{x}, t)$ are both linear in P and first order in time, but that the right-hand sides are quite different. Let us comment briefly on their similarities and differences. Despite the simpler appearance, equation (1) is the more general case, apart from the complications associated with discrete versus continuous variables. Thus, let us facilitate the comparison by considering a discrete version of equation (6), i.e. $t \to \tau\delta t$ and $\vec{x} \to \vec{\zeta}\delta x$, so that $P(\vec{x}, t) \to P(\vec{\zeta}, \tau)$. In this light, it is clear that the derivatives on the right correspond to various linear combinations of $P(\zeta_\alpha \pm 1, \zeta_\beta \pm 1; \tau)$. In other words, only a handful of the 'nearest configurations' are involved in the evolution of $P(\vec{\zeta}, \tau)$. By contrast, the range of w_i^j, as written in equation (1), is not restricted.

Let us illustrate by a specific example. Consider a system with N Ising spins (with any interactions between them) evolving according to random sequential Glauber spin-flip dynamics [53]. In a time step, a random spin is chosen and flipped with some probability. Now, as noted earlier, the configuration space is the set of vertices of an N dimensional cube. Therefore, the only transitions allowed are moves along an edge of the cube, so that the range of w_i^j is 'short'. In this sense, field theoretic formulations of the Ising system evolving with Glauber dynamics are possible, taking advantage of Fokker–Planck like equations, cast in terms of path integrals. On the other hand, consider updating according to a cluster algorithm, e.g. Swendsen–Wang [54], in which a large cluster of spins (say, M) are flipped in a single step. Such a move clearly corresponds to crossing the body diagonal of an M dimensional cube. Since M is conceivably as large as N, there is no limit to the range of this set of ws. It is hardly surprising that field theoretic approaches for such systems have yet to be formulated, as they would be considerably more complex.

2.2. Non-equilibrium versus equilibrium stationary states, persistent probability currents

Following the footsteps of Boltzmann and Gibbs, we study statistical mechanics of systems in thermal equilibrium by focusing on time-independent distributions such as $P^*(\mathcal{C}) \propto 1$ or $\exp[-\beta\mathcal{H}(\mathcal{C})]$ (where $\mathcal{H}$ is the total energy associated with $\mathcal{C}$ and β is the inverse temperature). Apart from a few model systems, it is not possible to compute, analytically and in general, averages of observable quantities, i.e.

$$\langle\mathcal{O}\rangle \equiv \sum_j \mathcal{O}(\mathcal{C}_j) P^*(\mathcal{C}_j). \tag{7}$$

Instead, remarkable progress over the last 50 years was achieved through computer simulations, in which a small subset of $\{\mathcal{C}\}$ is generated—with the appropriate (relative) weights—and used for computing the desired averages. This

[5] Note that $D_{\alpha\beta}(\vec{x})$ here derives from the rate of change of the variance of the distribution and is different from the diffusion coefficient used to define Fick's law. Here, both spatial derivatives operate on $D_{\alpha\beta}(\vec{x})$.

approach is an advanced art [55], far beyond the scope (or purpose) of this review. Here, only some key points will be mentioned and exploited—for highlighting the contrast between the stationary distributions of Boltzmann–Gibbs and those in NESS.

In a classic paper [56], Metropolis *et al* introduced an algorithm to generate a set of configurations with relative Boltzmann weights. This process also simulates a dynamical evolution of the system, in precisely the sense of the master equation. Starting from some initial $\mathcal{C}(0) = \mathcal{C}_0$, a new one, $\mathcal{C}_k$, is generated (by some well-defined procedure) and accepted with probability w_k^0. Thus, $\mathcal{C}(1)$ is $\mathcal{C}_k$ or $\mathcal{C}_0$. with relative probability w_k^0 or $(1 - w_k^0)$, respectively. After some transient period, the system is expected to settle into a stationary state, i.e. the frequencies of $\mathcal{C}_i$ occurring in the run are proportional to a time independent $P^*(\mathcal{C}_i)$. To implement this Monte-Carlo method, a set of transition rates, w_j^i, must be fixed. Further, if the desired outcome is $P^* \propto \mathrm{e}^{-\beta\mathcal{H}}$, then w_j^i cannot be arbitrary. A sufficient (but not necessary) condition is referred to, especially in the simulations community [55], as 'detailed balance':

$$w_k^i P^*(\mathcal{C}_i) = w_i^k P^*(\mathcal{C}_k). \tag{8}$$

In other words, it suffices to constrain the ratio w_k^i/w_i^k to be $\exp[-\beta\Delta\mathcal{H}]$, where $\Delta H \equiv \mathcal{H}(\mathcal{C}_k) - \mathcal{H}(\mathcal{C}_i)$ is just the difference between the configurational energies. A common and simple choice is $w_k^i = \min\{1, \mathrm{e}^{-\beta\Delta\mathcal{H}}\}$.

Of course, constraining the ratios still leaves us with many possibilities. To narrow the choices, it is reasonable to regard a particular set of ws as the simulation of a physical dynamics[6]. In that case, other considerations will guide our choices. For example, the Lenz–Ising system is used to model spins in ferromagnetism [57] as well as occupations in binary alloys [58, 59]. In the former, individual spins can be flipped and it is quite appropriate to exploit Glauber [53] dynamics, in which the ws connect $\mathcal{C}$s that differ by only one spin. In the latter, however, a Zn atom, say, cannot be changed into a Cu atom, so that exchanging a neighboring pair of different 'spins'—Kawasaki [60, 61] dynamics—is more appropriate. In terms of the N dimensional cube representation of $\{\mathcal{C}\}$, these ws connect two vertices along an edge (Glabuer) or across the diagonal of a square face or plaquette (Kawasaki). Both dynamics involve ws that only connect $\mathcal{C}$s with one or two different spins. The idea is that, in a short δt, exchanging energy with the thermal reservoir can randomly affect only one or two spins. Also, in this sense, we can regard the ws as how the system is coupled to the surrounding medium. Clearly, $\Delta\mathcal{H}$ measures the energy exchanged between the two. Another important quantity is entropy production, whether associated with the system or the medium, in which the ws will play a crucial role.

It is significant that regardless of the details of the associated dynamics, a set of ws that obey detailed balance (8) necessarily leads the system to a state in which *all* stationary currents vanish. This follows trivially from the definition (5). By contrast, transition rates that violate detailed balance necessarily lead to some *non-vanishing* stationary currents. To appreciate this statement, let us provide a better criterion, due to Kolmogorov [62], for rates that respect/violate detailed balance. In particular, while equation (8) gives the wrong impression that detailed balance is defined with respect to a given $\mathcal{H}$, the Kolmogorov criterion for detailed balance is applicable to all Markov processes, whether an underlying Hamiltonian exists or not.

Consider a closed loop in configuration space, e.g. $\mathcal{L} \equiv \mathcal{C}_i \to \mathcal{C}_j \to \mathcal{C}_k \to \cdots \to \mathcal{C}_n \to \mathcal{C}_i$. Define the product of the associated rates in the 'forward' direction by $\Pi[\mathcal{L}] \equiv w_j^i w_k^j \ldots w_i^n$ and also for the 'reverse' direction: $\Pi[\mathcal{L}_{rev}] \equiv w_i^j w_j^k \ldots w_n^i$. The set of rates are said to satisfy detailed balance if and only if

$$\Pi[\mathcal{L}] = \Pi[\mathcal{L}_{rev}] \tag{9}$$

for *all loops*. If this criterion is satisfied, then we can show that a (single valued) functional in configuration space can be constructed simply from the set of ratios w_k^i/w_i^k, and that it is proportional to $P^*(\mathcal{C})$. If this criterion is violated for certain loops, these will be referred to here as 'irreversible rate loops' (IRLs). Despite the lack of detailed balance, $P^*(\mathcal{C})$ exists and can still be constructed from the ws, though much more effort is required. Established some time ago [4, 63, 64], this approach to P^* is similar to Kirchhoff's for electric networks [65]. More importantly, this construction provides the framework for showing that, in the stationary state, some K^*s must be non-trivial [7, 66]. Since the divergence of these currents must vanish, they must form current loops. As time-independent current loops, they remind us of magnetostatics. The distinction between this scenario and the case with detailed balance ws is clear: the latter resembles electrostatics. In this light, it is reasonable to label a stationary state as an equilibrium one if and only if *all* its (probability) currents vanish, associated with a set of ws with no IRLs. Similarly, an NESS would be associated with non-trivial current loops, generated by detailed balance-violating rates with IRLs [7, 66]. Our proposal is that all stationary states should be characterized by the pair $\{P^*, K^*\}$. In this scheme, 'equilibrium states' correspond to the subset $\{P^*, 0\}$, associated with a dynamics that respects detailed balance and time reversal.

The presence of current loops and IRLs raises a natural and intriguing question: is there an intuitively accessible and simple relationship between them? Unfortunately, the answer remains elusive so far. Venturing further, it is tempting to speculate on the existence of a gauge theory, along the lines of that in electromagnetism, for NESM. If such a theory can be formulated, its consequences may be far-reaching.

Time-independent probability current loops also carry physical information about an NESS. Referring readers to a recent paper [7] for the details, we provide brief summaries here for a few key points.

(i) In particular, it is shown how the Ks can be used to compute currents associated with physical quantities, such as energy or matter. In addition, we have emphasized that a signature of NESS is the existence of a steady flux (of

[6] In this light, the sequence of configurations generated $(\mathcal{C}_{j_1}, \mathcal{C}_{j_2}, \ldots, \mathcal{C}_{j_\tau})$ can be regarded as a history, or trajectory, of the system. By collecting many (M) such sequences, $\{\mathcal{C}_j^\alpha\}, \alpha = 1, \ldots, M$, time-dependent averages $\langle\mathcal{O}\rangle_\tau \equiv \sum_j \mathcal{O}(\mathcal{C}_j)P_j(\tau)$ are simulated by $M^{-1}\sum_\alpha \mathcal{O}(\mathcal{C}_{j_\tau}^\alpha)$.

energy, for example) *through* the system. All aspects of such through-flux, such as averages and correlation, can also be computed with the Ks.

(ii) Following Schnakenberg [63], we may define the *total* entropy production $\mathbf{\Sigma}_{\rm tot}$ as a quantity associated with the rates $\{w^i_j\}$. This $\mathbf{\Sigma}_{\rm tot}$ can be written as the sum of two terms, $\mathbf{\Sigma}_{\rm sys} + \mathbf{\Sigma}_{\rm med}$. The first is associated with entropy production within our system (recognizable as the derivative of the Gibbs entropy, $-\sum_i P_i \ln P_i$, in the continuous-time limit):

$$\mathbf{\Sigma}_{\rm sys}(\tau) \equiv \frac{1}{2}\sum_{i,j} K^j_i(\tau) \ln \frac{P_j(\tau)}{P_i(\tau)}. \tag{10}$$

It is straightforward to show that for an NESS with $K^* \neq 0$, $\mathbf{\Sigma}_{\rm sys}$ vanishes as expected. However, a second contribution to entropy production is associated with the medium:

$$\mathbf{\Sigma}_{\rm med}(\tau) \equiv \frac{1}{2}\sum_{i,j} K^j_i(\tau) \ln \frac{w^j_i}{w^i_j}, \tag{11}$$

where the positivity of $\sum K^{*j}_i \ln(w^j_i/w^i_j)$ has been demonstrated. This result is entirely consistent with our description of an NESS, namely a system coupled to surroundings which continue to evolve and generate entropy.

(iii) The following inverse question for NESS is also interesting. As we noted, given a Boltzmann distribution, a well-known route to generate it is to use a dynamics which obeys detailed balance (8). If we accept that an NESS is characterized not only by the stationary distribution, but by the pair $\{P^*, K^*\}$, then the generalized condition is $w^i_k P^*_i = w^k_i P^*_k + K^{*i}_k$, or more explicitly,

$$w^i_k P^*(\mathcal{C}_i) = w^k_i P^*(\mathcal{C}_k) + K^*(\mathcal{C}_i \to \mathcal{C}_k). \tag{12}$$

It is possible to phrase this condition more elegantly (perhaps offering a little insight) by performing a well-known similarity transform on w^i_k: Define the matrix $\mathbb{U}$, the elements of which are

$$U^i_k \equiv (P^*_k)^{-1/2} w^i_k (P^*_i)^{1/2}.$$

The advantage of this form of 'coding' the dynamics is that $\mathbb{U}$ is symmetric if rates obey detailed balance. Meanwhile, since K^* is a current, we can exploit the analog $J = \rho v$ to define the 'velocity matrix' $\mathbb{V}$, the elements of which are

$$V^i_k \equiv (P^*_k)^{-1/2} K^{*i}_k (P^*_i)^{-1/2},$$

associated with the flow from $\mathcal{C}_i$ to $\mathcal{C}_k$. Our generalized condition (12) now reads simply: the antisymmetric part of $\mathbb{U}$ is $\mathbb{V}/2$. Similar ideas have also been pursued recently [67].

To summarize, if a dynamics is to lead a system to a desired $\{P^*, K^*\}$, then the associated antisymmetric part of $\mathbb{R}$ is completely fixed by K^*. By contrast, its symmetric part is still unconstrained, corresponding to dynamics that takes us to the same $\{P^*, K^*\}$.

(iv) As long as $K^* \neq 0$ for a transition, we can focus on the direction with positive current (say, $K^{*i}_k > 0$) and choose the maximally asymmetric dynamics, namely $w^k_i \equiv 0$ and $w^i_k = K^{*i}_k / P^*_i$. (Understandably, such choices are impossible for systems in thermal equilibrium, except for $T = 0$ cases.) Whether systems with such apparently unique dynamics carry additional significance remains to be explored. Certainly, TASEP—the paradigmatic model of NESS, to be presented next—belongs in this class. Before embarking on the next section, let us briefly comment on some typical features of NESS which are counter-intuitive, based on our notions of EQSM.

2.3. Beyond expectations of EQSM

EQSM has allowed us to develop physical intuition that can be valuable guides when we are faced with new problems in unfamiliar settings. A good example is energy–entropy competition, which tends to serve us well when we encounter novel phase transitions: the former/latter 'wins' for systems at low/high temperatures, so that it displays order/disorder phenomena. Another example is 'positive response': to ensure thermodynamic stability, we expect the system to respond in a certain manner (positively) when its control parameters are changed. Thus, it is reasonable to expect, e.g., positive specific heat and compressibility for systems in thermal equilibrium. A final example is long-range correlations, which are generically absent in equilibrium systems with short-range interactions and dynamics. There are exceptions, of course, such as in critical phenomena associated with second order phase transitions. When we encounter systems in NESS, however, we should be aware that such physical intuition often leads us astray. At present, we are not aware of another set of overarching principles which are generally applicable for NESS. Instead, in the following, we will provide two specific circumstances in which our expectations fail.

Negative response. In order for a system to be in thermal equilibrium, it must be stable against small perturbations. Otherwise, fluctuations will drive it into another state. Such consistent behaviors of a system may be labeled as 'positive response'. Related to the positivity of certain second derivatives of the free energy, elementary examples include positive specific heat and compressibility. By contrast, a surprisingly common hallmark of NESS is 'negative response.' For example, imagine a room in which the internal energy decreases when the thermostat is turned up! One of the first systems in NESS where this type of surprising behavior surfaced is the driven Ising lattice gas [36]. Referring the reader to, for example, reference [68] for details, the key ingredients are the following. An ordinary Ising system (with nearest neighbor (NN) ferromagnetic interactions on a square lattice) is subjected to an external drive, and observed to undergo the phase transition at a temperature *higher* than that expected from Onsager's solution. Since the external drive tends to break bonds, its effect is similar to coupling the system to another energy reservoir with a *higher* temperature. Nevertheless, this NESS system displays more order than its equilibrium counterpart. In other words, despite the fact that

more energy appears to be 'pumped into' the system, the internal energy decreases. A more direct manifestation of this form of 'negative response' has been observed in the two-temperature Ising lattice gas, in which particle hops in the x or y direction are updated by Metropolis rates appropriate to exchanging energy with a thermal reservoir set at temperature T_x or T_y. Changing T_x, with T_y held fixed, the average internal energy, U (i.e. $\langle\mathcal{H}\rangle$), is found to vary with $\partial U/\partial T_y < 0$ [69]! Such surprising negative response is so generic that it can be found in exceedingly simple, exactly solvable cases [70].

Of course, we should caution the reader that 'negative response' may be simply a misnomer, poor semantics, or careless interpretation of an observed phenomenon. After all, fluctuations of observables in a stationary state must be positive and if the appropriate conjugate variable is used, then the response to that variable will again be positive. In particular, for any observable $\mathcal{O}$, we can always define the cumulant generating function $\Xi(\omega) \equiv \ln\langle e^{\omega\mathcal{O}}\rangle$ and its derivative $X(\omega) \equiv \Xi'(\omega)$. Of course, the average $\langle\mathcal{O}\rangle$ is $\Xi'(0)$, while $X(\omega)$ is, in general, the average of $\mathcal{O}$ in the *modified distribution* $\tilde{P}^*(\mathcal{C}) \propto e^{\omega\mathcal{O}(\mathcal{C})}P^*(\mathcal{C})$. Then, we are guaranteed 'positive response:' $\partial X/\partial\omega > 0$. However, unlike internal energy and temperature for systems in thermal equilibrium, simple physical interpretations of these mathematical manipulations for NESSs are yet to be established. Clearly, this issue is related to the fluctuation–dissipation theorem in EQSM. General results valid for NESM have been derived during the last two decades; we refer the reader to the seminal papers [27, 28, 71–73]. The generalization of the fluctuation–dissipation theorem to NESM is a major topic [34, 74] and lies outside our scope. Here, let us remark that the foundations of this theorem lies in the time-reversal properties of the underlying dynamics [75, 76], which control the nature of the fluctuations of the random variables. To characterize these fluctuations quantitatively, large-deviation functions (LDFs) have been introduced. They play a crucial role in NESM, akin to that of thermodynamic potentials in EQSM [77, 78]. Valid for systems far from equilibrium, the fluctuation theorem can be stated as a symmetry property of the LDF (see the next section for a explicit example in the case of TASEP). Near an equilibrium state this theorem implies the fluctuation–dissipation relation, previously derived from linear response theory [79, 80]. A related set of significant results is the non-equilibrium work relations [27–35], also a topic worthy of its own review (see, e.g., [81, 82] and references therein). Here, in the context of the exact solution of TASEP (section 3), another result along this theme—the macroscopic fluctuation theory developed by Jona-Lasinio and co-workers [83]—plays an important role.

Generic long-range correlations. For systems with short-range interactions in thermal equilibrium, the static (i.e. equal time) correlations of the fluctuations are generically short-ranged. This is true even if the dynamics contains long-ranged components (e.g., the 'artificial' Swendsen–Wang [54] dynamics): as long as it obeys detailed balance, we are ensured of $P^* \propto e^{-\beta\mathcal{H}}$. Of course, time-dependent correlations are *not* similarly constrained. An excellent example is diffusive dynamics obeying certain conservation laws (e.g. hydrodynamics or Kawasaki [60, 61] dynamics modeling Cu–Zn exchange), where long time tails (power law decays) are well-known phenomena: the autocorrelation function, $G(r = 0, t)$, decays as $t^{-d/2}$ in d dimensions, even for a single particle. As pointed out by Grinstein [84], a simple scaling argument, along with $r \sim t^{1/z}$, would lead to *generic* long-range correlations, $G(r, t = 0) \to Ar^{-zd/2}$ (i.e. r^{-d} in the case of random walkers subjected to short-range interactions, where $z = 2$). Yet, $G(r, t = 0)$ generally decays as an exponential in equilibrium systems! These seemingly contradictory statements can be reconciled when the amplitude A is examined. In the equilibrium case, detailed balance (or the fluctuation–dissipation theorem) constrains A to vanish. For NESS, there is no such constraint, leaving us with long-range correlations generically. For further details of these considerations, the reader may consult [68, 85].

To end the discussion on such correlations, we should caution the readers on a subtle point. Although we emphasized how long-range correlations can emerge from a short-range dynamics that violates detailed balance, the latter is not *necessary*. An excellent example is a driven diffusive system with three species—the ABC model [86, 87]—in one dimension. The system evolves with a short-range dynamics which generally violates detailed balance, and displays long-range *order* (as well as correlations). Remarkably, for a special set of parameters, detailed balance is restored and so an exact P^* was easily found. When interpreted as a Boltzmann factor (i.e. $P^* \propto e^{-\beta\mathcal{H}}$), the Hamiltonian contains inter-particle interactions which range over the entire lattice! Despite having an $\mathcal{H}$ with long-range interactions, it is possible to construct a short-range dynamics (e.g. ws that involve only NN particle exchanges) that will lead the system to an EQSS: $\{P^* \propto e^{-\beta\mathcal{H}}, K^* \equiv 0\}$. To appreciate such a counter-intuitive situation, consider $\Delta\mathcal{H} = \mathcal{H}(\mathcal{C}_i) - \mathcal{H}(\mathcal{C}_j)$ for a pair of configurations that differ in some local variables. The presence of long-range terms in $\mathcal{H}$ typically induce similar terms in $\Delta\mathcal{H}$, leading to a long-range dynamics. If such terms conspire to cancel, then $\Delta\mathcal{H}$ becomes short-ranged and it is simple to choose ws with no long-range components. We believe it is important to investigate whether such examples belong to a class of mathematical curiosities or form the basis for a wide variety of physical/biological systems. With these two examples, we hope to have conveyed an important lesson we learned from our limited explorations of NESS: expect the unexpected, when confronted with a novel system evolving according to detailed balance-violating dynamics.

In this section, we attempted to provide a bird's eye view of the many facets of NESM, and then to focus on a particular aspect: stationary states associated with dynamics that violates detailed balance. We emphasized the importance of this class of problems and pointed out significant features of NESS that run counter to the physical intuition learned from EQSM. In the next two sections, we will turn our attention to specific systems. As common in all theoretical studies, there are two typically diverging goals associated with the models we pursue. One goal is to account for as many features found in nature as realistically possible. The other is to consider models with just

one or two features so that they are simple enough to be solved analytically and exactly. These goals obviously diverge since more realistic models are typically mathematically intractable while exactly solvable models generally lack essential aspects of physical systems (or those in chemistry, biology, finance, sociology, etc). Nevertheless, we believe is it worthwhile to devote our attention to both of them, albeit separately. In this spirit, we will next present a simple model: the exclusion process, with the TASEP being an extreme limit. Arguably the simplest possible model with a non-trivial NESS, the TASEP is not only amenable to exact and approximate solution strategies, but it also has shed considerable light on problems in the real world. In section 4, we turn to a number of generalizations of this model, each taking into account new physical features required for modeling various aspects of transport in biological systems.

3. A paradigmatic model: the asymmetric simple exclusion process

Building a simple representation for complex phenomena is a common procedure in physics, leading to the emergence of paradigmatic models: the harmonic oscillator, the random walker, the Ising magnet, etc. These beautiful models often display wonderful mathematical structures [88, 89]. In the field of NESM, and for investigating the role of detailed balance-violating dynamics in particular, the asymmetric simple exclusion process (ASEP) is reaching the status of such a paradigm. A model with possibly the simplest of rules, it nevertheless displays a rich variety of NESSs. Further, it is sufficiently simple to allow us to exploit rigorous mathematical methods and, over the last two decades, to arrive at a number of exact results. In this way, valuable insights into the intricacies of NESM have been garnered. In this section, we delve into some details of two such methods, in the hope that readers unfamiliar with these techniques can join in these efforts. Of course, as we consider models which are more suited for physical/biological systems, we will encounter more complex ingredients than in ASEPs. As a result, these models are not exactly solvable at present. In these cases, approximations are necessary for further progress. One successful scheme is the mean-field approximation, leading to hydrodynamics equations (PDEs) for density fields. Since this strategy is the only one to offer some quantitative understanding of the more realistic/complex models, we will devote the last section 3.11 here to this approach.

In the previous section, we presented the master equation (1) in discrete time, which is clearly the most appropriate description for computer simulations. On the other hand, for analytic studies, it is often far easier to use continuous variables (or infinite systems, in a similar vein). Thus, all the discussions in this section will be based on continuous time, t. As discussed in the context of the Fokker–Planck equation (6), we introduced this connection: $t = \tau\delta t$. Here, let us be explicit and write the continuous version of equation (2) as

$$\partial_t P_i(t) = \sum_j M_i^j P_j(t) \tag{13}$$

where the matrix on the right, $\mathbb{M}$, is just $\mathbb{L}/\delta t$. Taking the limit $\delta t \to 0$ in the formal solution, $P(\tau) = [\mathbb{I} + \mathbb{L}]^\tau P(0)$ ($\mathbb{I}$ being the identity), leads then to $P(t) = \exp[\mathbb{M}t]P(0)$.

3.1. Motivation and definition of ASEP and TASEP

The ASEP is a many-body dynamical system, consisting of particles located on a discrete lattice that evolves in continuous time. The particles hop randomly from a site on a lattice to one of its immediate neighbors, provided the target site is empty. Physically, this constraint mimics short-range interactions amongst particles. In order to drive this lattice gas out of equilibrium, non-vanishing currents must be established in the system. This can be achieved by various means: by starting from non-uniform initial conditions, by coupling the system to external reservoirs that drive currents [90] through the system (transport of particles, energy, heat), or by introducing some intrinsic bias in the dynamics that favors motion in a privileged direction. Then, each particle is an asymmetric random walker that drifts steadily along the direction of an external driving force. Due to its simplicity, this model has appeared in different contexts. As noted in the introduction, it was first proposed by Gibbs and co-workers in 1968 [13, 14] as a prototype to describe the dynamics of ribosomes translating along an mRNA. In the mathematical literature, Brownian processes with hard-core interactions were defined in 1970 by Spitzer [9] who coined the term 'exclusion process' (see also [10, 11, 91, 92]). In addition to motivation from issues in molecular biology—the main focus of section 4, the ASEP has also been used to describe transport in low-dimensional systems with strong geometrical constraints [93] such as macromolecules transiting through anisotropic conductors, or quantum dots, where electrons hop to vacant locations and repel each other via Coulomb interaction [94], while many of its variants are ubiquitous in modeling traffic flow [15, 95]. More generally, the ASEP belongs to the class of driven diffusive systems defined by Katz, Lebowitz and Spohn in 1984 [12, 36, 68, 93, 96]. We emphasize that the ASEP is defined through dynamical rules, while no energy is associated with a microscopic configuration. More generally, the kinetic point of view seems to be a promising and fruitful approach to non-equilibrium systems (see, e.g., [97]).

To summarize, the ASEP is a minimal model to study non-equilibrium behavior. It is simple enough to allow analytical studies; however, it contains the necessary ingredients for the emergence of a non-trivial phenomenology:

> *Asymmetry*. The external driving breaks detailed balance and creates a stationary current. The system settles into an NESS.
> *Exclusion*. The hard-core interaction implies that there is at most one particle per site. The ASEP is a genuine many-body problem, with arguably the simplest of all interactions.
> *Process*. With no underlying Hamiltonian, the dynamics is stochastic and Markovian.

Having a general picture of an ASEP, let us turn to a complete definition of the model. Focusing on only exactly solvable cases, we restrict ourselves here to a one-dimensional

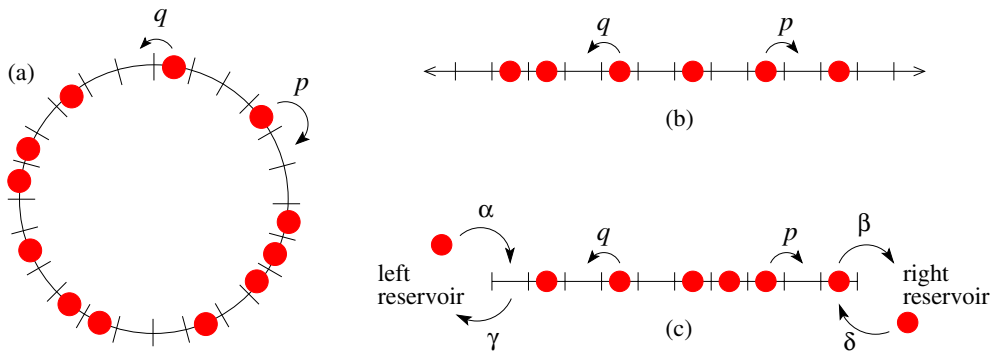

Figure 1. (*a*) The ASEP on a ring of L sites filled with N particles ($L = 24$, $N = 12$ here). The total number of configurations is just $\Omega = \binom{L}{N}$. (*b*) ASEP on an infinite lattice. The particles perform asymmetric random walks ($p \neq q$) and interact through the exclusion constraint. (*c*) A schematic of an ASEP with open boundaries on a finite lattice with $L = 10$ sites.

lattice, with sites labeled by $i = 1, \ldots, L$ (here, we will use i to label a site rather than a configuration). The stochastic evolution rules are the following: a particle located at site i in the bulk of the system jumps, in the interval $[t, t + \mathrm{d}t]$, with probability $p\mathrm{d}t$ to site $i + 1$ and with probability $q\mathrm{d}t$ to site $i - 1$, provided the target site is empty (*exclusion rule*). The rates p and q are the parameters of our system. By rescaling time, p is often set to unity, while q is left as a genuine control parameter. In the TASEP, the jumps are totally biased in one direction (e.g., $q = 0$). On the other hand, the *symmetric* exclusion process (SEP) corresponds to the choice $p = q$. The physics and the phenomenology of the ASEP is extremely sensitive to the boundary conditions. We will mainly discuss three types of boundary conditions:

Periodic boundary conditions. The exclusion process is defined on a ring, so that sites i and $L + i$ are identical. The system is filled with $N \leqslant L$ particles (figure 1(*a*)). Of course, the dynamics conserves N.

Infinite lattice. Here, the boundaries are sent to $\pm\infty$. Boundary conditions here are of a different kind. This system always remains sensitive to the initial conditions. Therefore, an initial configuration, or a statistical set of configurations, must be carefully specified. Figure 1(*b*) is an illustration of this system.

Open boundaries. Here, the boundary sites $i = 1, L$ play a special role, as they are coupled to particles in reservoirs just outside the system. Thus, if site 1 is empty, a particle can enter (from the 'left reservoir') with rate α. If it is occupied, the particle can exit (into this reservoir) with rate γ. Similarly, the interactions with the 'right reservoir' are the following: if site L is empty/occupied, a particle can enter/exit the system with rate δ/β, respectively. These rates can be regarded as the coupling of our finite system with infinite reservoirs set at different 'potentials'. Figure 1(*c*) illustrates this system. A much simpler limiting case is the TASEP, with $q = \gamma = \delta = 0$, with particles injected from the left, hopping along the lattice only to the right, and finally exiting to the right.

We emphasize that there are very many variants of the ASEP. The dynamical rules can be modified, especially in computer simulation studies using discrete-time updates (e.g. random sequential, parallel, or shuffle updates). The hopping rates can be modified to be either site- or particle-dependent, with motivations for such additions from biology provided in section 4. In modeling vehicular traffic, the former is suitable, e.g., for including road work or traffic lights. The latter can account for the range of preferred driving velocities, while a system can also be regarded as one with many 'species' of particles. In addition, these disorders can be dynamic or quenched [98–105]. Further, the exclusion constraint can be relaxed, so that fast cars are allowed to overtake slower ones, which are known as 'second class' or 'third class' particles [106–112]. Finally, the lattice geometry itself can be generalized to multi-lanes, higher dimensions, or complex networks. All these modifications drastically alter the collective behavior displayed in the system, as hundreds of researchers discovered during the last two decades. Although more relevant for applications, more realistic models cannot, in general, be solved exactly. As the primary focus of this section is exact solutions, we will focus only on the homogeneous systems presented above. These problems are amenable to sophisticated mathematical analysis thanks to a large variety of techniques: Bethe ansatz, quadratic algebras, Young tableaux, combinatorics, orthogonal polynomials, random matrices, stochastic differential equations, determinantal representations, hydrodynamic limits, etc. Each of these approaches is becoming a specific subfield that has its own links with other branches of theoretical physics and mathematics. Next, we will present some of these methods that have been developed for these three ideal cases.

3.2. Mathematical setup and fundamental issues

The evolution of the system is given by equation (13) and controlled by the Markov operator $\mathbb{M}$ as follows. In order to distinguish the two uses of i—label for configurations and for sites on our lattices, let us revert to using $\mathcal{C}$ for configurations. Then, this master equation reads

$$\frac{\mathrm{d}P(\mathcal{C}, t)}{\mathrm{d}t} = \sum_{\mathcal{C}'} M(\mathcal{C}, \mathcal{C}')P(\mathcal{C}', t). \tag{14}$$

As a reminder, the off-diagonal matrix elements of $\mathbb{M}$ represent the transition rates, and the diagonal part $M(\mathcal{C},\mathcal{C}) = -\sum_{\mathcal{C}'\neq\mathcal{C}} M(\mathcal{C}',\mathcal{C}')$ accounts for the exit rate from $\mathcal{C}$. Thus, the sum of the elements in any given column vanishes, ensuring probability conservation. For a finite ASEP, $\{\mathcal{C}\}$ is finite and the Markov operator $\mathbb{M}$ is a matrix. For the infinite system, $\mathbb{M}$ is an operator and its precise definition needs more sophisticated mathematical tools than linear algebra, namely functional analysis [10, 92]. Unless stated otherwise, we will focus here on the technically simpler case of finite L and deduce results for the infinite system by taking $L \to \infty$ limit formally. An important feature of the finite ASEP is ergodicity: any configuration can evolve to any other one in a finite number of steps. This property ensures that the Perron–Frobenius theorem applies (see, e.g., [45, 113]). Thus, $E = 0$ is a non-degenerate eigenvalue of $\mathbb{M}$, while all other eigenvalues have a strictly negative real part, $\mathrm{Re}(E) < 0$. The physical interpretation of the spectrum of $\mathbb{M}$ is clear: the right eigenvector associated with the eigenvalue $E = 0$ corresponds to the stationary state of the dynamics. Because all non-zero eigenvalues have strictly negative real parts, these eigenvectors correspond to relaxation modes, with $-1/\mathrm{Re}(E)$ being the relaxation time and $\mathrm{Im}(E)$ controlling the oscillations.

We emphasize that the operator $\mathbb{M}$ encodes all statistical information of our system, so that any physical quantity can be traced ultimately to some property of $\mathbb{M}$. We will list below generic mathematical and physical properties of our system that motivate the appropriate calculation strategies.

(i) Once the dynamics is properly defined, the basic question is to determine the steady state, P^*, of the system, i.e. the right eigenvector of $\mathbb{M}$ with eigenvalue 0. Given a configuration $\mathcal{C}$, the value of the component $P^*(\mathcal{C})$ is known as the measure (or stationary weight) of $\mathcal{C}$ in the steady state, i.e. it represents the frequency of occurrence of $\mathcal{C}$ in the stationary state.

(ii) The vector P^* plays the role of the Boltzmann factor in EQSM, so that all steady-state properties (e.g. all equal-time correlations) can be computed from it. Some important questions are the following: what is the mean occupation ρ_i of a given site i? What does the most likely density profile, given by the function $i \to \rho_i$, look like? Can one calculate density–density correlation functions between different sites? What is the probability of occurrence of a density profile that differs significantly from the most likely one? The last quantity is known as the large deviation of the density profile.

(iii) The stationary state is a dynamical state in which the system constantly evolves from one micro-state to another. This microscopic evolution induces macroscopic fluctuations (the equivalent of the Gaussian Brownian fluctuations at equilibrium). How can one characterize such fluctuations? Are they necessarily Gaussian? How are they related to the linear response of the system to small perturbations in the vicinity of the steady state? These issues can be tackled by considering tagged-particle dynamics, anomalous diffusion, time-dependent perturbations of the dynamical rules [114].

(iv) As expected, the ASEP carries a finite, non-zero, steady-state particle current, J, which is clearly an important physical observable. The dependence of J on the external parameters of the system allows us to define different phases of the system.

(v) The existence of a non-zero J in the stationary state implies the physical transport of an extensive number of particles, Q, through the lattice. The total number of particles, Q_t, transported up to time t is a random quantity. In the steady state, the mean value of Q_t is just Jt, while in the long time limit, the distribution of the random variable $Q_t/t - J$ represents exceptional fluctuations (i.e. large deviations) of the mean-current. This LDF is an important observable that provides detailed properties of the transport through the system. While particle current is the most obvious quantity to study in an ASEP, similar questions can be asked of other currents and the transport of their associated quantities, such as mass, charge, energy, etc in more realistic NESM models.

(vi) The way a system relaxes to its stationary state is also an important characteristic. The typical relaxation time of the ASEP scales with the system size as L^z, where z is the dynamical exponent. The value of z is related to the spectral gap of the Markov matrix $\mathbb{M}$, i.e. to the largest $-\mathrm{Re}(E)$. For a diffusive system, $z = 2$. For the ASEP with a periodic boundary condition, an exact calculation leads to $z = 3/2$. More generally, the transitory state of the model can be probed using correlation functions at different times.

(vii) The matrix $\mathbb{M}$ is generally a non-symmetric matrix and, therefore, its right eigenvectors differ from its left eigenvectors. For instance, a right eigenvector ψ_E corresponding to the eigenvalue E is defined as

$$\mathbb{M}\psi = E\psi. \tag{15}$$

Because $\mathbb{M}$ is real, its eigenvalues (and eigenvectors) are either real numbers or complex conjugate pairs. Powerful analytical techniques, such as the Bethe ansatz, can be exploited to diagonalize $\mathbb{M}$ in some specific cases, providing us with crucial information on its spectrum.

(viii) Solving the master equation (14) analytically would allow us to calculate exactly the evolution of the system. A challenging goal is to determine the finite-time Green function (or transition probability) $P(\mathcal{C}, t|\mathcal{C}_0, 0)$, the probability for the system to be in configuration $\mathcal{C}$ at time t, given that the initial configuration at time $t = 0$ was $\mathcal{C}_0$. Formally, it is just the $\mathcal{C}, \mathcal{C}_0$ element of the matrix $\exp[\mathbb{M}t]$ here. In principle, it allows us to calculate all the correlation functions of the system. However, explicit results for certain quantities will require not only the knowledge of the spectrum and eigenvectors of $\mathbb{M}$, but also explicit evaluations of matrix elements associated with the observable of interest.

The following sections are devoted to a short exposition of several analytical techniques that have been developed to answer some of these issues for the ASEP.

3.3. Steady-state properties of the ASEP

Given a stochastic dynamical system, the first question naturally concerns the stationary measure. We will briefly discuss the ASEP with periodic boundary conditions and the infinite line case. More details will be provided for the highly non-trivial case of the open ASEP.

Periodic boundary conditions. This is the simplest case, with the stationary measure being flat [96]. That the uniform measure is also stationary can be understood as follows. A given configuration consists of k clusters of particles separated by holes. A particle that leads a cluster can hop in the forward direction with rate p whereas a particle that ends a cluster can hop backward with rate q; thus the total rate of leaving a configuration consisting of k clusters is $k(p+q)$. Similarly, the total number of *ancestors* of this configuration (i.e. of configurations that can evolve into it) is also given by $k(p+q)$. The fact that these two quantities are identical suffices to show that the uniform probability is stationary. To obtain the precise value of P^*, $1/\Omega$, is also elementary. Since N is a constant, we only need the total number of configurations for N particles on a ring with L sites, which is just $\Omega = L!/[N!(L-N)!]$.

Infinite lattice. For the exclusion process on an infinite line, the stationary measures are studied and classified in [11, 92]. There are two one-parameter families of invariant measures. One family, denoted by ν_ρ, is a product of local Bernoulli measures of constant density ρ: this means that each site is occupied with probability ρ. The other family is discrete and is concentrated on a countable subset of configurations. For the TASEP, this second family corresponds to *blocking measures*, which are point-mass measures concentrated on step-like configurations (i.e. configurations where all sites to the left/right of a given site are empty/occupied).

Open boundaries. Turning to the case of the ASEP on a finite lattice with open boundaries, we note that the only knowledge we have, without detailed analysis, is the existence of a unique stationary measure (thanks to the Perron–Frobenius theorem), i.e. the vector P^* with 2^L components. We emphasize again that finding P^* is a non-trivial task because we have no *a priori* guiding principle at our disposal. With no underlying Hamiltonian and no temperature, no fundamental principles of EQSM are relevant here. The system is far from equilibrium with a non-trivial steady-state current that does not vanish for even large L.

To simplify the discussion, we focus on the TASEP where particles enter from the left reservoir with rate α, hop only to the right and leave the system from the site L with rate β. A configuration $\mathcal{C}$ can be represented by the binary string, $(\sigma_1, \ldots, \sigma_L)$, of occupation variables: $\sigma_i = 1$ if the site i is occupied and $\sigma_i = 0$ otherwise. Our goal is to determine $P^*(\mathcal{C})$, with which the steady-state current J can be expressed simply and *exactly*:

$$\begin{aligned} J &= \alpha(1-\langle\sigma_1\rangle) = \langle\sigma_1(1-\sigma_2)\rangle \\ &= \cdots = \langle\sigma_i(1-\sigma_{i+1})\rangle = \beta\langle\sigma_L\rangle. \end{aligned} \tag{16}$$

Here, the brackets $\langle\,\rangle$ denote expectation values as defined in equation (7). Even if J were known somehow, this set of equations is not sufficient for fixing the (unknown) density profile $\rho_i = \langle\sigma_i\rangle$ and the NN correlations $\langle\sigma_i\sigma_{i+1}\rangle$. Typical in a truly many-body problem, there is a hierarchy [47, 115–117] of equations that couple k-site and $(k+1)$-site correlations. A very important approximation, which often provides valuable insights, is the *mean-field assumption* in which the hierarchy is simply truncated at a given level. If the correlations beyond this level are small, this approximation can be quite good. Applying this technique here consists of replacing two-site correlations by products of single-site averages:

$$\langle\sigma_i\sigma_j\rangle \to \langle\sigma_i\rangle\langle\sigma_j\rangle = \rho_i\rho_j. \tag{17}$$

Thus, equation (16) becomes

$$\begin{aligned} J &\simeq \alpha(1-\rho_1) = \rho_1(1-\rho_2) \\ &= \ldots = \rho_i(1-\rho_{i+1}) = \beta\rho_L \end{aligned} \tag{18}$$

and we arrive at a closed recursion relation between ρ_{i+1} and ρ_i, namely $\rho_{i+1} = 1 - J/\rho_i$. Of course, J is an unknown, to be fixed as follows. Starting with $\rho_1 = 1 - J/\alpha$, the recursion eventually leads us to ρ_L as a rational function of J (and α). Setting this to J/β gives a polynomial equation for J. Solving for J, we obtain the desired dependence of the steady-state current on the control parameters: $J(\alpha, \beta, L)$. This approach to an approximate solution was known to Gibbs and co-workers [13, 14] (within the context of a more general version of TASEP) and explored further in [118] recently.

Analyzing $J(\alpha, \beta, L)$ gives rise to the phase diagram of the TASEP (see figure 2). For studying these aspects of the TASEP, the mean-field method provides us with a reasonably good approximation. Indeed, the correct phase diagram of the model was obtained in [90] [7] through physical reasoning using such mean-field arguments along with the hydrodynamic limit. Since this strategy is quite effective and more widely applicable, we will briefly discuss how it is applied to ASEP in section 3.11. Despite many effective mean-field theory (MFT)-based strategies, exact solutions to ASEP are desirable, especially for an in-depth analysis. In particular, MFT cannot account for correlations, fluctuations, or rare events. In fact, the mean-field density profile (from solving the recursion relation (18) numerically) does not agree with the exact profile (from evaluating the expression (23)). Of course, it is rare that we are able to calculate the stationary measure for a non-equilibrium interacting model. Not surprisingly, the exact steady-state solution of the TASEP [118–121] was considered a major breakthrough.

3.4. The matrix representation method for the open TASEP

The exact calculation of the stationary measure for the TASEP with open boundaries and the derivation of its phase diagram triggered an explosion of research on exactly solvable models in NESM. The fundamental observation [118] is the existence of recursion relations for the stationary probabilities between systems of different sizes. These recursions are particularly striking when $\alpha = \beta = 1$ [118]; they can be generalized to arbitrary values of α and β [120, 121] and also to the more

[7] See also [10, 119] for a pedagogical example.

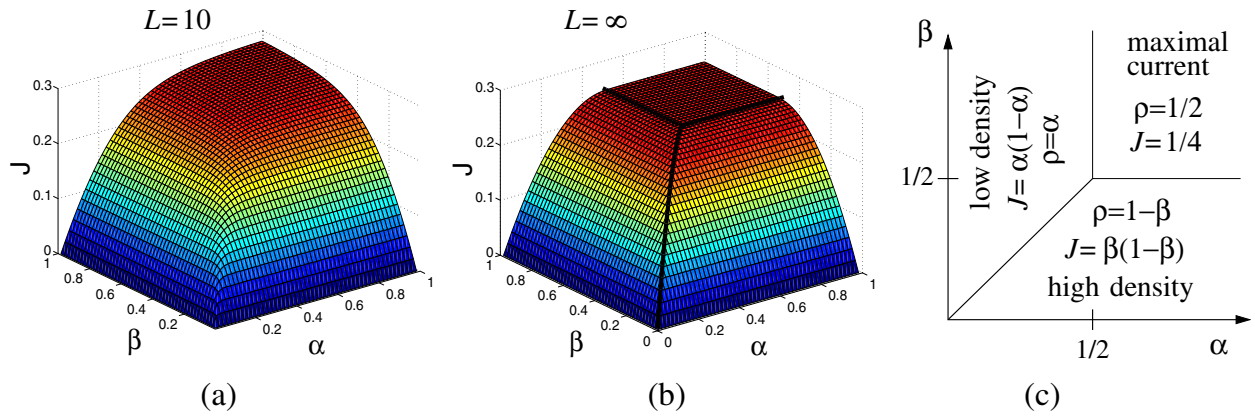

Figure 2. (*a*) Exact solution (derived from equations (24) and (22) for the steady-state current J of a TASEP with $L = 10$ sites. (*b*) The steady-state current J plotted in the $L \to \infty$ limit. (*c*) The phase diagram for the current of an infinite lattice ($L = \infty$) TASEP as a function of the injection and extraction rates.

general case in which backward jumps are allowed (also known as a partially asymmetric exclusion process, or PASEP). The most elegant and efficient way to encode these recursions is to use the matrix ansatz [120]. We caution readers that the matrices to be presented in this subsection have nothing to do with the transition matrices $\mathbb{M}$ discussed above. They do not represent the intrinsic physics of TASEP but, instead, provide a convenient framework for representing the algebra that arises from the recursion relations. In particular, we need only two matrices ($\boldsymbol{D}$ and $\boldsymbol{E}$) and two 'eigenvectors' (a bra $\langle W|$ and a ket $|V\rangle$, normalized by $\langle W|V\rangle = 1$) here. The algebra we need is

$$\begin{aligned} \boldsymbol{D}\boldsymbol{E} &= \boldsymbol{D} + \boldsymbol{E} \\ \boldsymbol{D}\,|V\rangle &= \frac{1}{\beta}|V\rangle \\ \langle W|\,\boldsymbol{E} &= \frac{1}{\alpha}\langle W|. \end{aligned} \tag{19}$$

We emphasize that in general the operators $\boldsymbol{D}$ and $\boldsymbol{E}$ do not commute with each other, so that an explicit representation would be typically infinite dimensional.

Remarkably, it was shown that the stationary $P^*(\mathcal{C})$ for TASEP can be written as the scalar

$$P^*(\sigma_1, \ldots, \sigma_L) = \frac{1}{Z_L}\langle W|\prod_{i=1}^{L}(\sigma_i \boldsymbol{D} + (1-\sigma_i)\boldsymbol{E})|V\rangle \tag{20}$$

where

$$Z_L = \langle W|(\boldsymbol{D}+\boldsymbol{E})^L|V\rangle \tag{21}$$

is a normalization constant. Each operation of the matrices $\boldsymbol{D}$ or $\boldsymbol{E}$ is associated with a filled or empty site on the lattice. For example, the weight of the configuration shown in figure 1(*c*) is $\langle W|\boldsymbol{E}\boldsymbol{D}\boldsymbol{D}\boldsymbol{E}\boldsymbol{D}\boldsymbol{E}\boldsymbol{D}\boldsymbol{E}\boldsymbol{D}\boldsymbol{E}|V\rangle/Z^{10}$. To obtain explicit values for (20), one method is to find an explicit representation of this algebra. Another possibility is to systematically use the algebraic rules (19) without referring to any representation. Indeed, a product of $\boldsymbol{D}$s and $\boldsymbol{E}$s in an arbitrary order can be decomposed as a linear combination of monomials of the type $\boldsymbol{E}^n\boldsymbol{D}^m$ repeatedly using the rule $\boldsymbol{D}\boldsymbol{E} = \boldsymbol{D} + \boldsymbol{E}$. Then, using $\langle W|\boldsymbol{E}^n\boldsymbol{D}^m\,|V\rangle = \alpha^{-n}\beta^{-m}$, we find that any matrix element of the type (20) is a polynomial in $1/\alpha$ and $1/\beta$. In particular, we find the following general formula [120] for Z_L:

$$\begin{aligned} Z_L &= \langle W|(\boldsymbol{D}+\boldsymbol{E})^L|V\rangle \\ &= \sum_{p=1}^{L} \frac{p\,(2L-1-p)!}{L!\,(L-p)!}\,\frac{\beta^{-p-1}-\alpha^{-p-1}}{\beta^{-1}-\alpha^{-1}}. \end{aligned} \tag{22}$$

When $\alpha = \beta = 1$, Z_L is a Catalan number [120]. Another special case is $\alpha = 1-\beta$, for which the scalar representation, $\boldsymbol{D} = 1/\beta$, $\boldsymbol{E} = 1/\alpha$, suffices and P^* simplifies considerably. In all cases, quantities of physical interest (current, profile, correlations) can be explicitly computed using the algebra (19). In this sense, the TASEP is 'solved': all equal-time correlations in the stationary state are known.

The matrix method may look puzzling at first sight. One informal way to motivate it is the following: the steady-state weight of a configuration cannot be expressed in general as a product of single site occupancy or vacancy probabilities because in the presence of interactions there are non-zero correlations (i.e. MFT is not exact). However, by writing the stationary measure as a product of matrices, a sort of factorization still holds and at the same time correlations are taken into account by the fact that the matrices do not commute.

3.5. Phase diagram of the open TASEP

Thanks to the matrix representation method, exact expressions for the phase diagram of the TASEP, as well as stationary equal-time correlations and density profiles, can be readily obtained. For example, the mean occupation of a site i (with $1 \leqslant i \leqslant L$) is given by

$$\langle \sigma_i \rangle = \frac{1}{Z_L}\langle W|(\boldsymbol{D}+\boldsymbol{E})^{i-1}\boldsymbol{D}(\boldsymbol{D}+\boldsymbol{E})^{L-i}|V\rangle. \tag{23}$$

This expression is obtained by summing over all configurations in which site i is occupied.

Similarly, the average value of the steady-state current J through the 'bond' connecting site i and $i+1$ can be

calculated as

$$J(\alpha,\beta,L) = \langle \sigma_i(1-\sigma_{i+1})\rangle = \frac{1}{Z_L}\langle W|(\boldsymbol{D}+\boldsymbol{E})^{i-1}\boldsymbol{D}\boldsymbol{E}(\boldsymbol{D}+\boldsymbol{E})^{L-i-1}|V\rangle = \frac{Z_{L-1}}{Z_L} \tag{24}$$

where we have used the algebra (19). We note that this value does not depend on the specific bond considered. This was expected because particles are neither created nor destroyed in the system.

In the limit of large system sizes, the phase diagram (figure 2) consists of three main regions.

- In the *low-density phase*, when $\alpha < \min\{\beta, 1/2\}$, the bulk-density is $\rho = \alpha$ and the average current $J = \alpha(1-\alpha)$ is a function only of the rate-limiting injection process.
- In the *high-density phase*, when $\beta < \min\{\alpha, 1/2\}$, the typical density is characterized by $\rho = 1-\beta$ and the steady-state current, $J = \beta(1-\beta)$, is a function only of the rate-limiting extraction step.
- In the *maximal current phase,* when $\alpha > 1/2$ and $\beta > 1/2$, the bulk behavior is independent of the boundary conditions and one finds $\rho = 1/2$ and $J = 1/4$. In this phase, particle–particle correlations decay only algebraically away from the boundaries, in contrast to exponentially decaying correlations in both the low- and high-density phases.
- The low- and high-density phases are separated by the 'shock-line', $\alpha = \beta \leqslant 1/2$, across which the bulk-density is discontinuous. In fact, the profile on this line is a mixed-state of shock profiles interpolating between the lower density $\rho = \alpha$ and the higher density $\rho = 1-\beta$.

Detailed properties of the phase diagram are reviewed in [96, 122, 123].

The particle density profiles in the large L limit, described in each phase above, are only approximately uniform in that they are asymptotically accurate only in the bulk, but must vary near the boundaries in order to satisfy conditions determined by the steady-state particle injection and extraction [124]. It turns out that the MFT approaches, recursion and hydrodynamic equations, reproduce the exact $L \to \infty$ phase diagram; however, the matrix product approach finds the correct density profile which is not obtained by mean-field approximations.

3.6. Some extensions of the matrix ansatz

Extension to the general ASEP model. If we allow jumps in both directions and entrance/exit at both ends of the system, the matrix technique can still be applied. The algebra (19) must be replaced by the more general rules

$$\begin{aligned} p\boldsymbol{D}\boldsymbol{E} - q\,\boldsymbol{E}\boldsymbol{D} &= \boldsymbol{D}+\boldsymbol{E} \\ (\beta\boldsymbol{D}-\delta\boldsymbol{E})|V\rangle &= |V\rangle \\ \langle W|(\alpha\,\boldsymbol{E}-\gamma\boldsymbol{D}) &= \langle W|. \end{aligned} \tag{25}$$

This new algebra allows one to calculate the general phase diagram of the open ASEP using orthogonal polynomials [123, 125–127]. The phase diagram of the ASEP turns out to be identical to that of the TASEP in a two-dimensional slice across effective parameters that are functions of the intrinsic rates $\alpha, \beta, \gamma, \delta, p, q$.

Multispecies exclusion processes. The matrix method can be used to represent the stationary measure of periodic systems with defects or with different classes of particles [106–112]. In particular, this allows us to investigate shock profiles that appear in the ASEP and to prove that these shocks, predicted by Burgers' equation, do exist at the microscopic level and are not artifacts of the hydrodynamic limit [106, 128–130].

Macroscopic density profiles. Knowing exactly the microscopic invariant measure allows us to rigorously coarse-grain the problem and to determine the probability of occurrence of a density profile that differs from the average profile. The calculation of such 'free energy functionals' is an important step in understanding how non-equilibrium macroscopic behavior emerges from the microscopic model. For a review of these very important issues and for relevant references, we refer the reader to [77, 131].

Other models. We emphasize that the matrix product representation method has proved to be very fruitful for solving many one-dimensional systems; a very thorough review of this method can be found in [123].

3.7. Time-dependent properties: the Bethe ansatz

In order to investigate the behavior of the system away from stationarity, the spectrum of the Markov matrix is needed. For an arbitrary stochastic system, the evolution operator cannot be diagonalized analytically for any system sizes. However, the ASEP belongs to a very special class of models: it is *integrable* and it can be solved using the Bethe ansatz as first noticed by Dhar in 1987 [132]. Indeed, the Markov matrix that encodes the stochastic dynamics of the ASEP can be rewritten in terms of Pauli matrices; in the absence of a driving field, the *symmetric* exclusion process can be mapped exactly into the Heisenberg spin chain. The asymmetry due to a non-zero external driving field breaks the left/right symmetry and the ASEP becomes equivalent to a non-Hermitian spin chain of the XXZ type with boundary terms that preserve the integrable character of the model. The ASEP can also be mapped into a six vertex model [88, 133, 134]. These mappings suggest the use of the Bethe ansatz to derive spectral information about the evolution operator, such as the spectral gap [132, 135–139] and LDFs [140, 141].

Here, we will apply the Bethe ansatz to the ASEP on a ring. A configuration can also be characterized by the positions of the N particles on the ring, $(x_1, x_2, \ldots, x_N)$ with $1 \leqslant x_1 < x_2 < \cdots < x_N \leqslant L$. With this representation, the

eigenvalue equation (15) becomes

$$\begin{aligned} E\psi(x_1,\ldots,x_N) &= \sum_i p[\psi(x_1,\ldots,x_{i-1},\ x_i-1,\ x_{i+1},\ldots,x_N) \\ &\quad -\psi(x_1,\ldots,x_n)] \\ &\quad +\sum_j q[\psi(x_1,\ldots,x_{j-1},\ x_j+1,\ x_{j+1},\ldots,x_N) \\ &\quad -\psi(x_1,\ldots,x_N)] \end{aligned} \tag{26}$$

where the sum runs over the indices i such that $x_{i-1} < x_i - 1$ and over the indices j such that $x_j + 1 < x_{j+1}$; these conditions ensure that the corresponding jumps are allowed.

We observe that equation (26) is akin to a discrete Laplacian on a N-dimensional lattice: the major difference is that the terms corresponding to forbidden jumps are absent. Nevertheless, this suggests that a trial solution, or *ansatz*, in the form of plane waves may be useful. This is precisely the idea underlying the Bethe ansatz, originally developed to study the Heisenberg spin chain model of quantum magnetism [142]. Following Bethe's method, we will also refer to ψ as a 'wave function,' but the reader should not confuse our problem with one in quantum mechanics. In our opinion, the ASEP is one of the simplest systems with which one can learn the Bethe ansatz. The next subsection is devoted to such a tutorial.

3.8. Bethe ansatz for ASEP: a crash-course

Our aim is to solve the linear eigenvalue problem (26) which corresponds to the relaxation modes of the ASEP with N particles on a ring of L sites. We will study some special cases with small N to illustrate the general structure of the solution.

The single-particle case. For $N = 1$, equation (26) reads

$$E\psi(x) = p\psi(x-1) + q\psi(x+1) - (p+q)\psi(x) \tag{27}$$

with $1 \leqslant x \leqslant L$ and where periodicity is assumed

$$\psi(x+L) = \psi(x). \tag{28}$$

Equation (27) is simply a linear recursion of order 2 that is solved as

$$\psi(x) = Az_+^x + Bz_-^x \tag{29}$$

where $r = z_\pm$ are the two roots of the characteristic equation

$$qr^2 - (E+p+q)r + p = 0. \tag{30}$$

The periodicity condition imposes that at least one of the two characteristic values is an Lth root of unity (Note that because $z_+ z_- = p/q$, only one of them can be a root of unity when $p \neq q$). The general solution is given by

$$\psi(x) = Az^x \qquad \text{with } z^L = 1 \tag{31}$$

i.e. simple *plane waves* with 'momenta' being integer multiples of $2\pi/L$ and associated with eigenvalue

$$E = \frac{p}{z} + qz - (p+q). \tag{32}$$

The two-particle case. The case $N = 2$ where two particles are present is more interesting because when the particles are located on adjacent sites the exclusion effect plays a role. Indeed, the general eigenvalue equation (26) can be split into two different cases.

- In the generic case, x_1 and x_2 are separated by at least one empty site:

$$\begin{aligned} E\psi(x_1,x_2) &= p[\psi(x_1-1,x_2) + \psi(x_1,x_2-1)] \\ &\quad +q[\psi(x_1+1,x_2) + \psi(x_1,x_2+1)] \\ &\quad -2(p+q)\psi(x_1,x_2). \end{aligned} \tag{33}$$

- In the (special) adjacency case, $x_2 = x_1 + 1$, some jumps are forbidden and the eigenvalue equation reduces to

$$\begin{aligned} E\psi(x_1,x_1+1) &= p\psi(x_1-1,x_1+1) + q\psi(x_1,x_1+2) \\ &\quad -(p+q)\psi(x_1,x_1+1). \end{aligned} \tag{34}$$

  This equation differs from the generic equation (33) in which we substitute $x_2 = x_1 + 1$. An equivalent way to take into account the adjacency case is to impose that the generic equation (33) is valid *for all values* of x_1 and x_2 and add to it the following *cancellation boundary condition:*

$$\begin{aligned} &p\psi(x_1,x_1) + q\psi(x_1+1,x_1+1) \\ &\quad -(p+q)\psi(x_1,x_1+1) = 0. \end{aligned} \tag{35}$$

We now examine how these equations can be solved. In the generic case particles behave totally independently (i.e. they do not interact). The solution of the generic equation (33) can therefore be written as a product of plane waves $\psi(x_1,x_2) = Az_1^{x_1}z_2^{x_2}$, with the eigenvalue

$$E = p\left(\frac{1}{z_1} + \frac{1}{z_2}\right) + q(z_1+z_2) - 2(p+q). \tag{36}$$

However, the simple product solution cannot be the full answer: the cancellation condition for the adjacency case (35) also has to be satisfied. The first crucial observation, following Bethe [142], is that the eigenvalue E, given in (36), is invariant by the permutation $z_1 \leftrightarrow z_2$. In other words, there are two plane waves $Az_1^{x_1}z_2^{x_2}$ and $Bz_2^{x_1}z_1^{x_2}$ with the same eigenvalue E which has a two-fold degeneracy. The full eigenfunction corresponding to E can thus be written as

$$\psi(x_1,x_2) = A_{12}z_1^{x_1}z_2^{x_2} + A_{21}z_2^{x_1}z_1^{x_2} \tag{37}$$

where the amplitudes A_{12} and A_{21} are arbitrary. The second key step is to understand that these amplitudes can now be chosen to fulfil the adjacency cancellation condition: substitution of (37) into equation (35) leads to

$$\frac{A_{21}}{A_{12}} = -\frac{qz_1z_2 - (p+q)z_2 + p}{qz_1z_2 - (p+q)z_1 + p}. \tag{38}$$

The eigenfunction (37) is therefore determined, but for an overall multiplicative constant. We now implement the periodicity condition that takes into account the fact that the system is defined on a ring. This constraint can be written as follows for $1 \leqslant x_1 < x_2 \leqslant L$:

$$\psi(x_1,x_2) = \psi(x_2,x_1+L). \tag{39}$$

This relation plays the role of a quantification condition for the scalars z_1 and z_2, which we will call *Bethe roots*. If we now impose the condition that the expression (37) satisfies equation (39) for all generic values of the positions x_1 and x_2, new relations between the amplitudes arise:

$$\frac{A_{21}}{A_{12}} = z_2^L = \frac{1}{z_1^L}. \tag{40}$$

Comparing equations (38) and (40) leads to a set of algebraic equations obeyed by the Bethe roots z_1 and z_2:

$$z_1^L = -\frac{qz_1z_2 - (p+q)z_1 + p}{qz_1z_2 - (p+q)z_2 + p} \tag{41}$$

$$z_2^L = -\frac{qz_1z_2 - (p+q)z_2 + p}{qz_1z_2 - (p+q)z_1 + p}. \tag{42}$$

These equations are known as the *Bethe ansatz equations*. Finding the spectrum of the matrix $\mathbb{M}$ for two particles on a ring of size L is reduced to solving these two coupled polynomial equations of degree $L+2$ with unknowns z_1 and z_2. Surely, this still remains a very challenging task but the Bethe equations are explicit and very symmetric. Moreever, we emphasize that the size of the matrix $\mathbb{M}$ (and the degree of its characteristic polynomial) is of order L^2.

The three-particle case. We are now ready to consider the case $N = 3$. For a system containing three particles, located at $x_1 \leqslant x_2 \leqslant x_3$, the generic equation, valid when the particles are well separated, can readily be written using equation (26). But now, the special adjacency cases are more complicated.

(i) Two particles are next to each other and the third one is far apart; such a setting is called a two-body collision and the boundary condition that results is identical to the one obtained for the case $N = 2$. There are now two equations that correspond to the cases $x_1 = x \leqslant x_2 = x+1 \ll x_3$ and $x_1 \ll x_2 = x \leqslant x_3 = x+1$:

$$p\psi(x,x,x_3) + q\psi(x+1,x+1,x_3) - (p+q)\psi(x,x+1,x_3) = 0 \tag{43}$$

$$p\psi(x_1,x,x) + q\psi(x_1,x+1,x+1) - (p+q)\psi(x_1,x,x+1) = 0. \tag{44}$$

We emphasize again that these equations are identical to equation (35) because the third particle, located far apart, is simply a *spectator* (x_3 is a spectator in the first equation; x_1 in the second one).

(ii) There can be three-body collisions, in which the three particles are adjacent, with $x_1 = x$, $x_2 = x+1$, $x_3 = x+2$. The resulting boundary condition is then given by

$$p[\psi(x,x,x+2) + \psi(x,x+1,x+1)] + q[\psi(x+1,x+1,x+2) + \psi(x,x+2,x+2)] - 2(p+q)\psi(x,x+1,x+2) = 0. \tag{45}$$

The fundamental remark is that *three-body collisions do not lead to an independent constraint*. Indeed, equation (45) is simply a linear combination of the constraints (43) and (44) imposed by the two-body collisions. To be precise: equation (45) is the sum of equation (43), with the substitutions $x \to x$ and $x_3 \to x+2$, and of equation (44) with $x_1 \to x$ and $x \to x+1$. Therefore, *it is sufficient to fulfil the two-body constraints because then the three-body conditions are automatically satisfied.* The fact that three-body collisions decompose or 'factorize' into two-body collisions is the *crucial property* that lies at the very heart of the Bethe ansatz. If it were not true, the ASEP would not be exactly solvable or 'integrable'.

For $N = 3$, the plane wave $\psi(x_1,x_2,x_3) = Az_1^{x_1}z_2^{x_2}z_3^{x_3}$ is a solution of the generic equation with the eigenvalue

$$E = p\left(\frac{1}{z_1} + \frac{1}{z_2 + z_3^{-1}}\right) + q(z_1+z_2+z_3) - 3(p+q). \tag{46}$$

However, such a single plane wave does not satisfy the boundary conditions (43) and (44). Again, we note that the eigenvalue E is invariant under the permutations of z_1, z_2 and z_3. There are six such permutations, that belong to S_3, the permutation group of three objects. The Bethe wave function is therefore written as a sum of the six plane waves, corresponding to the same eigenvalue E, with unknown amplitudes:

$$\begin{aligned}\psi(x_1,x_2,x_3) &= A_{123}\, z_1^{x_1}z_2^{x_2}z_3^{x_3} \\ &+A_{132}\, z_1^{x_1}z_3^{x_2}z_2^{x_3} + A_{213}\, z_2^{x_1}z_1^{x_2}z_3^{x_3} \\ &+A_{231}\, z_2^{x_1}z_3^{x_2}z_1^{x_3} + A_{312}\, z_3^{x_1}z_1^{x_2}z_2^{x_3} + A_{321}\, z_3^{x_1}z_2^{x_2}z_1^{x_3} \\ &= \sum_{s\in S_3} A_s z_{s(1)}^{x_1} z_{s(2)}^{x_2} z_{s(3)}^{x_3}.\end{aligned} \tag{47}$$

The six amplitudes A_s are uniquely and unambiguously determined (up to an overall multiplicative constant) by the two-body collision constraints. It is therefore absolutely crucial that three-body collisions do not bring additional independent constraints that the Bethe wave function could not satisfy. We encourage the reader to perform the calculations (which are very similar to the $N = 2$ case) of the amplitude ratios.

Finally, the Bethe roots z_1, z_2 and z_3 are quantized through the periodicity condition

$$\psi(x_1,x_2,x_3) = \psi(x_2,x_3,x_1+L) \tag{48}$$

for $1 \leqslant x_1 < x_2 < x_3 \leqslant L$. This condition leads to the Bethe ansatz equations (the equations for general N are given below).

The general case. Finally, we briefly discuss the general case $N > 3$. Here one can have k-body collisions with $k = 2, 3, \ldots N$. However, all multi-body collisions 'factorize' into two-body collisions and ASEP can be diagonalized using the Bethe wave function

$$\psi(x_1,x_2,\ldots,x_N) = \sum_{s\in S_N} A_s z_{s(1)}^{x_1} z_{s(2)}^{x_2} \cdots z_{s(N)}^{x_N} \tag{49}$$

where S_N is the permutation group of N objects. The $N!$ amplitudes A_s are fixed (up to an overall multiplicative constant) by the two-body collisions constraints. The corresponding eigenvalue is given by

$$E = p\sum_{i=1}^{N}\frac{1}{z_i} + q\sum_{i=1}^{N} z_i - N(p+q). \tag{50}$$

The periodicity condition

$$\psi(x_1, x_2, \ldots, x_N) = \psi(x_2, x_3, \ldots, x_N, x_1 + L) \tag{51}$$

where $1 \leqslant x_1 < x_2 < \ldots < x_N \leqslant L$, leads to a set of algebraic equations satisfied by the Bethe roots $z_1, z_2, \ldots, z_N$. The Bethe ansatz equations are given by

$$z_i^L = (-1)^{N-1} \prod_{j \neq i} \frac{q z_i z_j - (p+q) z_i + p}{q z_i z_j - (p+q) z_j + p} \tag{52}$$

for $i = 1, \ldots N$. The Bethe ansatz thus provides us with a set of N coupled algebraic equations of order L (recall that the size of the matrix $\mathbb{M}$ is of order 2^L, when $N \simeq L/2$). Although the degree of the polynomials involved is extremely high, a large variety of methods have been developed to analyze them [88, 143, 144].

We remark that for $p = q = 1$ the Bethe equations are the same as the ones derived by Bethe in 1931. Indeed, the symmetric exclusion process is mathematically equivalent to the isotropic Heisenberg spin chain (although the two systems describe totally different physical settings).

3.9. Some applications of the Bethe ansatz

The Bethe ansatz allows us to derive information about the spectrum of the Markov matrix that governs the evolution of ASEP. Below, we review some applications and refer to the original works.

Structure of the Bethe wave function. In the totally asymmetric case (TASEP), the Bethe equations simplify and it is possible to perform analytical calculations even for finite values of L and N. Moreover, the TASEP Bethe wave function takes the form of a determinant:

$$\psi(\xi_1, \ldots, \xi_N) = \det(\mathbb{R}) \tag{53}$$

where $\mathbb{R}$ is a $N \times N$ matrix with elements

$$R_{ij} = \frac{z_i^{\xi_j}}{(1 - z_i)^j} \qquad \text{for } 1 \leqslant i, j \leqslant N \tag{54}$$

with $(z_1, \ldots, z_N)$ being the Bethe roots. By expanding the determinant, one recovers the generic form (49) for the Bethe wave function. The formulae (53) and (54) can be verified directly by proving that the eigenvalue equation (26) and all the boundary conditions are satisfied [112, 145]. As we will see in the next subsection, determinantal representations of the eigenvectors and of the exact probability distribution at finite-time play a very important role in the study of the TASEP [146–149].

Spectral gap and dynamical exponent. The Bethe ansatz allows us to determine the spectral gap which amounts to calculating the eigenvalue E_1 with the largest real part. For a density $\rho = N/L$, one obtains for the TASEP

$$E_1 = \underbrace{-2\sqrt{\rho(1-\rho)}\frac{6.509\,189\,337\ldots}{L^{3/2}}}_{\text{relaxation}} \pm \underbrace{\frac{2\mathrm{i}\pi(2\rho - 1)}{L}}_{\text{oscillations}}. \tag{55}$$

The first excited state consists of a pair of conjugate complex numbers when ρ is different from $1/2$. The real part of E_1 describes the relaxation towards the stationary state: we find that the largest relaxation time scales as $T \sim L^z$ with the dynamical exponent $z = 3/2$ [132, 135, 136, 138, 150]. This value agrees with the dynamical exponent of the one-dimensional Kardar–Parisi–Zhang (KPZ) equation that belongs to the same universality class as ASEP (see the review of Halpin-Healy and Zhang [151]). The imaginary part of E_1 represents the relaxation oscillations and scales as L^{-1}; these oscillations correspond to a kinematic wave that propagates with the group velocity $2\rho - 1$; such traveling waves can be probed by dynamical correlations [99, 152]. The same procedure also allows us to classify the higher excitations in the spectrum [153]. For the partially asymmetric case ($p, q > 0$, $p \neq q$), the Bethe equations do not decouple and analytical results are much harder to obtain. A systematic procedure for calculating the finite size corrections of the upper region of the ASEP spectrum was developed by Kim [136, 137].

Large deviations of the current. The exclusion constraint modifies the transport properties through the ASEP system. For instance, if one considers the ASEP on a ring and tags an individual particle (without changing its dynamics), the particle displays diffusive behavior in the long time limit, but with a tracer diffusion coefficient $\mathcal{D}$ that depends on the size of the system. It is different from the free, non-interacting particle diffusion constant: $\mathcal{D}_{\text{ASEP}} \neq \mathcal{D}_{\text{free}}$. In a ring of size L, $\mathcal{D}_{\text{ASEP}}$ scales as $L^{-1/2}$ in the presence of an asymmetric driving. In the case of symmetric exclusion, one has $\mathcal{D}_{\text{SEP}} \sim L^{-1}$. These scaling behaviors indicate that in the limit of an infinite system the diffusion constant vanishes and fluctuations become anomalous [154]. In the classic result [91, 92, 97] of the SEP on an infinite line, root-mean square displacement of a tagged particle scales as $t^{1/4}$. In the ASEP, subtleties associated with the initial conditions arise. For a *fixed initial condition*, the position of the tagged particle spreads as $t^{1/3}$. However, if an average is carried out by choosing random initial conditions (with respect to the stationary measure), then a normal $t^{1/2}$ diffusion is recovered. The latter is a trivial effect due to the local density fluctuations that result from varying the initial condition; these fluctuations completely overwhelm and mask the intrinsic dynamical fluctuations. Another feature that one expects is a non-Gaussian behavior, i.e. cumulants beyond the second are present.

An alternative observable that carries equivalent information (and is amenable to analytical studies) is the total current transported through the system. Consider the statistics of Y_t, the total distance covered by all the particles between the time 0 and t. It can be shown (see, e.g., [112] and references therein) that in the long time limit the cumulant generating function of the random variable Y_t behaves as

$$\langle e^{\mu Y_t} \rangle \simeq \mathrm{e}^{E(\mu)t}. \tag{56}$$

This equation implies that all the cumulants of Y_t grow linearly with time and can be determined by taking successive derivatives of the function $E(\mu)$ at $\mu = 0$. Another way to

characterize the statistics of Y_t is to consider the LDF of the current, defined as follows:

$$\text{Prob}\left(\frac{Y_t}{t} = j\right) \sim \mathrm{e}^{-tG(j)}. \tag{57}$$

From equations (56) and (57), we see that $G(j)$ and $E(\mu)$ are the *Legendre transforms* of each other. LDFs play an increasingly important role in non-equilibrium statistical physics [78], especially through application of the fluctuation theorem [76]. Thus, determining exact expressions for these LDFs for interacting particle processes, either analytically or numerically, is a major challenge in the field [155–157]. Moreover, higher cumulants of the current and large deviations are also of experimental interest in relation to counting statistics in quantum systems [158].

The crucial step in the calculation of the cumulants is to identify the generating function $E(\mu)$ as the dominant eigenvalue of a matrix $\mathbb{M}(\mu)$, obtained by the following deformation of the original Markov matrix $\mathbb{M}$:

$$\mathbb{M}(\mu) = \mathbb{M}_0 + \mathrm{e}^{\mu}\mathbb{M}_1 + \mathrm{e}^{-\mu}\mathbb{M}_{-1} \tag{58}$$

where $\mathbb{M}_0$ is the matrix of the diagonal of $\mathbb{M}$, and $\mathbb{M}_1$ ($\mathbb{M}_{-1}$) is a matrix containing the transition rates of particle hopping in the positive (negative) direction. Hence, the statistics of the transported mass has been transformed into an eigenvalue problem. The deformed matrix $\mathbb{M}(\mu)$ can be diagonalized by the Bethe ansatz by solving the following Bethe ansatz equations:

$$z_i^L = (-1)^{N-1}\prod_{j=1}^{N}\frac{q\mathrm{e}^{-\mu}z_iz_j - (p+q)z_i + pe^{\mu}}{q\mathrm{e}^{-\mu}z_iz_j - (p+q)z_j + pe^{\mu}}. \tag{59}$$

The corresponding eigenvalues are given by

$$E(\mu; z_1, z_2 \ldots z_N) = pe^{\mu}\sum_{i=1}^{N}\frac{1}{z_i} + q\mathrm{e}^{-\mu}\sum_{i=1}^{N}z_i - N(p+q). \tag{60}$$

For $\mu = 0$ we know that the largest eigenvalue is 0. For $\mu \neq 0$ the cumulant generating function corresponds to the continuation of this largest eigenvalue (the existence of this continuation, at least for small values of μ is guaranteed by the Perron–Frobenius theorem).

We remark that equations (59) and (60) are invariant under the transformation

$$\begin{aligned} z &\to \frac{1}{z} \\ \mu &\to \mu_0 - \mu \qquad \text{with } \mu_0 = \log\frac{q}{p}. \end{aligned} \tag{61}$$

This symmetry implies that the spectra of $\mathbb{M}(\mu)$ and of $\mathbb{M}(\mu_0 - \mu)$ are identical. This functional identity is in particular satisfied by the largest eigenvalue of $\mathbb{M}$ and we have

$$E(\mu) = E(\mu_0 - \mu). \tag{62}$$

Using the fact that the LDF $G(j)$ is the Legendre transform of $E(\mu)$, we obtain the canonical form of the *fluctuation theorem* (or Gallavotti–Cohen relation)

$$G(j) = G(-j) - \mu_0 j. \tag{63}$$

We observe that in the present context this relation manifests itself as a symmetry of the Bethe equations. However, it is satisfied by a large class of systems far from equilibrium [71–73]. The validity of the fluctuation theorem does not rely on the integrability of the system and it can be proved for Markovian or Langevin dynamical systems using time-reversal symmetry [75, 76] as well as measure-theoretic considerations [159, 160].

The complete calculation of the current statistics in the ASEP is a difficult problem that required more than a decade of effort. The breakthrough was the solution of the TASEP, by Derrida and Lebowitz in 1998 [140]. These authors obtained the following parametric representation of the function $E(\mu)$ in terms of an auxiliary parameter B:

$$E(\mu) = -N\sum_{k=1}^{\infty}\binom{kL-1}{kN}\frac{B^k}{kL-1} \tag{64}$$

where $B(\mu)$ is implicitly defined through

$$\mu = -\sum_{k=1}^{\infty}\binom{kL}{kN}\frac{B^k}{kL}. \tag{65}$$

These expressions allow us to calculate the cumulants of Y_t, for example the mean-current J and a 'diffusion constant' D:

$$\begin{aligned} J &= \lim_{t\to\infty}\frac{\langle Y_t\rangle}{t} = \left.\frac{\mathrm{d}E(\mu)}{\mathrm{d}\mu}\right|_{\mu=0} = \frac{N(L-N)}{L-1} \\ D &= \lim_{t\to\infty}\frac{\langle Y_t^2\rangle - \langle Y_t\rangle^2}{t} = \left.\frac{\mathrm{d}^2E(\mu)}{\mathrm{d}\mu^2}\right|_{\mu=0} \\ &= \frac{N^2\,(2L-3)!\,(N-1)!^2\,(L-N)!^2}{(L-1)!^2\,(2N-1)!\,(2L-2N-1)!}. \end{aligned} \tag{66}$$

When $L \to \infty$, $\rho = L/N$, and $|j - L\rho(1-\rho)| \ll L$, the LDF $G(j)$ can be written in the following scaling form:

$$G(j) = \sqrt{\frac{\rho(1-\rho)}{\pi N^3}}H\left(\frac{j - L\rho(1-\rho)}{\rho(1-\rho)}\right) \tag{67}$$

with

$$H(y) \simeq -\frac{2\sqrt{3}}{5\sqrt{\pi}}y^{5/2} \qquad \text{for } y \to +\infty \tag{68}$$

$$H(y) \simeq -\frac{4\sqrt{\pi}}{3}|y|^{3/2} \qquad \text{for } y \to -\infty. \tag{69}$$

The shape of the LDF is skewed: it decays with a $5/2$ power as $y \to +\infty$ and with a $3/2$ power as $y \to -\infty$. For the general case $q \neq 0$ on a ring, the solution was found by rewriting the Bethe ansatz as a functional equation and restating it as a purely algebraic problem [161, 162]. For example, this method allows us to calculate the first two cumulants, J and D:

$$\begin{aligned} J &= \frac{(p-q)}{p}\frac{N(L-N)}{L-1} \sim \frac{(p-q)}{p}L\rho(1-\rho) \\ &\quad \text{for } L \to \infty \\ D &= \frac{(p-q)}{p}\frac{2L}{L-1}\sum_{k>0}k^2\frac{C_L^{N+k}}{C_L^N}\frac{C_L^{N-k}}{C_L^N}\left(\frac{p^k+q^k}{p^k-q^k}\right), \end{aligned} \tag{70}$$

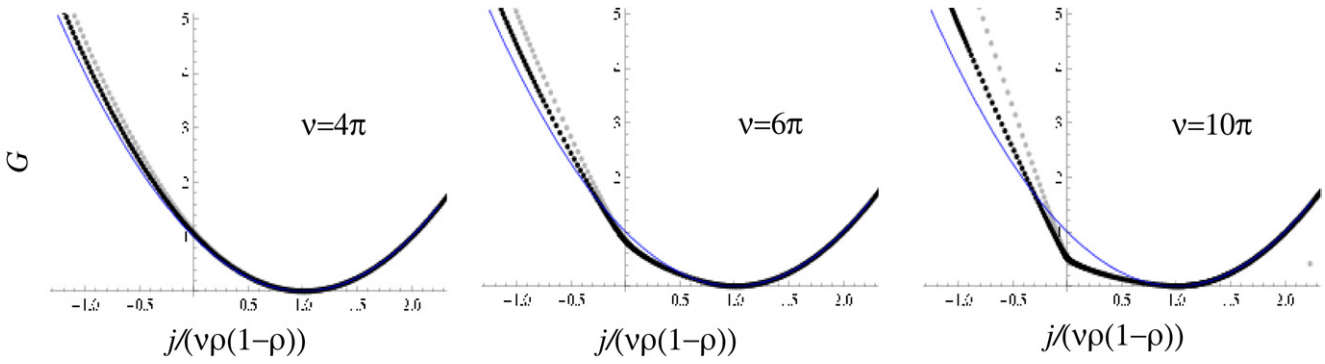

Figure 3. Behavior of the LDF G as a function of the current $j/(\nu\rho(1-\rho))$ for different values of ν. The gray dots correspond to $L = 50$, $N = 25$ and the black dots correspond to $L = 100$, $N = 50$. The curves are formally obtained by numerically solving the Bethe ansatz equations (59) and Legendre transforming $E(\mu)$. The thin blue curve represents the leading Gaussian behavior indicated by equation (73).

where C_L^N are the binomial coefficients. Note that the formula for D was previously derived using the matrix product representation discussed above [163]. Higher cumulants can also be found and their scaling behavior investigated. For ASEP on a ring, the problem was completely solved recently by Prolhac [164], who found a parametric representation analogous to equations (64) but in which the binomial coefficients are replaced by combinatorial expressions enumerating some tree structures. A particularly interesting case [165] is a weakly driven limit defined by $q/p = 1 - \frac{\nu}{L}$, $L \to \infty$. In this case, we need to rescale the fugacity parameter as μ/L and the following asymptotic formula for the cumulant generating function can be derived

$$E\left(\frac{\mu}{L}, 1-\frac{\nu}{L}\right) \simeq \frac{\rho(1-\rho)(\mu^2+\mu\nu)}{L} - \frac{\rho(1-\rho)\mu^2\nu}{2L^2} + \frac{1}{L^2}\phi[\rho(1-\rho)(\mu^2+\mu\nu)] \tag{71}$$

$$\text{with } \phi(z) = \sum_{k=1}^{\infty} \frac{B_{2k-2}}{k!(k-1)!} z^k \tag{72}$$

and where B_js are Bernoulli numbers. We observe that the leading order (in $1/L$) is quadratic in μ and describes Gaussian fluctuations. It is only in the subleading correction (in $1/L^2$) that the non-Gaussian character arises. This formula was also obtained for the symmetric exclusion case $\nu = 0$ in [166]. We observe that the series that defines the function $\phi(z)$ has a finite radius of convergence and that $\phi(z)$ has a singularity for $z = -\pi^2$. Thus, non-analyticities appear in $E(\mu, \nu)$ as soon as

$$\nu \geqslant \nu_c = \frac{2\pi}{\sqrt{\rho(1-\rho)}}.$$

By Legendre transform, non-analyticities also occur in the LDF $G(j)$ defined in (57). At half-filling, the singularity appears at $\nu_c = 4\pi$ as can be seen in figure 3. For $\nu < \nu_c$ the leading behavior of $G(j)$ is quadratic (corresponding to Gaussian fluctuations) and is given by

$$G(j) = \frac{(j-\nu\rho(1-\rho))^2}{4L\rho(1-\rho)}. \tag{73}$$

For $\nu > \nu_c$, the series expansions (71) and (72) break down and the LDF $G(j)$ becomes non-quadratic even at leading order. This phase transition was predicted by Bodineau and Derrida using macroscopic fluctuation theory [167–169]. These authors studied the optimal density profile that corresponds to the total current j over a large time t. They found that this optimal profile is flat for $j < j_c$ but it becomes linearly unstable for $j > j_c$. In fact, when $j > j_c$ the optimal profile is time dependent. The critical value of the total current for which this phase transition occurs is $j_c = \rho(1-\rho)\sqrt{\nu^2 - \nu_c^2}$ and therefore one must have $\nu \geqslant \nu_c$ for this transition to occur. One can observe in figure 3 that for $\nu \geqslant \nu_c$, the LDF $G(j)$ becomes non-quadratic and develops a kink at a special value of the total current j.

Bethe ansatz for other systems out of equilibrium. We have discussed in this review the Bethe ansatz for a system on a periodic ring where the total number of particles is a conserved quantity. It is possible to extend the Bethe ansatz for the finite ASEP with open boundaries in which the total number of particles is not constant. The resulting Bethe equations have a more complicated structure; they have been thoroughly analyzed in a series of papers by de Gier and Essler [153, 170, 171] who calculated the spectral gaps in the different phases of the open ASEP. In particular, they discovered sub-phases in the phase diagram that could not be predicted from the steady-state measure alone. We note that the Bethe ansatz can be applied to variants of the ASEP, such as models with impurities [141], multispecies exclusion processes [172–174] as the zero-range process [175], the raise and peel model [125], vicious walkers [176], or the Bernoulli matching model of sequence alignment [177, 178].

3.10. ASEP on an infinite lattice: Bethe ansatz and random matrices

In this last subsection, we briefly review some important analytical results that have been obtained for exclusion processes on an infinite line, especially in connection with the Bethe ansatz method discussed above. This will allow us to derive some insight into the dynamics of the system. More detailed results and historical discussions can be found in the literature cited in the text.

We first consider the case of the ASEP on the infinite lattice $\mathbb{Z}$ but with only a *finite* number N of particles. Because the particles cannot overtake one another, the ordering of the particles is conserved by the dynamics, and we can label the particles from right to left. Suppose that at $t = 0$, the particles are located at positions $y_1 > \cdots > y_N$ and at some later time t, they are located at $x_1 > \cdots > x_N$.

The transition probability, $P(x_1, \ldots, x_N, t|y_1, \ldots, y_N, 0)$, for reaching the final configuration $x_1, \ldots, x_N$ at t starting from $y_1, \ldots, y_N$ at $t = 0$, has the following exact expression:

$$P(x_1, \ldots, x_N, t|y_1, \ldots, y_N, 0) = \sum_{s\in S_N} \prod_{k=1}^{N} \oint_{C_R} \frac{\mathrm{d}z_k}{2\pi \mathrm{i} z_k} A_s(\{z\}) \mathrm{e}^{(\frac{p}{z_k}+qz_k-1)t} z_{s(k)}^{x_k-y_{s(k)}}. \quad (74)$$

The crucial observation is that there exists a closed formula for the amplitude A_s, given by

$$A_s(\{z\}) = \mathrm{sgn}(s) \frac{\prod_{i<j}(p + qz_{s(i)}z_{s(j)} - z_{s(i)})}{\prod_{i<j}(p + qz_iz_j - z_i)} \quad (75)$$

where we use the convention $p + q = 1$. The expressions (74) and (75) are reminiscent of the formulae given by the Bethe ansatz. These results were initially derived for the TASEP on $\mathbb{Z}$ by Schütz in 1997, who constructed them from the Bethe ansatz [147] and then proved rigorously that equation (74) solves exactly the time-dependent Markov equation with the correct initial condition (generalized to the periodic case by Priezzhev in [148, 149]). The general result for the ASEP was found by Tracy and Widom in 2008 [179] and has motivated many studies in the last few years. Equation (74) is a seminal result: it is an exact expression for the Green function of the ASEP from which, in principle, individual particle distributions and correlations functions can be extracted (this can be an extremely difficult task in practice). Finally, we emphasize that the 'Bethe roots' z_i are not quantified in the infinite system: each of them takes a continuous set of values along the circular contour C_R of radius R, so small that the poles of $A_s(\{z\})$ lie outside C_R.

To give one specific example, consider the *totally* asymmetric exclusion with unit hopping rate $p = 1$ (and $q = 0$) and with a *step initial condition*, where all sites right of the origin ($i > 0$) are empty and all to the left ($i \leqslant 0$) are occupied. If we are interested in the behavior of *only* the right most N particles after time t, then we can replace the semi-infinite string by a finite segment of N particles. The point is, in a TASEP, none of the particles hops to the left and so particles to the left of our N-particle string cannot affect their behavior. Thus, it is sufficient to consider $P(x_1, \ldots, x_N, t|y_1 = 0, \ldots, y_N = 1 - N, 0)$. Now, suppose we ask a more restricted question: what is $\tilde{P}(M, N, t)$, the probability that the Nth particle (initially located at $i = 1-N$), has performed at least M hops by time t? In terms of P, we write

$$\tilde{P}(M, N, t) = \sum_{\substack{x_1 > \ldots > \\ x_N > M - N}} P(x_1, \ldots, x_N, t|y_1 = 0, \ldots, y_n = 1 - N, 0). \quad (76)$$

We next exploit a determinantal representation, analogous to (53) and (54) for ψ, and express P as

$$P(x_1, \ldots, x_N, t|y_1, \ldots, y_N, 0) = \det(\mathbb{B}) \quad (77)$$

where $\mathbb{B}$ is an $N \times N$ matrix with elements

$$B_{ij} = \oint_{C_R} \frac{\mathrm{d}z}{2\pi \mathrm{i} z} z^{x_i-y_j}(1 - z)^{j-i} \mathrm{e}^{(\frac{1}{z}-1)t} \quad \text{for } 1 \leqslant i, j \leqslant N. \quad (78)$$

After some calculation [180], these equations allow us to express $\tilde{P}(M, N, t)$ compactly:

$$\tilde{P}(M, N, t) = \frac{1}{Z_{M,N}} \int_{[0,t]^N} \mathrm{d}^N x \prod_{1\leqslant i<j\leqslant N} (x_i - x_j)^2 \times \prod_{j=1}^{N} x_j^{M-N} \mathrm{e}^{-x_j}. \quad (79)$$

where $Z_{M,N}$ is a normalization factor. The integral on the right-hand side has a direct interpretation in random matrix theory: it is the probability that the largest eigenvalue of the random matrix $\mathbb{A}\mathbb{A}^\dagger$ is less than or equal to t, with $\mathbb{A}$ being an $N \times M$ matrix of complex random variables with zero mean and variance $1/2$ (unitary Laguerre random matrix ensemble).

Finally, we note that $\tilde{P}(N, N, t)$ can also be interpreted as the probability that the integrated current Q_t through the bond (0,1) is at least equal to N (Q_t is the number of particles that have crossed the bond (0,1) between time 0 and t). From the classical Tracy–Widom laws for the distribution of the largest eigenvalue of a random matrix [181], one can write

$$Q_t = \frac{t}{4} + \frac{t^{1/3}}{2^{4/3}}\chi \quad (80)$$

where the distribution of the random variable χ is given by

$$\mathrm{Prob}(\chi \leqslant s) = 1 - F_2(-s). \quad (81)$$

The Tracy–Widom function $F_2(s)$ is the cumulative distribution of the maximum eigenvalue λ_{max} in the Gaussian unitary ensemble (self-adjoint Hermitian matrices), i.e.

$$\mathrm{Prob}\left(\frac{\lambda_{\max} - \sqrt{2N}}{(8N)^{-1/6}} \leqslant s\right) = F_2(s) \quad (82)$$

where $N \gg 1$ represents here the size of the random matrix. Exact expressions for $F_2(s)$ can be found, for example, in [182]. This crucial relation between random matrix theory and the asymmetric exclusion process, first established by Johansson in 2000 [183], has stimulated many works in statistical mechanics and probability theory (see, e.g., [184–186]). The mathematical study of the infinite system has grown into a subfield *per se* that displays fascinating connections with random matrix theory, combinatorics and representation theory. We note that Johansson did not use the Bethe ansatz in his original work. He studied a discrete-time version of the TASEP in which the trajectories of the particles were encoded in a waiting-time matrix, which specifies how

long a given particle stays at each given site. This integer-valued matrix can be mapped via the Robinson–Schensted–Knuth correspondence into a Young tableau. The value of the total current through the bond (0,1) is linearly related to the length of the longest line of this Young tableau. The statistics of the length of the longest line can be found using asymptotic analysis techniques *à la* Tracy–Widom. In fact, a closely related question, the classical Ulam problem of the longest increasing subsequence in a random permutation, was solved a few years earlier by Baik *et al* using related methods [187].

Very recently, in a series of papers [179, 188–191], Tracy and Widom have generalized Johansson's results to the partially asymmetric exclusion process by deriving some integral formulae for the probability distribution of an individual particle starting from the step initial condition. These expressions can be rewritten as a single integral involving a Fredholm determinant that is amenable to asymptotic analysis. In particular, a limit theorem is proved for the total current distribution. Going from TASEP to ASEP is a crucial progress because the weakly asymmetric process leads to a well-defined continuous limit: the KPZ equation, a universal model for surface growth. Indeed, a very important outgrowth of these studies is the exact solution of the KPZ equation in one dimension. The distribution of the height of the surface at any finite time is now known exactly (starting from some special initial conditions), solving a problem that remained open for 25 years: a description of the historical development of these results and the contributions of the various groups can be found in [186, 192–199]. One important feature to keep in mind is that the results (and therefore the universality class) depend strongly on the chosen initial conditions. Lately, n-point correlation functions of the height in KPZ have also been exactly derived by Spohn and Prolhac [200, 201]. For an overview of these fascinating problems, we recommend the paper by Kriecherbauer and Krug [182], and the reviews by Aldous and Diaconis [202] and Corwin [203].

3.11. Hydrodynamic mean-field approach

Although elegant and rigorous, the methods presented above cannot be applied to systems much more complex than the TASEP. Typically, further progress relies on a very successful approach, based on the mean-field approximation and a continuum limit, leading to PDEs for various densities in the system. Known as the hydrodynamic limit, such equations can be 'derived' from the master equation (14). The strategy starts with the exact evolution equation for $\rho_i(t) \equiv \langle \sigma_i \rangle_t = \sum_{\mathcal{C}} \sigma_i P(\mathcal{C}, t)$. Differentiating this $\rho_i(t)$ with respect to t and using equation (14), we see that new operators appear:

$$\mathcal{O}(\mathcal{C}') = \sum_{\mathcal{C}} \sigma_i(\mathcal{C}) M(\mathcal{C}, \mathcal{C}'). \tag{83}$$

In the case of ASEP, $M(\mathcal{C}, \mathcal{C}')$ is sufficiently simple that the sum over $\mathcal{C}$ can be easily performed, leaving us with products of σs (associated with configurations $\mathcal{C}'$). Applying the mean-field approximation (equation (17)), the right-hand side now consists of products of $\rho_i(t)$ and $\rho_{i\pm1}(t)$.

Taking the thermodynamic and continuum limit, we let $i, L \to \infty$ with finite $x = i/L$ and write $\rho_i(t) \simeq \rho(x, t)$. Next, we expand $\rho_{i\pm1}(t) \simeq \rho(x, t) \pm \varepsilon \partial_x \rho + (\varepsilon^2/2)\partial_x^2 \rho + \ldots$, where $\varepsilon \equiv 1/L \to 0$. The result is a hydrodynamic PDE for the particle density [124]:

$$\frac{\partial \rho(x,t)}{\partial t} = \varepsilon \frac{\partial}{\partial x}[(q-p)\rho(1-\rho)] + \frac{\varepsilon^2}{2}\frac{\partial}{\partial x}\left[(1-\rho)\frac{\partial}{\partial x}[(p+q)\rho] + (p+q)\rho\frac{\partial \rho}{\partial x}\right] \tag{84}$$

where $\varepsilon \equiv 1/L \to 0$. Note that even slow variations in the hopping rates ($p_i \to p(x)$ and $q_i \to q(x)$) can be straightforwardly incorporated [204]. Analogous hydrodynamic equations have also been derived for ASEPs with particles that occupy more than one lattice site [205–207]. In addition to spatially slowly varying hopping rates, this approach is useful for exploring more complex models, e.g. a TASEP with particles that can desorb and/or attach to every site (section 4.2). Of course, such equations are also the starting point for very successful field theoretic approaches to dynamic critical phenomena near-equilibrium [208–211] as well as ASEPs (even with interacting particles) in higher dimensions [212–217]. Supplemented with noise terms, these become Langevin equations for the density or mangnetization fields. Then, fluctuations and correlations can be computed within, typically, a perturbative framework.

Returning to equation (84), it is especially easy to analyze in the steady-state limit where the resulting equation is an ODE in x. But, the highest power of ε multiplies the largest derivative, so that we are dealing with 'singularly perturbed' differential equations [124–219]. The solutions for the steady-state mean-field density $\rho(x)$ consist of 'outer solutions' that hold in the bulk, matched to 'inner solutions' corresponding to boundary layers of thickness ε at the open ends. For the ASEP, this approach correctly determines the phase boundaries and the self-consistently determined steady-state current J (which arise both in the integration constant of equation (84) and in the boundary conditions). However, as anticipated, the density profiles are not exactly determined, even when $L \to \infty$. Nevertheless, for more realistic physical models such as the ones to be discussed in the next section, such a mean-field approach (or one of its variants) is often the only available analytical method at our disposal.

4. Biological and related applications of exclusion processes

In this section, we review a number of applications of stochastic exclusion models to problems of transport in materials science, cell biology and biophysics. While quantitative models of these real-world applications often require consideration of many microscopic details (and their corresponding parameters), simple one-dimensional lattice models nonetheless can be used to capture the dominant mechanisms at play, providing a succinct representation of the system. Moreover, these types of models can be extended in a number of ways, and are amenable to concise analytic

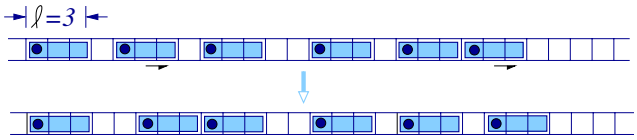

Figure 4. An interior section of an asymmetric exclusion process with extended particles of size $\ell = 3$. The individual particles occlude three of the lattice sites on which the hops occur.

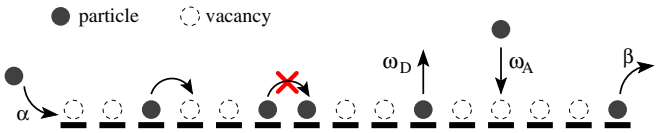

Figure 5. A TASEP with Langmuir kinetics where particles can spontaneously detach and attach at every site with rates ω_D and ω_A, respectively. Adapted from [221].

solutions. As we will see, the application of lattice models to complex biophysical systems is aided by a few main extensions and modifications to the TASEP presented above. These modified dynamics are illustrated, respectively, by figures 4–9.

(i) *Longer-ranged interactions.* Objects represented by particles in an exclusion process may have molecular structure that carry longer-ranged particle–particle interactions. For example, to model ribosomes on an mRNA or cargo-carrying molecular motors, we should use large particles taking small discrete steps and introduce a rule beyond on-site exclusion. We may regard these as 'extended particles' that occlude $\ell > 1$ lattice sites (figure 4).

(ii) *Particle detachment and attachment.* Particles such as molecular motors have finite processivity. That is, they can spontaneously detach from their lattices before reaching their destination. Conversely, particles in a bulk reservoir can also attach at random positions on the lattice. The coupling of the particle number to a bulk reservoir is analogous to the problem of Langmuir kinetics [219, 220] on a one-dimensional lattice, except that the particles are directionally driven on the substrate (figure 5).

(iii) *Multiple species.* Usually, biological transport involves multiple interacting species in confined geometries, often one-dimensional in nature. For example, these secondary species may represent particles that are co-transported or counter-transported with the primary particles, or, they may represent species that bind to pores and regulate primary particle transport [222](figure 6).

(iv) *Partial exclusion and coupled chains.* Often, the strict one-dimensional nature of the exclusion dynamics can be relaxed to account for particles that, while strongly repelling each other, can on occasion pass over each other. This scenario might arise when pores are wide enough to allow particle passing. Related extensions of single-chain exclusion processes are exclusion processes across multiple interacting chains (figure 7).

(v) *Internal states and nonexponentially distributed dwell times.* The physical mechanisms of how excluding particles are inserted, extracted, and hop in the interior of the lattice are often complex, involving many intermediate chemical steps [225, 226]. Therefore, the distribution of times between successive hops, even when unimpeded by exclusion interactions, is often non-exponential. Specific hopping time distributions can be incorporated into lattice particle models by explicitly evolving internal particle states (figure 8).

(vi) *Variable lattice lengths.* The lattices on which the exclusion processes occur may not be fixed in some settings. A dynamically varying length can arise in systems where growth of the lattice is coupled to the

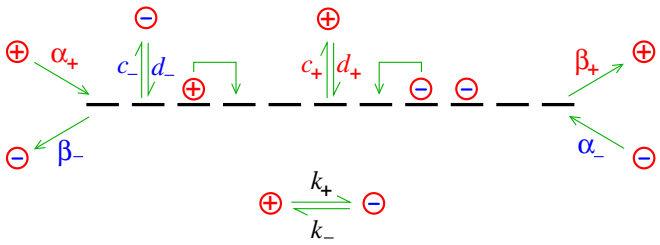

Figure 6. A two-species exclusion model, adapted from [223], where + and − particles move in opposite directions but can interconvert with rate $k_\pm$. Attachment and detachment are also allowed with rates $c_\pm$ and $d_\pm$, respectively.

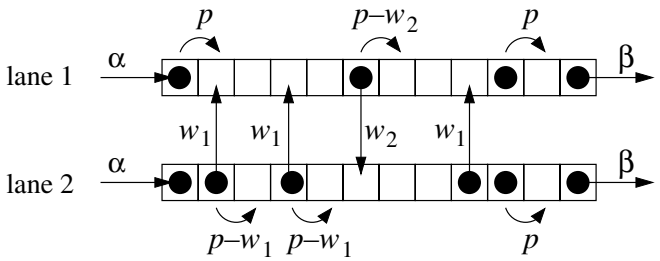

Figure 7. Two coupled TASEP lattices with interchain hopping rates w_1 and w_2. Adapted from [224].

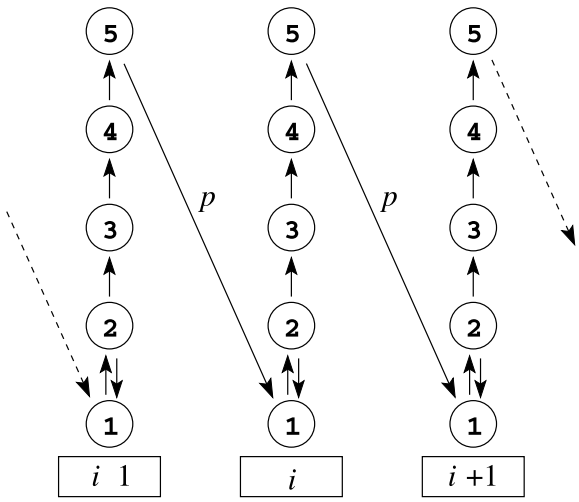

Figure 8. Internal states (1–5) that determine the timing between particle hops (adapted from [226]). Here, a linear sequence of Poisson processes generates a Gamma-distributed [227] interhopping time distribution (dwell time). This model for the internal dynamics has been used to model mRNA translation by ribosome enzymes.

transport of particles to the dynamically varying end of the lattice [228–231]. While no exact solutions have been found, mean-field and hydrodynamic approaches have been successfully applied [232]. In the continuum limit, this problem is analogous to the classic Stefan problem [232, 233], except with nonlinear particle density dynamics (figure 9).

Not surprisingly, the techniques presented in the previous section are typically not powerful enough for obtaining exact results for these variants of the basic exclusion processes. Of course, for sufficiently small systems (e.g. $L \lesssim 10$), high performance computers can be used to diagonalize $\mathbb{M}$, but that method is not viable for many physical or biological systems. There are also some cases, including special cases of two-species exclusion and ASEP with extended particles on a ring (to be discussed below, within their own contexts), where exact solutions can be found for all L. Despite the lack of progress in finding analytic results, there are two other approaches which provide valuable insights into these more complex yet more realistic systems. One is computer simulations, exploiting Monte Carlo techniques on our lattice models. Once the stochastic rules of a model are specified, then, this technique corresponds to implementing equation (1). In addition, molecular-dynamics (MD) simulations with off-lattice systems also proved to be very successful. The other approach is based on designing good approximation schemes for attacking exact equations (or expressions for specific quantities). MFT, or mean-field *approximation*, is most often used. An example is equation (17) for the TASEP. However, systematically improving these generalizations is not generally straightforward. Thus, we will see that, for TASEP with extended objects, the substitution (17) is very poor (when compared with simulation results). Instead, a more sophisticated scheme, implemented by Gibbs and co-workers [13, 14], is much more successful at predicting, say, the average current. In turn, when this scheme fails to predict other quantities, another level of approximation [103] (in the spirit of the Bethe–Williams approximation for the Ising model) is needed. Nevertheless, if the predictions are in good agreement with simulations, the MFT provides some confidence that we are 'on the right track' toward our goal: understanding these generalized ASEPs which have found wide applicability in modeling complex biological processes.

4.1. Pore transport

Transport of atoms and small molecules arises in both man-made structures and cell biological systems. Materials such as zeolites form networks of one-dimensional channels within which molecules, such as light hydrocarbons, can pass through and/or react. A number of authors have used exclusion processes as simple descriptions of single-file or near single-file transport. It has long been known that tracer diffusion in single-file channels follows subdiffusive dynamics [97, 234–237]. A mean-square displacement of the form $\langle x^2 \rangle \sim \sqrt{t}$ is found by considering equilibrium fluctuations of the density around the tagged particle in an infinite system. For steady-state particle transport across finite pores, the lattice

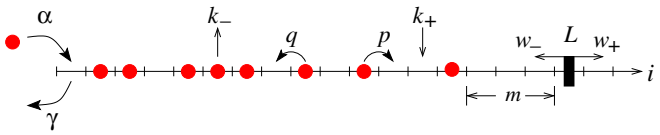

Figure 9. Schematic of an ASEP (adapted from [232]) with detachment and attachment rates k_- and k_+, respectively, and a 'confining' wall at site L. The wall has intrinsic dynamics described by hopping rates $w_\pm$.

exclusion process has proved a more useful starting point. Given the frequent application of exclusion processes to pore transport, two important points should be stressed.

First, the standard lattice exclusion process assumes that waiting times are exponentially distributed and, other than lattice site exclusion, are independent. This assumption can fail if, say, an attractive interaction between particles is comparable to the interaction between substrate (e.g. atoms that make up the pore walls) and the particles. Here, concerted motion can arise and has been shown to be important in particle transport. For example, Sholl and Fichthorn have shown using MD simulations how concerted motions of clusters of water affects its overall transport in molecular sieves [238]. Similarly, Sholl and Lee also showed that concerted motions of clusters of CF_4 and Xe in $AlPO_4$-5 and $AlPO_4$-31 zeolites, respectively, contribute significantly to their overall mobilities [239]. Concerted motion has also been predicted to occur in transport across carbon nanotubes [240]. These concerted motions arise from frustration due to a mismatch between particle–particle and particle–pore interaction ranges, allowing for a lower barrier of motion for bound pair of particles that for an isolated, individual particle. Although concerted motion arises from geometrically complicated arrangements of particles that form low energy pathways in the high-dimensional energy landscapes, if a small number of these pathways support most of the probability flux, simplifying assumptions can be made. For example, coarse-grained treatments of concerted motion were developed by Sholl and Lee [239]. Concerted motion has also been incorporated within lattice models of exclusion processes in a more severe manner. Gabel, Krapivsky and Redner have formulated a 'facilitated exclusion' process on a ring whereby a particle hops forward to an empty site *only* if the site behind it is also occupied [241]. They find a maximal current of $3 - 2\sqrt{2}$ which is less than the maximal current of $1/4$ arising in the standard TASEP. A model that incorporates concerted motion might be described by a facilitated exclusion model where motion in either direction occurs faster if the particle is adjacent to another one. The hopping rate might also be increased if an isolated particle moves to a site that results in it having an additional adjacent particle. If these accelerated steps occur much faster than individual particle hops, then the dynamics will resemble motion of pairs of particles. It would be interesting to determine how this model of near-concerted hops increase the overall particle flux.

A second important point to emphasize is that different physical systems are best modeled with varying degrees of asymmetry in the exclusion processes. Two extreme limits

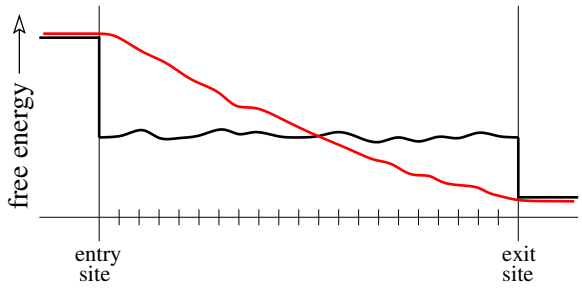

Figure 10. Representative single-particle, one-dimensional free energy landscapes over which excluding particles travel. The black curve free energy profile could represent a symmetric exclusion process, while the red landscape would describe an asymmetric exclusion processes. In the former, detailed balance is assumed to be violated at the entrance and exit sites and the particle flux is driven by differences between the chemical potentials of the two reservoirs.

are the totally asymmetric process, where particles only hop in one direction, and symmetric exclusion, where particle hopping between any two adjacent sites obeys detail-balance. In this case, detailed balance is violated only at the two ends of the lattice. Net particle current arises only when there exists an asymmetry in the injection and extraction rates at the two ends. This latter scenario corresponds to boundary-driven exclusion processes where differences in the chemical potential of the particles in the two reservoirs drive the flux. Osmotic and pressure-driven flows (when local equilibrium thermodynamics holds and particle inertia is negligible) are examples of processes best described using *symmetric* exclusion processes [242]. However, when particles in the lattice are charged, and an external field is applied, the internal jumps are asymmetric since there is a direct force acting on the particles, breaking detailed balance. A heuristic delineation between asymmetric and symmetric (boundary-driven) exclusion processes can be motivated by considering the *single-particle* free energy profiles. Figure 10 depicts two hypothetical single-particle free energy profiles experienced by an isolated particle under local thermodynamic equilibrium.

In biological systems, channels that transport water and neutral (e.g. sugars) or charge-screened molecules can be described by symmetric exclusion, while motion of charged ions in single-file channels would be best characterized by partially asymmetric exclusions. Modeling uncharged particles allows equal internal hopping rates ($p = q$) with drive originating only at the boundaries. The steady-state current is easily found and is a function of the asymmetry in the boundary injection and extraction rates [242, 243]

$$J = \frac{p(\alpha\beta - \gamma\delta)}{(L-1)(\alpha+\delta)(\beta+\gamma) + p(\alpha+\beta+\gamma+\delta)}. \qquad (85)$$

The boundary injection and extraction rates are those defined in figure 1(*c*). As expected, this expression for J is similar to that arising from simple diffusive flux in the $L \to \infty$ limit. However, as discussed, non-trivial current fluctuations, which cannot be accounted for by simple diffusion, have also been worked out [161, 162, 164, 244, 245].

When particles are 'charged', the level of asymmetry (the relative difference between an ion hopping forward and hopping backward) is controlled by the magnitude of the externally applied 'electric field'. In addition to the exact solutions for the steady-state current [125], cumulants of the current in a weakly asymmetric exclusion process have also been derived [165], the slowest dynamic relaxation mode computed [171], and the tracer diffusivity derived [163].

Specific biological realizations of driven transport include ion transport across ion channels [242], while transport across nuclear pore complexes (NPCs) [246, 247], and osmosis [248] are typically boundary-driven, or ratcheted (see the section on molecular motors).

In 1998, the x-ray crystal structure of the K^+ ion channel was published[8], allowing a more detailed mechanistic understanding of the ion conduction and selectivity across a wide class of related, and biologically important, ion channels [249]. The crystal structure showed three approximately in-line vestibules that can each hold one K^+ ion. Representations of the voltage-gated Kv1.2 channel are shown in figure 11. Ion conduction can thus be modeled by a simple three-site partially asymmetric exclusion process provided the hopping rates at each occupation configuration are physically motivated [248, 250, 251]. However, note that there is evidence that ion dynamics within some ion channels is 'concerted' because the free energy barriers between ion binding sites are small and ions entering an occupied channel can knock the terminal ion out of the channel. This 'knock-on' mechanism [252] has been motivated by MD simulations [253, 254] and studied theoretically via a reduced one-dimensional dynamical model [255].

The symmetric exclusion process has also been used to consider osmotic flow across membrane-spanning, single-file channels [248]. Here, the solvent flux is driven by differences in the injection rates at the two pore ends connected to two separate particle reservoirs. Simple osmosis across a strictly semipermeable membrane can be described by a single species symmetric exclusion process where the injection rate of the solvent from one of the reservoirs is reduced due to its smaller mole fraction arising from the presence of solute in that reservoir [248]. The solvent current is approximately linearly proportional to the difference in injection rates at the two ends of the lattice, inversely proportional to the length of the lattice, but with a weak suppression due to multiple pore occupancy [242].

Another transport channel in cells is nuclear NPCs, responsible for the selective shuttling of large molecules and proteins (such as transcription factors, histones, ribosomal subunits) through the double nuclear membrane. Exclusion processes have been employed as theoretical frameworks for describing the efficiency and selectivity NPC transport [247, 256].

In all of the above applications, extensions exploiting multispecies exclusion processes are often motivated. In biological systems ion transport is typically 'gated' by cofactors that bind to the pore, either blocking ion transport, or inducing a conformational change in the pore structure

[8] This achievement was partially responsible for Peter Agre and Roderick MacKinnon being awarded the Nobel Prize in Chemistry in 2003, 'for discoveries concerning channels in cell membranes.'

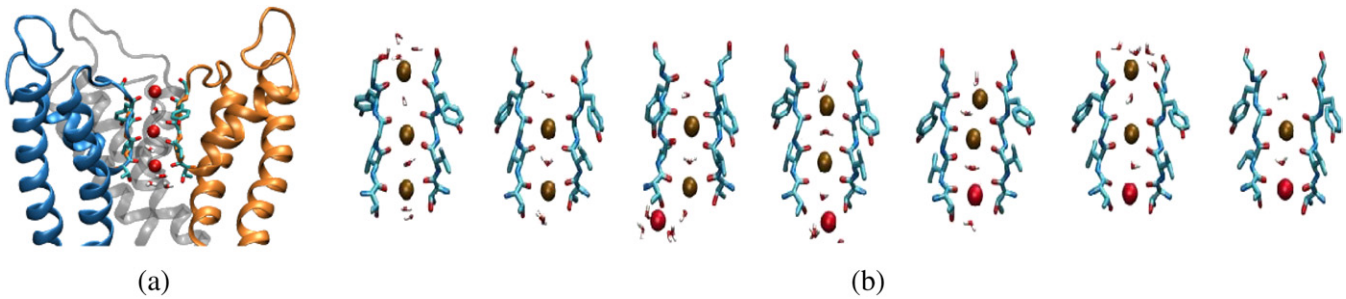

Figure 11. (*a*) A ribbon figure of the Kv1.2 voltage-gated potassium ion channel embedded in a model lipid membrane. The pore structure clearly shows three dominant interior binding sites. This potassium channel image was made with VMD and is owned by the Theoretical and Computational Biophysics Group, NIH Resource for Macromolecular Modeling and Bioinformatics, at the Beckman Institute, University of Illinois at Urbana-Champaign. (*b*) A time series of an MD simulation suggesting a concerted 'knock-on' mechanism. Image adapted from [254] with original labels removed, and used with their permission.

thereby affecting the entrance, exit, and internal hopping rates [222]. The inclusion of additional species of particles in the exclusion process has been used to describe 'transport factor' mediated nuclear pore transport [246, 247, 256]. For osmosis, solutes that are small enough to enter membrane pores may also interfere with the transport of solvent particles through channels. The solvent and solute species would have different entry, exit, and internal hopping rates, describing their different interactions with the pore. In [248], a simple two-species, three-site, partially asymmetric exclusion model was used to show how solutes that can enter a pore and suppress solvent flux. Moreover, it was found that a small amount of slippage (passing of the solvent and solute particles over each other) and a pore that was slightly permeable to solute can very effectively shunt osmotic flow. When both solute and solvent can pass through the channel (with equal forward and backward hopping rates in the interior), an interesting possibility arises whereby the flux of one of the species can drive the other species from its low concentration reservoir to the high concentration reservoir. Since the mechanism relies on entrainment of particles that are driven up its chemical potential, slippage between the pumping and convected particles destroys this entropic pumping mechanism. The efficiency of using a pumping particle that travels from high chemical potential reservoir to low chemical potential reservoir to pump the secondary particle was found using Monte-Carlo simulations [257].

An even more interesting application of multispecies exclusion processes to biological transport arises when the transported ion is a proton. In addition to regulating ionic concentrations, pH regulation is an important aspect of cellular function. It has been known for quite some time that the diffusivity of protons is about an order of magnitude faster than that of small cations [259, 260]. The physical mechanism invoked to explain accelerated motion of protons is based on a proton transfer or shuttling mechanism, analogous to electronic conduction. For a simple ion to traverse a narrow ion channel, it must shed its hydration shell and push any possible water molecules ahead of it within the pore. An extra proton, however, can hop along an oxygen 'backbone' of a line of water molecules, transiently converting each water molecule it visits into a hydronium ion H_3O^+. The Grotthuss mechanism of proton conduction has been conjectured to occur across many narrow pores, including those in gramicidin-A

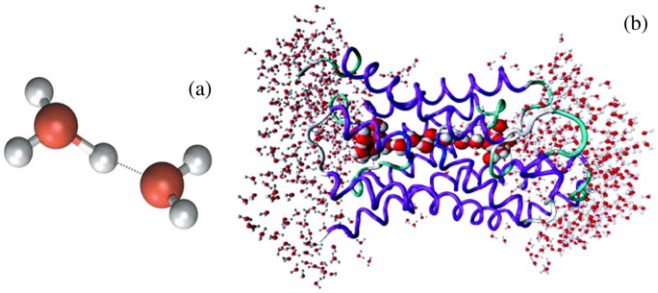

Figure 12. (*a*) Schematic of the Grotthuss proton transfer mechanism. (*b*) An MD simulation showing the persistence of a 'water wire' within a membrane-spanning Aquaporin-1 water channel protein [258]. The waters within the pore are shown magnified.

channels [261, 262], proton transfer enzymes such as carbonic anhydrase [263], voltage-gated proton channels such as Hv1 [264], Aquaporin water channels [258, 265, 266], and carbon nanotubes [267]. All of these structures have in common the existence of a relatively stable water wire as shown on the right of figure 12.

The basic water-wire mechanism can be mapped onto a three-species exclusion model as shown in figure 13.[9] Unlike models where only one extra proton is allowed in the channel at any given time [270], the general exclusion model allows each site to be in one of three states, protonated, water lone-pair electrons pointing to the left and to the right. In this particular application, no exact results are known, but mean-field treatments have been used to extract qualitative phenomena [268, 269]. For example, in order to sustain a steady-state proton current, the lone-pair electrons of a water molecule need to flip in order to relay successive protons. Not only was proton conduction found to be mediated by water flipping, but nonlinear effects such as saturation at high voltages and even negative differential resistances were exhibited by the model [268, 269].

The issue of concerted motions and precise definitions of the proton carrier species also arises in more detailed

[9] We caution the reader that the usage of '*M* species' in the literature is not uniform or unique. Thus, 'three species' here refers to three types of particles on the lattice, *without* holes. Thus, in terms of states at each site, it is the same as the 'two species' model describing solvent, solute, and holes at each site.

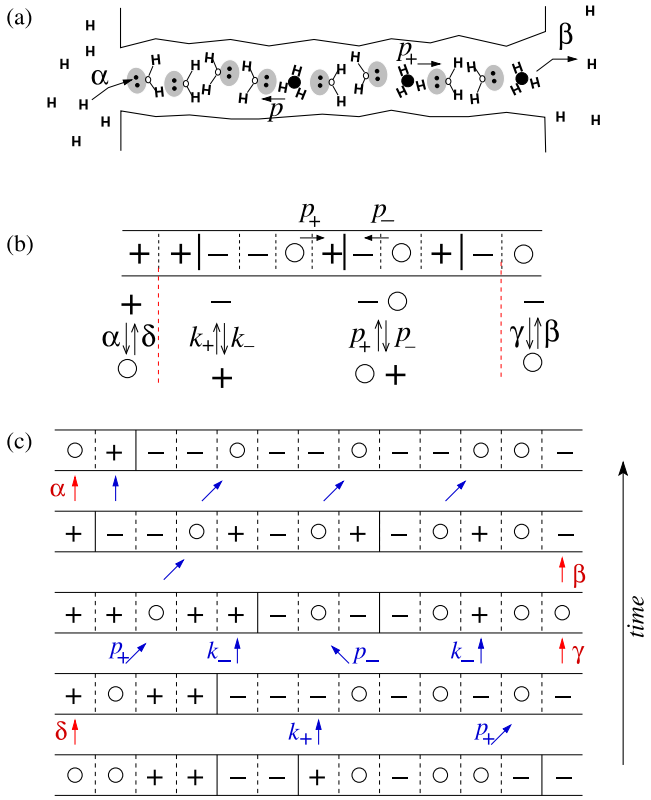

Figure 13. (*a*) A cartoon of water-wire proton conduction. Hydrogen atoms and lone electron pairs of the water oxygen are shown. (*b*) A lattice model for the Grotthuss proton conduction mechanism. The symbols ○, + and − correspond to hydronium ions, water with lone pair pointing to the left, and water with lone electron pair pointing to the right, respectively. Proton movement from left to right leaves the donor site in a − configuration and can occur only if the receptor site is originally in the + configuration. The spontaneous left-right water flipping rates are $k_\pm$ and the proton forward and backward hopping rates (assuming a compatible configuration) are $p_\pm$. (*c*) A time-sequence of a trajectory of configurations. Figures adapted from [268, 269].

considerations of proton transport. There has been considerable effort devoted to identifying the precise molecular species that solvates and relays the protons [271]. Moreover, there is some evidence that proton dynamics in water wire conduction may be concerted [263]. Nonetheless, the three-species exclusion model and its potential extensions are fruitful ways of understanding the gross mechanisms in proton conduction.

4.2. Simple models of molecular motors

Perhaps the simplest models of active biological transport are those of isolated molecular motors that move along one-dimensional tracks such as actin, microtubules, DNA or RNA. Motors are enzymes such as dynein, kinesin and myosin that hydrolyze molecules such as ATP or GTP, turning the free energy released to directed motion along their one-dimensional substrate [272, 273]. Motoring is necessary for sustaining cell functions such as mediating cell swimming and motility and intracellular transport of biomolecules, particularly at length scales where diffusion is not efficient, or where spatial specificity is required. Due to the importance of molecular motors in intracellular transport and cell motility, there is an enormous literature on the detailed structure and chemo-mechanical transduction mechanisms of molecular motors.

From the theoretical physics point of view, molecular motors are useful examples of non-equilibrium systems. Indeed, such motors typically operate far from equilibrium, in a regime where the usual thermodynamic laws do not apply. A molecular motor is kept far from equilibrium by a coupling with some external 'agent' (e.g. a chemical reaction, or a load-force): under certain conditions, work can be extracted, although the motor operates in a medium with constant (body) temperature. We emphasize that there is no contradiction with thermodynamics: the system is far from equilibrium and the motor simply plays the role of a transducer between the energy put in by the agent (e.g. chemical energy) and the mechanical work extracted. Molecular motors have been described theoretically either by continuous ratchet models or by models based on master equations on a discrete space, which are similar to exclusion-type systems, to which some of the exact analytical techniques described above can be applied. Using an extension of the discrete two-state motor model, Lau *et al* [274] investigated theoretically the violations of Einstein and Onsager relations and calculated the efficiency for a single processive motor in [274]. Furthermore, it can be shown that the fluctuation relations (such as the Gallavotti–Cohen theorem, the Jarzysnki–Crooks relations) play the role of a general organizing principle. Indeed, cellular motors are systems of molecular size which operate with a small number of molecules, and for these reasons undergo large thermal fluctuations. The fluctuation relations impose general constraints on the function of these nanomachines that go beyond classical thermodynamics. They provide a way to better understand the non-equilibrium energetics of molecular motors and to map out various operating regimes [274–276].

Significant effort in the investigation into molecular motors has focused on identifying and understanding the molecular mechanics and the coupling of molecular motion with a chemical reaction such as ATP hydrolysis. From these studies, complex descriptions of molecular motors have been developed, including a somewhat artificial classification of motors employing 'power-stroke' or 'Brownian ratchet' mechanisms. This classification refers to how detailed balance is violated *within* the large motor molecule or enzyme. If certain internal degrees of freedom in a molecule are made inaccessible at the right times, a net flux along these states can arise, ratcheting the motion. If a particular transition is strongly coupled to specific chemical step such as the hydrolysis of an ATP molecule bound in a pocket of the motor molecule, the motion has been described as a power stroke motor. It has been shown that this distinction is quantitative, rather than qualitative [277]. From a stochastic processes point of view, when the dynamics of the microscopic internal motor degrees of freedom is represented by, e.g., a Markov chain, power-stroke and ratchet mechanisms can be distinguished where detailed balance is violated in the cycle. For example, if the relative amount of violation occurs during transitions across states that are directly coupled to motion against a load, the motor will be 'ratchet-like'.

If the abscicca in figure 10 represents sequential internal molecular states, a purely ratchet mechanism is naturally represented by a state evolving along the flat energy profile. In this case, a steady-state probability flux, or molecular motion, arises from the absorbing and emitting boundary conditions that ratchet the overall motion. In this stochastic picture, the power-stroke/Brownian ratchet distinction is mathematically recapitulated by state-space boundary conditions and by the relative amount of convection through state-space. How much a motor utilizes a power-stroke mechanisms would be described by the Peclet number within the framework of single-particle convection–diffusion or Fokker–Planck type equations. For a more detailed delineation of regimes of mechanical–chemical coupling, see the review by Astumian [278].

In many cellular contexts, molecular motors are crowded and interact with each other and exhibit collective behavior [279]. Examples include connected myosin motors in muscle, multiple motors and motor types on cellular filaments and microtubules (often carrying large cargo such as vesicles), and motors that process DNA and RNA. To model such systems, the details of how an isolated motor generates force and moves may be best subsumed into a single parameter representing the mean time between successive motor displacements. The internal dynamics, whether power-stroke or Brownian ratchet, moves the motor one step against a load or resistance at random times. These times are drawn from a distribution of hopping times that is determined by the underlying, internal stochastic process.

One can simplify the modeling of molecular motors by assuming that the motor stepping time is exponentially distributed with an inverse mean that defines the hopping rate. Each motor hops along a one-dimensional track and can exclude other motors. Typically, concerted motions are also neglected in this application. That is, a motor is not allowed to push another one in front of it, moving both motors ahead simultaneously. In the extreme limit, multiple motors are coupled with, e.g., elastic elements and have been extensively modeled using simple Fokker–Planck equations that incorporate mechanical and thermal forces [281–287]. Weaker interactions that do not bound the distance between motors can be modeled using the excluding particle picture by assigning different rules for the hopping of two adjacent particles, analogous to the facilitated diffusion models of Gabel *et al* [241]. Given the assumptions discussed above, exclusion processes can be directly used to model collections of motors moving on one-dimensional tracks. Additional effects particular to applications in biomolecular motors include detachment and attachment kinetics and different types of motors that move in opposing directions.

Molecular motors 'walk' along filaments but have a finite 'processivity' since they can spontaneously detach. Thus, they have a distribution of run lengths. Conversely, motor molecules diffusing in the 'bulk' cytoplasmic space can attach to interior locations of the lattice. Detachment violates particle conservation on the lattice and has been studied using mean-field models, hydrodynamic approximations [288, 289] and Monte-Carlo simulations [218, 219, 290, 291]. The detachment and possible reattachment of particles on a lattice have been extensively studied in the context of gas adsorption isotherms or 'Langmuir kinetics' (see [292] and references within). While many models of Langmuir isotherms exist, previous studies considered only passive, undriven particles. In new work combining Langmuir kinetics with driven exclusion processes, analytic progress can be made by considering the infinite site, continuum hydrodynamic limit. If attachment and/or detachment occurs, the hopping rates must be rescaled by the number of lattice sites such that the rates $\omega_{A,D}$ (cf figure 5) at each site are inversely proportional to the number of sites L. If this is not done, particles only occupy a small region near the injection end of a long lattice. To arrive at a non-trivial structure, the attachment and detachment rates must be decreased so that the cumulative probability of desorption is a length-independent constant.

As we mentioned in section 3, continuum hydrodynamic equations allow more complicated models to be approximately treated. This has been the case for one-dimensional exclusion processes with Langmuir kinetics. In the steady-state limit, Parmeggiani *et al* find [219]

$$\frac{\varepsilon}{2}\frac{\partial^2\rho(x)}{\partial x^2} + (2\rho - 1)\frac{\partial\rho(x)}{\partial x} + \Omega_A(1 - \rho(x)) - \Omega_D\rho(x) = 0 \tag{86}$$

where $\Omega_{A,D} = \omega_{A,D}L \equiv \omega_{A,D}/\varepsilon$ represents appropriately rescaled detachment and attachment rates that in this simple model are *independent* of L. A detailed asymptotic analysis of equation (86) was performed and a phase diagram as a function of four parameters (the injection and extraction rates at the ends of the lattice, and the adsorption and desorption rates) was derived [218, 219]. They find a rich phase diagram with coexisting low- and high-density phases separated by boundaries induced by the Langmuir kinetics. Langmuir kinetics have also been investigated in the presence of bottlenecks [293]. Klumpp and Lipowsky [294] have considered asymmetric exclusion in tube-like structures such as those seen in axons or in filapodia [295, 296]. In this simplified geometry, the diffusion of motors within the tube can be explicitly modeled [294].

Since motors are used to carry cargoes across the different regions within a cell, they travel on directed filaments and microtubules. Different motors are used to carry cargo in one direction versus the other. For example, kinesins travel along microtubules in the '+' direction, while dynein travels in the '−' direction, as shown in figure 14. This scenario can be modeled using a two-species exclusion process with Langmuir kinetics overtaking. Moreover, microtubules are composed of multiple twisted filamentous tracks. Not only can motors travel in opposite directions on the same track, but filaments may be oppositely directed within confined spaces such as axons. Motors traveling in opposite directions on the same filament or on a nearby parallel filament can be modeled using coupled chains of exclusion processes. Many groups have explored the dynamical properties of two-species and two-lane asymmetric exclusion processes (as shown in figure 7) [297–301]. With the proper biophysical identification of the parameters, results from these studies of interacting lattices should provide illuminating descriptions of more complex scenarios of molecular motor-mediated transport.

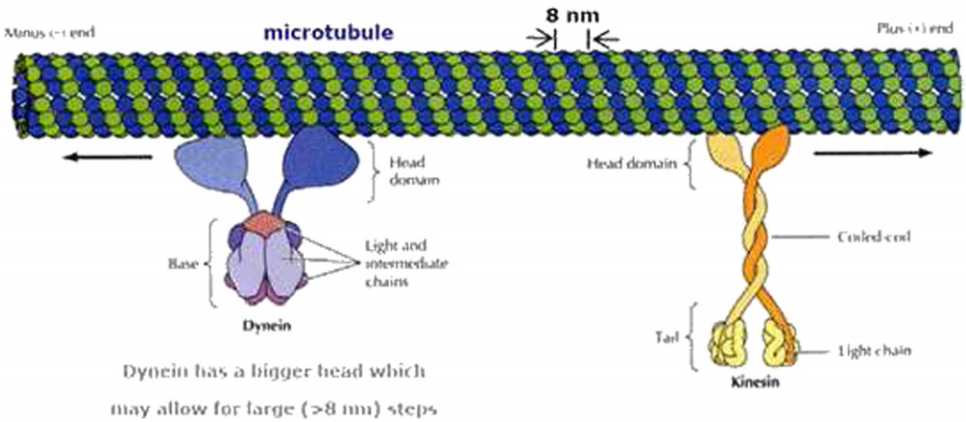

Figure 14. A schematic of two types of molecular motors moving along a cellular microtubule (adapted from [280]). In this picture, kinesin moves to the right while dynein moves to the left. Each motor can be attached to large cargoes such as vesicles or other filaments. Note that the microtubule consists of twisted lanes of repeated molecular subunits.

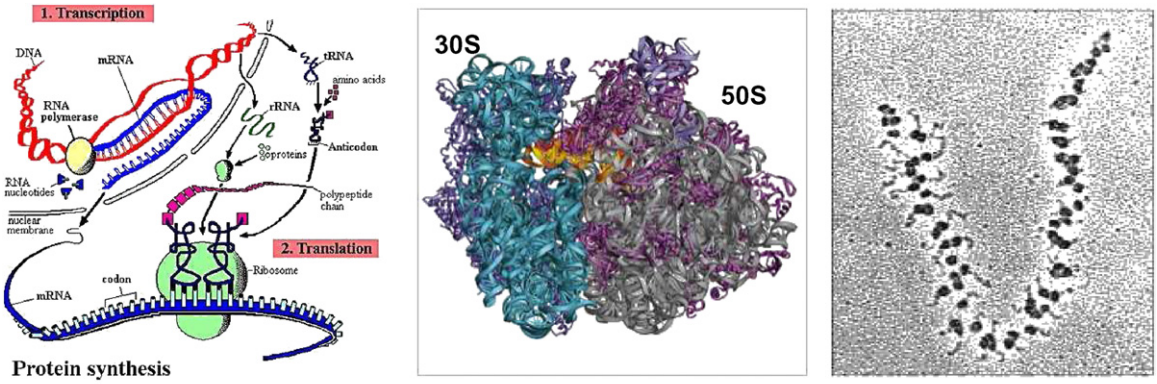

Figure 15. (*a*) A cartoon of the 'central dogma' in biology where mRNA is synthesized from cellular DNA and transported to the cytoplasm. The cytoplasmic mRNAs are then translated by ribosomes into polypeptides which may then finally be folded and processed into functioning proteins. (*b*) Crystal structure of both subunits of bacterial ribosome. (*c*) An electron micrograph of multiple ribosomes translating a single mRNA.

4.3. mRNA translation and protein production

One very special case of interacting motors moving along a one-dimensional track arises in cell biology. In all cells, proteins are synthesized by translation of messenger RNA (mRNA) as schematized in figure 15. Complex ribosome enzymes (shown in figure 15(*b*)) unidirectionally scan the mRNA polymer, reading triplets of nucleotides and adding the corresponding amino acid to a growing polypeptide chain. Typically, many ribosomes are simultaneously scanning different parts of the mRNA. An electron micrograph of such a *polysome* is shown in figure 15(*c*).

The ribosomes are actually comprised of two subunits, each made up mostly of RNA and a few proteins. Not only do these 'ribozymes' catalyze the successive addition of the specific amino acid as they scan the mRNA, their unidirectional movement from the 5′ end to the 3′ end, (where the 5′ denotes the end of the mRNA that has the fifth carbon of the sugar ring of the ribose as the terminus) constitutes a highly driven process. Therefore, each ribosome is also a molecular motor that rarely backtracks as it moves forward. The fuel providing the free energy necessary for codon recognition and unidirectional movement is supplied in part by the hydrolysis of GTP [302]. Quantitatively, mRNA translation is different from typical molecular motors in that ribosome processivity is very high, allowing one to reasonably neglect detachments except at the termination end. Moreover, there are no known issues with 'concerted motions' or 'facilitated exclusion'. If one ribosome prematurely pushes the one ahead of it, one would expect many polypeptides to be improperly synthesized.

Thus, at first glance, the TASEP seems to be the perfect model for this translation process, with the particles being ribosomes and a site being a codon—a triplet of nucleotides. On closer examination, it is clear that protein production is much more complicated. Many biophysical features relevant to mRNA translation are missing from the basic TASEP. The desire to have more 'realistic' models of protein production has motivated the development of various extensions to the basic TASEP. In this subsection, we will discuss only two efforts to generalize TASEP: allowing particles of size $\ell > 1$ and incorporating inhomogeneous, site-dependent hopping rates. In each case, we will describe the cell biology which motivates the modifications.

Although the fundamental step size of ribosomes is a codon, the large size of each ribosome (20 nm for prokaryotic

ribosomes and 25–30 nm for eukaryotic ribosomes) means that they each cover approximately ten codons along the mRNA chain and exclude each other at this range. Therefore, TASEPs comprised of extended objects, occluding $\ell > 1$ lattice sites have therefore been developed, dating back to the late 1960s [13, 14]. Although exact results for such a generalized TASEP on a ring are available [303], the problem with open boundaries remains unsolved. Instead, various MFTs have been successful at capturing many important properties for modeling mRNA translation. Let us devote the next paragraphs to this system.

First, consider a ring of L sites filled with N particles, and note that every configuration with particles of extent ℓ can be matched with a configuration with N point particles ($\ell = 1$) on a ring of $L - N(\ell - 1)$ sites. This mapping is easily understood by regarding a configuration, $\mathcal{C}$, as clusters of adjoining vacancies followed by clusters of adjoining particles (regardless of their sizes). Therefore, the stationary distribution, $P^*(\mathcal{C})$, is again flat and independent of ℓ for all p, q. Of course, the sum of the particle density ($\rho \equiv N/L$) and the hole density (ρ_{hole}) now satisfy $\ell\rho + \rho_{\text{hole}} = 1$, but with ρ lying in a limited interval $[0, 1/\ell]$. With $P^* \propto 1$, finding the probability of particle–hole pairs is straightforward, resulting in an exact expression [205] for the current density relation, $J(\rho) = \rho\rho_{\text{hole}}/(\rho + \rho_{\text{hole}} - 1/L)$, in the TASEP case. To lowest order in $1/L$, the formula

$$J = \frac{\rho(1 - \ell\rho)}{1 - (\ell - 1)\rho} \tag{87}$$

was known as early as 1968 [13, 14], and leads to a maximal current of $(1 + \sqrt{\ell})^{-2}$ associated with the optimal density of $\hat{\rho} = (\ell + \sqrt{\ell})^{-1}$. Note that, though $J(\rho)$ is no longer symmetric about $\hat{\rho}$, the particle–hole symmetry ($\rho \leftrightarrow \rho_{\text{hole}}$) is preserved. This invariance is expected on physical grounds, as the current arises only from exchanges of particle–hole pairs. Although the stationary measure is trivial and $G(r)$, the expectation value of two particles separated by r sites, can be written formally as a sum of products of binomials. Of course, period-ℓ structures are to be expected in $G(r)$. Despite the conceptual simplicity of this problem, remarkably intricate patterns emerge [304], especially near complete filling, $L \cong N\ell$ [305]. Such structures are completely absent from the $\ell = 1$ case (whether in periodic or open TASEP), showing us that, even in seemingly trivial situations, statistics of extended objects can produce surprises.

Turning to the open boundary TASEP, we must first specify how a particle enters/exits the lattice. One possibility is 'complete entry, incremental exit' [306], where a particle may enter completely provided the first ℓ sites are empty, while it may exit moving one site at a time. In the NESS, exact expressions for the current like (16) can still be written. When both i and $i + \ell$ are within $[1, L]$, we have $J = \langle\sigma_i(1 - \sigma_{i+\ell})\rangle$. From the 'incremental exit' rule, we have $J = \langle\sigma_{L-\ell}\rangle = \cdots = \langle\sigma_{L-1}\rangle = \beta\langle\sigma_L\rangle$, leading to a simple profile next to the exit. The major challenge comes from the 'complete entry' condition: $J = \alpha\langle\prod_{k=1}^{\ell}(1 - \sigma_k)\rangle$. Since this problem can no longer be solved exactly, many conclusions can only be drawn from simulation studies or imposing mean-field approximations. For the latter, the naïve replacement of averages of products of σ by products of $\langle\sigma\rangle$ (e.g. $\langle\sigma_i\sigma_{i+\ell}\rangle \to \langle\sigma_i\rangle\langle\sigma_{i+\ell}\rangle$) leads to extremely poor predictions. Gibbs and co-workers [13, 14] took into account some of the effects of exclusion at a distance and approximated $J = \langle\sigma_i(1 - \sigma_{i+\ell})\rangle$ by

$$J = \frac{\rho_i\bar{\rho}_i}{\rho_{i+\ell} + \bar{\rho}_i} \tag{88}$$

where $\bar{\rho}_i \equiv 1 - \sum_{k=i+1}^{i+\ell}\rho_k$ is an effective hole density in the ℓ sites following i. For the ring, the profile is flat and $\rho_i = \rho$, so that (88) reduces to (87). Supplemented with the appropriate boundary equations, (88) can be regarded as a recursion relation for the profile. The successes of this approach include predicting a phase diagram that is the same as the one in figure 2(*c*), except that the boundaries of the maximal current phase are now at $\alpha, \beta = (1 + \sqrt{\ell})^{-1}$. Simulations largely confirm such predictions [205, 306], suggesting that the correlations neglected by the scheme of Gibbs and co-workers [13, 14] are indeed small. On the other hand, for more sensitive quantities like the profile, this MFT is less successful, especially for the high-density phase ($\beta \ll \alpha \sim 1$). To produce better predictions, Shaw *et al* [103] introduced a more sophisticated MFT, taking into account some pair correlations. So far, no higher level of MFT has been attempted.

The second modification to the basic TASEP we consider here is site-dependent hopping rates. Since the translation of mRNA into polypeptides depends on the sequence of nucleotides, the hopping rates of the ribosome TASEP particles can vary dramatically as a function of its position on the lattice. The local hopping rates depend on the effective abundance of the specific amino-acid-charged tRNA that participates in each elongation step at each site. One of the first treatments of TASEPs on a non-uniform lattice considered a single defect, or slow hopping site[10], in the middle of an asymptotically long lattice. Kolomeisky derived the expected steady-state particle flux across a lattice with a single slow hopping site by ignoring particle–particle correlations across the defect [307]. He self-consistently matched the exit rate from the first half of the chain with the injection rate of the second half of the chain. This approach indicated that each long uniform region between slow sites can approximately be treated as separate, but self-consistently connected, uniform exclusion processes. Later work by Chou and Lakatos developed a more refined method of connecting the current between sections separated by interior defects. Their method generalizes MFT by explicitly enumerating the configurations of the sites straddling the inhomogeneity, and self-consistently matching the current across this segment with the asymptotically exact steady-state currents across the rest of the homogeneous lattice. Steady-state particle currents across localized defects can be accurately computed [308]. Using this approach, the synergistic effects of two nearby slow hopping sites were analyzed. It was shown that two defects decreased the current more when they are placed close to each other. The decrease in current approaches

[10] If an isolated site has faster hopping than all its neighbors, the average current is hardly affected, though there are noticeable changes to the profile. Thus, we focus on slow sites.

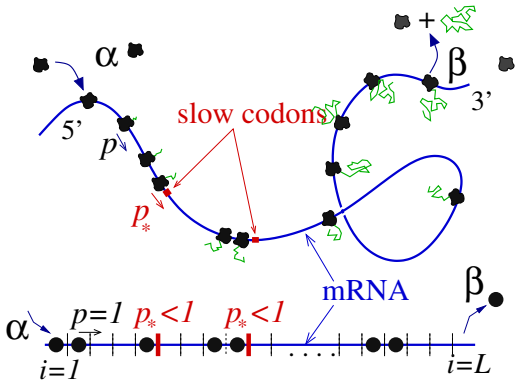

Figure 16. mRNA translation with fixed slow codons, or bottlenecks across which ribosome motion is slower ($p^* < p$) than across other codons. This local slowing down can arise from a limited supply of the appropriate amino acid-charged tRNA corresponding to the slow site.

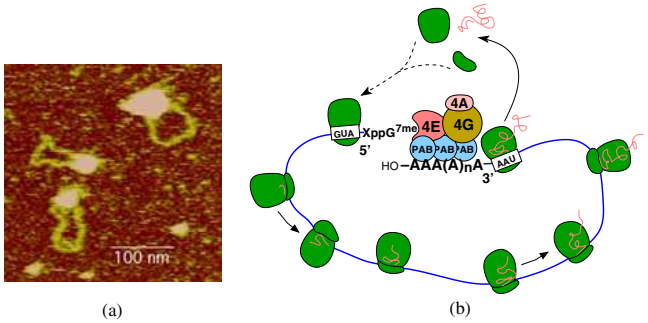

Figure 17. (*a*) Atomic force microscopy image of circularized mRNA. (*b*) Schematic of a model where ends of mRNA are sticky (the poly-A tails are known to bind to initiation factors [316–318]), increasing the probability of loop formation.

that of a single defect as the distance between two defects diverges since the dynamical 'interaction' from overlap of density boundary layers vanishes.

Another method for approximately treating inhomogeneous hopping rates was developed by Shaw *et al* [103] where the original mean-field equations of Gibbs and co-workers [13, 14] were generalized to include site-dependent elongation rates. Dong *et al* [309, 310] systematically analyzed the effects of defects on the steady-state current of extended particles that occupy multiple ($w > 1$) sites. They used a combination of self-consistent MFT and Monte-Carlo simulations to show the importance of the location of the defect, especially if the defect is placed close entry or exit sites where they may possibly 'interact' with the end-induced density boundary layers.

As mentioned in section 3.3 hydrodynamic MFT developed for analyzing systems with slowly varying hopping rates. Continuum equations, such as (84), that incorporate spatially varying hopping rate functions $p(x)$ and $q(x)$ have been derived for the mean-field ribosome density $\rho(x)$ [124, 205–207]. For single-site particles, these hydrodynamic equations can be integrated once to arrive at singular nonlinear first order differential equation where the integration constant is the steady-state particle current. Using singular perturbation theory, analytic solutions for density profiles have been found for very specific hopping rate functions $p(x)$ and $q(x)$ [124, 204].

The stochastic process underlying the models of mRNA translation described above all assume an exponentially distributed waiting time between elongation events. Dwell time distributions would be difficult to incorporate into simple ODEs for the mean-field particle density or continuum hydrodynamic equations. Although different dwell time distributions would not qualitatively affect steady-state ribosome current and protein production rate, to model them explicitly requires incorporation of intermediate biochemical steps involved in initiation, elongation, and termination of the individual ribosomes. These steps include binding of an amino-acid charged transfer RNA (tRNA) to one of the binding sites, hydrolysis, etc [311]. Models that include more complex elongation steps have also been developed by a number of researchers [225, 226, 312–315]. The main qualitative result of these studies is that the standard current phase diagram is shifted due to a varying *effective* elongation (internal hopping) rate. Since the internal hopping rate depends on the details of their models, it cannot be nondimensionalized and the standard phase diagram is roughly reproduced with $\alpha_{\rm eff}/p_{\rm eff}$ and $\beta_{\rm eff}/p_{\rm eff}$ as the tuning variable. Here $\alpha_{\rm eff}$, $\beta_{\rm eff}$, and $p_{\rm eff}$ are are effective rates that might be estimated as the inverse of the mean of the associated dwell time distributions.

Finally, the mRNA translation process, much like molecular motor-facilitated intracellular transport, occurs in complex, spatially heterogeneous environments and involves many molecular players that initiate and terminate the process. For example, certain initiation factors that prime the initiation site for ribosomal entry have been shown to bind to the polyadenylated tails of mRNA, thereby forming circularized RNA. One hypothesis is that mRNA circularization facilitates the recycling of ribosomes. In circularized mRNA (figure 17(*b*)), ribosomes that detach from the termination site after completing translation have a shorter distance to diffuse before rebinding to the initiation site. A model for this effect was developed in [319], where an effective injection rate $\alpha_{\rm eff}$ was self-consistently found by balancing the steady-state ribosome concentration at the initiation site with the diffusive ribosome flux emanating from the nearly termination site. In this model, the diffusive feedback tends to increase the protein production rate, especially when overall ribosome concentrations are low. One can also imagine a strong feedback if factors regulating translation initiation were themselves products of translation. Newly produced cofactors can readily maintain the initiation rate α at a high value.

An even more important aspect of mRNA translation is that ribosomes and initiation factors [320], and mRNAs [321] can be actively localized to endoplasmic reticular (ER) membranes and compartments, depending on what types of proteins they code for, and where these proteins are needed. In confined cellular spaces, the supply of ribosomes and initiation factors may be limited. Moreover, there are many different mRNA copies that compete with each other for ribosomes. This global competition has been modeled by Cook *et al* [322, 323] who defined an effective initiation

rate $\alpha_{\rm eff}(N)$ which is a monotonically increasing function of the free ribosome concentration. They considered mRNAs of different length (but of identical initiation, elongation and termination rates) and found that steady-state protein production for different length mRNAs were comparable, but that their ribosome loading levels exhibit varying levels of sensitivity on the total ribosome mass.

4.4. Free boundary problems and filament length control

Our final example of a class of biological application of exclusion processes involves changes in the length of the underlying one-dimensional substrate. A dynamically varying lattice length arises in at least three different cellular contexts: growth of filaments such as hyphae and cellular microtubules, replication forks, and mRNA secondary structure. In each of these examples, there is a 'moving boundary' whose dynamics depends on transport within the domain bounded by the boundary.

An analogy can be made with the classic free boundary problem arising in continuum physics. In the 'Stefan problem' a diffusive quantity mediates the growth of an interface bounding the dynamics. This diffusing quantity may be heat which melts away the water–ice interface [324], or a particulate systems that deposits and makes the interface grow [233]. In systems relevant to cell biology, the dynamics (i) occurs in confined, often one-dimensional geometries, and (ii) occurs on a fluctuating mesoscopic or molecular scale. In confined geometries, particle–particle exclusion become important. By contrast, this exclusion is absent when the transported field is say, heat. On small scales, statistical fluctuations of the interface, and its coupling with the fluctuating particle field can also be important.

A stochastic one-dimensional moving boundary problem can also be described within an exclusion process where the number of sites is allowed to fluctuate. Such models have been described in [228–331, 232], and [231]. In [232], a fluctuating wall is coupled to an asymmetric exclusion process as shown in figure 9. The wall particle acts like a piston and defines one boundary of the lattice and has its own intrinsic forward and backward hopping rates. Particles impinge on the wall and have a certain detachment rate. Using a moving frame version of asymptotic matching [308] the expected position and fluctuations of the wall were accurately computed. The wall was found to either extend the lattice indefinitely, compress the particles and fall off the lattice at the injection site, or find an equilibrium lattice length.

In terms of specific biological applications, Evans and Sugden [228] and Sugden *et al* [229] consider a free boundary TASEP as a model for hyphae growth in fungi (cf figure 18(*a*)). The hypothesis is that kinesin motors carry cargo and move unidirectionally toward the tip. The delivered cargo can then extend the tip by incrementing the number of lattice sites of the TASEP. In this case, there is no confining wall, and the velocity tip extension is proportional to the number of arriving TASEP particles. Even though the tip is always growing with a fixed velocity, the particle density profiles can acquire different structure, including a jammed, high-density phase.

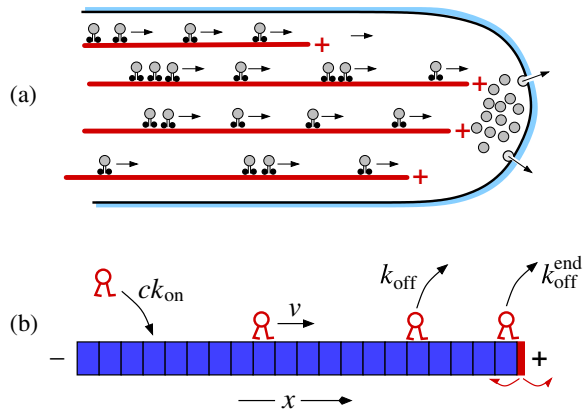

Figure 18. (*a*) Schematic of multiple TASEPs for dynamically growing tips. The particles are motors carrying building blocks of the underlying filaments [228]. (*b*) A model of microtubule length control where particles reaching the tip depolymerize the last subunit [231]. Figures are adapted from those in [228, 231].

Another application of dynamic-boundary TASEPs involving molecular motors was described by Hough *et al* [231]. In their model of microtubule length control, kinesin-8 motors move along a microtubule and *depolymerize* the tip when it is reached. The tip also has an intrinsic degradation and assembly rate, the latter depending on the concentration of subunits in the bulk. Therefore, this model is similar to a TASEP with a confining wall [232] representing the end of the lattice. However, in this model, the kinesis motors also undergo Langmuir kinetics by attaching to, and detaching from, the microtubule lattice. Hough *et al* find regimes where microtubule length-dependent depolymerization rates arise, as well as how the behavior depends on bulk motor concentrations [231].

A number of potentially new models remain relatively unexplored. For example, molecular motors often encounter an obstacle. As the helicase motor separates DNA strands for transcription, it must break base pair bonds and push the replication fork forward [325–328]. The fork may be represented by a confining wall that tends to reseal the single strands of DNA. Similarly, mRNA translation by ribosome 'motors' typically occur in the presence of hairpins that must be separated before the ribosomes can progress. In both of these applications the motor–wall interaction may be considered passive (ratchet-like) or active (forced separation) [328]. These limits are again related to the issue of concerted motion or facilitated exclusion mentioned earlier. The motor can actively advance the replication fork, whereby the forward motions of the leading particle and the wall occur simultaneously in a concerted fashion. Alternatively, the opening of the fork can be thermally activated, temporarily allowing the leading motor to ratchet the wall. Sometimes, due to the particular geometry, a motor may not need to move against a barrier, but may pass through it. An interesting realization arises in mRNA translation where ribosome may jump over hairpins, effectively making hops to an empty site far away on the lattice. This kind of 'short-cut' model has been studied using mean-field theory and simulations by Kim *et al* [329] and have been found to exhibit coexistence of empty and jammed phases. The

consequences of these rich mechanisms on cell biology remain to be explored.

5. Summary and outlook

Non-equilibrium statistical mechanics is the study of stochastic processes for a system involving many interacting degrees of freedom. As such, it concerns essentially the entire spectrum of natural phenomena, ranging over all length scales and relevant for all areas in science and engineering. While a small encyclopedia would be needed to adequately cover NESM, reviews dealing with more specialized topics are abundant in the literature. In this paper, we attempt a compromise by providing (*a*) a bird's eye view of NESM, and (*b*) a 'bridge' between the two different approaches to the subject. For the former, we review some of the fundamental issues associated with NESM and why the techniques (and assumptions) of equilibrium statistical mechanics cannot be easily generalized. Using the language of stochastic processes, we base our discussions on master equations and focus on systems which violate detailed balance (or time reversal). One serious consequence is that, given a set of such rates, even the stationary distribution, P^*—an NESS analog of the Boltzmann factor $e^{-\beta\mathcal{H}}$—is generally unknown. There is an additional challenge: the presence of persistent *probability currents* (forming closed loops, of course), K^*, much like the steady electric current loops in mangnetostatics. By contrast, $K^* \equiv 0$ if the transition rates obey detailed balance, in analog to electrostatics. We emphasized that these currents play important roles in an NESS, as they lead to persistent fluxes of physically observable quantities (e.g. mass, energy, etc) as well as constant entropy production in the surrounding medium.

Naturally, our 'bird's eye view' is both limited and colored. For example, we offer only a brief glance on fluctuation theorems and symmetry relations, a topic of NESM which has witnessed considerable progress over the past two decades. Even more generally, our focus on master equations implicitly assumes that the dynamics can be decomposed into a series of Markov processes with exponentially distributed waiting times in each configuration. Age-dependent processes described by more complex waiting-time distributions of each configuration may often be better studied using theories of branching processes. Moreover, master equation approaches are not very suited for studying the statistics of individual trajectories or realizations. Understanding properties of individual trajectories in configuration space is important, for example, in problems of inference and reconstruction of the stochastic rules from data. These attributes are better analyzed using techniques of, e.g., stochastic calculus or path integrals. Therefore, a comprehensive overview of the foundations of NESM and stochastic processes would include concepts and formalism from other disciplines such as probability theory, statistics and control theory—a task far beyond our scope.

To meet the challenges posed by NESM, a wide range of approaches have been developed. On the one hand, we have model systems, sufficiently simple that rigorous mathematical analysis is feasible. At the other extreme are models which account for many ingredients deemed essential for characterizing the large variety of phenomena found in nature. Understandably, those working on either end of this spectrum are not typically familiar with the progress at the other end. A historic example appeared in the late 1960s when Spitzer [9] and Gibbs and co-workers [13, 14] investigated independently the same stochastic process, but were unaware of each others' studies. In this paper, we attempt to bridge this divide by providing brief reviews of a limited set of topics from both ends.

For the exclusion process, we presented many exact results, along with two complementary techniques to obtain them. The stationary distribution for a system with periodic boundary conditions (i.e. ASEP on a ring) was known to be trivial [9]. On the other hand, a rich variety of dynamic properties, even for SEP, have been discovered over the last four decades. With open boundaries, particles may enter or exit the lattice at both ends, so that the total occupation becomes a dynamic variable. As a result, this system poses much more of a challenge. Little was known until the 1990s, when the exact P^* was found [118–121] through an ingenious recognition of a matrix representation. For simplicity, we presented the details of this method only for the extreme case of TASEP, in which particles enter/exit with rate α/β (section 3.4). Once P^* is known, it is straightforward to compute the exact *particle* current, J, and the mean density profile ρ_i. A non-trivial phase diagram in the α–β plane emerged, with three distinct phases separated by both continuous and discontinuous transitions (section 3.5). In addition, algebraic singularities are always present in one of the phases. Such phenomena are novel indeed, since the conventional wisdom from EQSM predicts no phase transitions (i.e. long-range order), let alone generic algebraic singularities, for systems in one dimension, with short-ranged interactions! Beyond NESS, another powerful method—the Bethe ansatz—has been applied successfully to obtain time-dependent properties (section 3.7). Analyzing the spectrum and the eigenvectors (Bethe wave functions) of the full Markov matrix, other physically interesting quantities in an NESS can be also computed. Examples include the fluctuations of the current (around the mean J), encoded in the LDF, $G(j)$. Knowledge of dynamic properties also allows us to explore, in principle, ASEPs on *infinite* lattices, for which the initial configuration must be specified and the system properties after long times are of interest. In practice, however, these problems are attacked by another technique, fascinatingly related to the theory of random matrices, representations and combinatorics (section 3.10). These powerful methods have yielded mathematically elegant and physically comprehensible results, rendering exclusion models extremely appealing for modeling real systems.

Apart from exact solutions, we also presented an important approximation scheme—the MFT. Based on physically reasonable and intuitive arguments, we consider coarse-grained densities as continuum fields, obeying hydrodynamic equations, e.g., the density $\rho(x,t)$ in ASEP. Remarkably, such an MFT predicted some aspects of TASEP exactly (e.g. the current density relation $J = \rho(1-\rho)$). Although neither rigorous nor a systematic expansion (such as perturbation theory with a small parameter), MFT has provided valuable

insights into behavior which we cannot compute exactly. This is especially true when appropriate noise terms are added, so that we can access not only the (possibly inhomogeneous) stationary profiles but also the fluctuations and correlations near them. A good example is the average power spectrum associated with $N(t)$, the total mass in an open TASEP. Intimately related to the time-dependent correlation of the currents at the two ends, this quantity has eluded efforts to find an exact expression, despite our extensive knowledge about the full Markov matrix. Instead, starting with an MFT and expanding around a flat profile in the high/low-density phase, many interesting properties of this power spectrum can be reasonably well understood [330, 331]. Undoubtedly, there are many other physically interesting quantities (in ASEP and other 'exactly solvable systems') for which theoretical predictions can be obtained only from mean-field approximations. Of course, as we consider modeling transport phenomena in biological systems, more realistic features must be included. Then, MFT typically offers the only route toward some quantitative understanding.

We next turned to specific generalizations of the ASEP which are motivated by problems in biological transport. While the exactly solvable ASEP consists of a single lattice of fixed length with at most one particle occupying each site and hopping along from site to site with the same rate, the variety of transport phenomena in cell biology calls for different ways to relax these constraints. Thus, in the first model for translation in protein synthesis, Gibbs and co-workers already introduced two features [13, 14] absent from the standard ASEP. Representing ribosomes/codons by particles/sites, and being aware that ribosomes are large molecules covering $O(10)$ codons, they considered ASEP with *extended objects*. They were also mindful that the sequence of codons in a typical mRNA consists of different codons, leading to a ribosome elongating (moving along the mRNA) with possibly different rates. The result is an ASEP with *inhomogeneous hopping rates*. Beyond these two aspects, we know that there are typically thousands of copies of many different mRNAs (synthesizing different proteins) within a single cell. Now, they compete for the same pool of ribosomes. To account for such competition, we should study multiple TASEPs, with different lengths, 'interacting' with each other through a common pool of particles. Within the cell, the ribosomes presumably diffuse around, leading to possibly more complex pathways of this 'recycling of ribosomes.'

Of course, ribosome motion along mRNA is only one specific example of molecular motors. Therefore, the TASEP is also suited for modeling cargo transport by molecular motors 'walking' along cellular microtubules. In this case, many essential biological features are also absent from the standard TASEP model. Motors are known to detach from the microtubule and reattach at other points, so that Langmuir kinetics [292] should be introduced. The cargoes they carry are typically much larger than their step size, leading us again to long-ranged particle–particle interactions. There are many lanes on a microtubule, so that we should include multiple TASEPs in parallel, with particles transferring from one lattice to another, much like vehicular traffic on a multilane highway. Molecular motors come in many varieties (dynein, kinesin, etc) which move in opposite directions and at different speeds. Consequently, a proper model would consist of several particle species hopping in different directions. The variety of speeds is the result of complex, multi-step chemical reactions, so that the dwell times are not necessarily distributed according to simple exponentials. To account for such details, particles with internal states can be used. This level of complexity is also sufficient for modeling another important biological process: transport through channels on membranes (pores). Various ions, atoms and molecules are driven in both directions, often 'squeezing by' each other. Finally, microtubules grow and shrink, a process modeled by a dynamic L, the length of our lattice. Typically, the associated rates are governed by the densities of particles at the tip, leading us to an entirely new dimension in mathematical complexity.

Let us also provide an outlook of NESM beyond the topics presented in the sections here. In the realm of exactly solvable models, ASEP is just one of many. Not surprisingly, all but a few are one-dimensional systems. For example, we noted in section 3.9 the zero-range process. Also introduced by Spitzer [9], it is a closely related model for mass transport. Multiple occupancy is allowed at each site, while some of the particles hop to the next site. Thus, this process is well suited to describe passengers at bus stops, with some of them being transported to the next stop. Particularly interesting is the presence of a 'condensation transition,' where a macroscopic number of particles occupy a single site as the overall particle density on a ring is increased beyond a critical value. Much progress has emerged, especially in the last two decades (see [332] for a review). Another notable example of transport is the ABC model [86, 87], mentioned at the end of section 2. In general, it also displays transitions of a non-equilibrium nature, admitting long-range order despite evolving with only short-ranged dynamics.

Apart from transport models, exact results are also known for systems with no conservation law. A good example is the kinetic Ising chain [53], coupled to two thermal reservoirs at different temperatures ($T > T'$). As a result, it settles down to an NESS, with generally unknown P^*. Depending on the details of the coupling, exact results are nevertheless available. In particular, if every other spin is updated by a heat-bath dynamics associated with T and T', then *all* multi-spin correlations are known exactly [333, 334]. Remarkably, even the full time dependence of these correlations can be obtained exactly, so that the full $P(\mathcal{C}, t)$ can be displayed explicitly as well [335] [11]. As a result, it is possible to compute the energy flow *through* the system (from the hotter bath to the cooler one) in the NESS, as well as the entropy production associated with the two baths [333]. Similar exact results are available in a more common form of imposing two baths, namely, joining two semi-finite chains (coupled to T and T') at a single point. Since the energy flows from the hotter bath, across this junction, to the cooler side, we may ask for, say, (a) the power injected to the latter and (b) the profile of how this injected energy is lost to the colder bath. Only the average

[11] Indeed, due to the simplicity of heat-bath dynamics, some exact results are known even if the rates are *time dependent* [336].

of the latter is known [337], but the LDF of the total injected power can be computed exactly [338, 339]. These are just some of the examples of other exactly solvable systems which evolve with detailed balance-violating dynamics.

In the realm of potential applications, exclusion processes extend well beyond the examples in biological transport presented here. In the general area of 'soft condensed matter,' the exclusion mechanism arises in many other systems, such as motion of confined colloids [340, 341]. Further afield, the process of surface growth in a particular two-dimensional system can be mapped to an ASEP [182, 342]. On larger scales, exclusion processes lends themselves naturally to modeling traffic flow [343–345] and service queues [346]. For each of these applications, though ASEP and its variants may not be sufficiently 'realistic', they nonetheless provide a succinct physical picture, some insights from mean-field analysis and a precise language on which sophisticated mathematical techniques can be applied. Along with the overall improvement of various technologies (in e.g. nanoscience, renewable energy), we expect that there will be many opportunities for exclusion processes to play a role, both in modeling newly discovered phenomena and in shaping directions of further research.

Broadening our outlook from exactly solvable models and potential applications to NESM in general, the vistas are expansive. It is beyond our scope to provide an exhaustive list of such systems, which would include problems in ageing and branching processes, directed percolation, dynamic networks, earthquake prediction, epidemics spreading, granular materials, financial markets, persistence phenomena, population dynamics, reaction diffusion, self organized critically, etc. On the purely theoretical front, many fundamental issues await further exploration. For example, the implications of probability currents, beyond the computation of physical fluxes, may be far reaching. If we pursue the analog with electromagnetism, we could ask if these currents can be linked to a form of 'magnetic fields,' if there is an underlying gauge theory, and if these concepts are constructive. Perhaps these ideas will lead us to a meaningful framework for *all* stationary states, characterized by the pair of distributions $\{P^*, K^*\}$, which encompasses the very successful Boltzmann–Gibbs picture for the equilibrium states. In particular, in attempting to describe systems which affect, and are affected by, their environment (through, e.g., entropy production) NESS represents a significant increase of complexity from EQSS. Of course, the hope is that an overarching theory for NESM, from the full dynamics to predicting NESS from a given set of rates, will emerge in the near future. Such a theory should help us reach the ultimate goal for, say, biology—which would be the ability to predict the form and behavior of a living organism, based only on its intrinsic DNA sequence and the external environment it finds itself in. For the latter, we have in mind both sources of input (e.g. light, air, food, stimulations) and output (e.g. waste disposal, work, reproduction). In the absence of such interactions with the environment, an isolated DNA will evolve to an equilibrium state—probably just an inert macromolecule. To fully understand the physics of life, we believe a firm grasp of non-equilibrium statistical mechanics is absolutely vital.

Acknowledgments

We are indebted to many colleagues for enlightening discussions on many topics. In particular, we wish to thank C Arita, J J Dong, M R Evans, C V Finkielstein, O Golinelli, G Lakatos, S Mallick, S Prolhac, B Schmittmann, U Seifert and B Shargel for their collaborations and continuing support in our endeavors. The authors also thank F W Crawford and A Levine for helpful comments on the manuscript. One of us (RKPZ) is grateful for the hospitality of H W Diehl in the Universität Duisburg–Essen and H Orland at CEA-Saclay, where some of this work was carried out. This research is supported in part by the Alexander von Humboldt Foundation, and grants from the Army Research office through grant 58386MA (TC) and the US National Science Foundation, DMR-0705152 (RKPZ), DMR-1005417 (RKPZ), DMS-1032131 (TC), ARO-58386MA (TC) and DMS-1021818 (TC).

References

[1] Young A P (ed) 1998 *Spin Glasses and Random Fields* (*Directions in Condensed Matter Physics* vol 12) (Singapore: World Scientific)
[2] de Dominicis C and Giardina I 2010 *Random Fields and Spin Glasses: A Field Theory Approach* (Cambridge: Cambridge University Press)
[3] Henkel M and Pleimling M 2010 *Nonequilibrium Phase Transitions Ageing and Dynamical Scaling far from Equilibrium* vol 2 (Heidelberg: Springer)
[4] Hill T L 1966 Studies in irreversible thermodynamics: IV. Diagrammatic representation of steady state fluxes for unimolecular systems *J. Theor. Biol.* **10** 442
[5] Committee on CMMP 2010 *Condensed-Matter and Materials Physics: The Science of the World Around Us* (Washington, DC: The National Academies Press)
[6] BESAC Subcommittee on Grand Challenges for Basic Energy Sciences 2007 *Directing Matter and Energy: Five Challenges for Science and the Imagination* (Washington, DC: US Department of Energy)
[7] Zia R K P and Schmittmann B 2007 Probability currents as principal characteristics in the statistical mechanics of non-equilibrium steady states *J. Stat. Mech.* **2007** P07012
[8] Jiang D Q, Qian M and Qian M P 2004 *Mathematical Theory of Nonequilibrium Steady States: On the Frontier of Probability and Dynamical Systems* (Berlin: Springer)
[9] Spitzer F 1970 Interaction of Markov processes *Adv. Math.* **5** 246
[10] Spohn H 1991 *Large Scale Dynamics of Interacting Particles* (Heidelberg: Springer)
[11] Liggett T M 1999 *Stochastic Interacting Systems: Contact, Voter, and Exclusion Processes* (Berlin: Springer)
[12] Schütz G 2000 *Exactly Solvable Models for Many-Body Systems far from Equilibrium* (*Phase Transitions and Critical Phenomena* vol 19) (New York: Academic)
[13] MacDonald C T, Gibbs J H and Pipkin A C 1968 Kinetics of biopolymerization on nucleic acid templates *Biopolymers* **6** 1
[14] MacDonald C T and Gibbs J H 1969 Concerning the kinetics of polypeptide synthesis on polyribosomes *Biopolymers* **7** 707
[15] Chowdhury D, Santen L and Schadschneider A 2000 Statistical physics of vehicular traffic and some related systems *Phys. Rep.* **329** 199
[16] Kardar M, Parisi G and Zhang Y C 1986 Dynamic scaling of growing interfaces *Phys. Rev. Lett.* **56** 889

[17] Wolf D E and Tang L H 1990 Inhomogeneous growth processes *Phys. Rev. Lett.* **65** 1591

[18] Wang G C and Lu T M 1985 Physical realization of two-dimensional Ising critical phenomena: oxygen chemisorbed on the W(112) surface *Phys. Rev.* B **31** 5918

[19] Lynn J W *et al* 1989 2D and 3D magnetic behavior of Er in $ErBa_2Cu_3O_7$ *Phys. Rev. Lett.* **63** 2606

[20] Wolf W P 2000 The Ising model and real magnetic materials *Braz. J. Phys.* **30** 794

[21] Wilson Kenneth G 1983 The renormalization group and critical phenomena *Rev. Mod. Phys.* **55** 583

[22] Quinn H R 2009 Time reversal violation *J. Phys.: Conf. Ser.* **171** 012001

[23] Onsager L 1931 Reciprocal relations in irreversible processes: I. *Phys. Rev.* **37** 405

[24] Green M S 1954 Markoff random processes and the statistical mechanics of time-dependent phenomena: II. Irreversible processes in fluids *J. Chem. Phys.* **22** 398

[25] Kubo R 1957 Statistical-mechanical theory of irreversible processes: I. General theory and simple applications to magnetic and conduction problems *J. Phys. Soc. Japan* **12** 570

[26] de Groot S R and Mazur P 1962 *Non-Equilibrium Thermodynamics* (Amsterdam: North Holland)

[27] Jarzynski C 1997 Nonequilibrium equality for free energy differences *Phys. Rev. Lett.* **78** 2690

[28] Crooks G E 1998 Nonequilibrium measurements of free energy differences for microscopically reversible Markovian systems *J. Stat. Phys.* **90** 1481

[29] Crooks G E 2000 Path-ensemble averages in systems driven far from equilibrium *Phys. Rev.* E **61** 2361

[30] Hatano T and Sasa S I 2001 Steady-state thermodynamics of Langevin systems *Phys. Rev. Lett.* **86** 3463

[31] Hummer G and Szabo A 2001 Free energy reconstruction from nonequilibrium single-molecule pulling experiments *Proc. Natl Acad. Sci. USA* **98** 3658

[32] Seifert U 2005 Entropy production along a stochastic trajectory and an integral fluctuation theorem *Phys. Rev. Lett.* **95** 040602

[33] Speck T and Seifert U 2006 Restoring a fluctuation-dissipation theorem in a nonequilibrium steady state *Europhys. Lett.* **74** 391

[34] Seifert U and Speck T 2010 Fluctuation-dissipation theorem in nonequilibrium steady states *Europhys. Lett.* **89** 10007

[35] Chetrite R and Gawedzki K 2008 Fluctuation relations for diffusion processes *Commun. Math. Phys.* **282** 469

[36] Katz S, Lebowitz J L and Spohn H 1984 Non-equilibrium steady states of stochastic lattice gas models of fast ionic conductors *J. Stat. Phys.* **34** 497

[37] Prigogine I 1967 *Introduction to Thermodynamics of Irreversible Processes* 3rd edn (New York: Interscience)

[38] Gyarmati I 1970 *Non-Equilibrium Thermodynamics: Field Theory and Variational Principles* (Berlin: Springer)

[39] Jaynes E T 1980 The minimum entropy production principle *Annu. Rev. Phys. Chem.* **31** 579

[40] Gallavotti G 2004 Entropy production and thermodynamics of nonequilibrium stationary states: a point of view *Chaos* **14** 680

[41] Phil A 2006 Theory for non-equilibrium statistical mechanics *Phys. Chem. Chem. Phys.* **8** 3585

[42] Martyushev L M and Seleznev V D 2006 Maximum entropy production principle in physics, chemistry and biology *Phys. Rep.* **426** 1

[43] Otten M and Stock G 2010 Maximum caliber inference of nonequilibrium processes *J. Chem. Phys.* **133** 034119

[44] Monthus C 2011 Non-equilibrium steady states: maximization of the Shannon entropy associated with the distribution of dynamical trajectories in the presence of constraints *J. Stat. Mech.* **2011** P03008

[45] Seneta E 1981 *Non-Negative Matrices and Markov Chains* 2nd edn (London: Springer)

[46] Van Kampen N G 2007 *Stochastic Processes in Physics and Chemistry* 3rd edn (Amsterdam: Elsevier)

[47] Reichl L E 2009 *A Modern Course in Statistical Physics* 3rd edn (New York: Wiley)

[48] Risken H 1989 *The Fokker–Planck Equation: Methods of Solutions and Applications* 2nd edn (Berlin: Springer)

[49] Schadschneider A, Chowdhury D and Nishinari K 2011 *Stochastic Transport in Complex Systems: From Molecules to Vehicles* (Amsterdam: Elsevier)

[50] Brown R 1828 A brief account of microscopical observations made on the particles contained in the pollen of plants *Phil. Mag.* **4** 161

[51] Einstein A 1905 Über die von der molekularkinetischen theorie der wärme geforderte bewegung von in ruhenden flüssigkeiten suspendierten teilchen *Ann. Phys., Lpz.* **322** 549

[52] von Smoluchowski M 1906 Zur kinetischen theorie der Brownschen molekularbewegung und der suspensionen *Ann. Phys., Lpz.* **326** 756

[53] Glauber R J 1963 Time dependent statistics of the Ising model *J. Math. Phys.* **4** 294

[54] Swendsen R H and Wang J S 1987 Nonuniversal critical dynamics in Monte Carlo simulations *Phys. Rev. Lett.* **58** 86

[55] Landau D P and Binder K 2009 *A Guide to Monte Carlo Simulations in Statistical Physics* 3rd edn (Cambridge: Cambridge University Press)

[56] Metropolis N, Rosenbluth A W, Rosenbluth M N, Teller A H and Teller E 1953 Equation of state calculations by fast computing machines *J. Chem. Phys.* **21** 1087

[57] Ising E 1925 Beitrag zur theorie des ferromagnetismus *Z. Phys.* **31** 253

[58] Yang C N and Lee T D 1952 Statistical theory of equations of state and phase transitions: I. Theory of condensation *Phys. Rev.* **87** 404

[59] Huang K 1987 *Statistical Mechanics* 2nd edn (New York: Wiley)

[60] Kawasaki K 1966 Diffusion constants near the critical point for time-dependent Ising models: II. *Phys. Rev.* **148** 375

[61] Kawasaki K 1970 Kinetic equations and time correlation functions of critical fluctuations *Ann. Phys.* **61** 1

[62] Kolmogorov A N 1936 Zur theorie der Markoffschen ketten *Math. Ann.* **112** 155

[63] Schnakenberg J 1976 Network theory of microscopic and macroscopic behavior of master equation systems *Rev. Mod. Phys.* **48** 571

[64] Haken H 1983 *Synergetics: An Introduction* 3rd edn (Berlin: Springer)

[65] Kirchhoff G 1847 Über die auflösung der gleichungen, auf welche man bei der untersuchung der linearen verteilung galvanischer ströme geführt wird *Ann. Phys. Chem.* **72** 497

[66] Zia R K P and Schmittmann B 2006 A possible classification of nonequilibrium steady states *J. Phys. A: Math. Gen.* **39** L407

[67] Chetrite R and Gupta S 2011 Two refreshing views of fluctuation theorems through kinematics elements and exponential martingale *J. Stat. Phys.* **143** 543

[68] Schmittmann B and Zia R K P 1995 Statistical mechanics of driven diffusive systems *Phase Transitions and Critical Phenomena* vol 17 (London: Academic)

[69] Praestgaard E L, Schmittmann B and Zia R K P 2000 A lattice gas coupled to two thermal reservoirs: Monte Carlo and field theoretic studies *Eur. Phys. J.* B **18** 675

[70] Zia R K P, Praestgaard E L and Mouritsen O G 2002 Getting more from pushing less: negative specific heat and conductivity in non-equilibrium steady states *Am. J. Phys.* **70** 384

[71] Evans D J, Cohen E G D and Morriss G P 1993 Probability of second law violations in shearing steady states *Phys. Rev. Lett.* **71** 2401

[72] Evans D J and Searles D J 1994 Equilibrium microstates which generate second law violating steady states *Phys. Rev.* E **50** 1645

[73] Gallavotti G and Cohen E G D 1995 Dynamical ensembles in non-equilibrium statistical mechanics *Phys. Rev. Lett.* **74** 2694

[74] Baiesi M, Maes C and Wynants B 2009 Fluctuations and response of nonequilibrium states *Phys. Rev. Lett.* **103** 010602

[75] Kurchan J 1998 Fluctuation theorem for stochastic dynamics *J. Phys. A: Math. Gen.* **31** 3719

[76] Lebowitz J L and Spohn H 1999 A Gallavotti–Cohen type symmetry in the large deviation functional for stochastic dynamics *J. Stat. Phys.* **95** 333

[77] Derrida B 2007 Non-equilibrium steady states: fluctuations and large deviations of the density and of the current *J. Stat. Mech.* **2007** P07023

[78] Touchette H 2009 The large deviation approach to statistical mechanics *Phys. Rep.* **478** 1

[79] Kubo R, Toda M and Hashitsume N 1998 *Statistical Physics II: Nonequilibrium Statistical Mechanics* 2nd edn (Berlin: Springer)

[80] Marconi U M B, Puglisi A, Rondoni L and Vulpiani A 2008 Fluctuation–dissipation: response theory in statistical physics *Phys. Rep.* **461** 111

[81] Gallavotti G 2008 Fluctuation theorem and chaos *Eur. Phys. J.* B **64** 315

[82] Jarzynski C 2008 Nonequilibrium work relations: foundations and applications *Eur. Phys. J.* B **64** 331

[83] Bertini L, De Sole A, Gabrielli D, Jona-Lasinio G and Landim C 2002 Macroscopic fluctuation theory for stationary non-equilibrium states *J. Stat. Phys.* **107** 635

[84] Grinstein G 1991 Generic scale invariance in classical nonequilibrium systems *J. Appl. Phys.* **69** 5441

[85] Dorfman J R, Kirkpatrick T R and Sengers J V 1994 Generic long range correlations in molecular fluids *Annu. Rev. Phys. Chem.* **45** 213

[86] Evans M R, Kafri Y, Koduvely H M and Mukamel D 1998 Phase separation and coarsening in one-dimensional driven diffusive systems: local dynamics leading to long-range Hamiltonians *Phys. Rev.* E **58** 2764

[87] Clincy M, Derrida B and Evans M R 2003 Phase transition in the ABC model *Phys. Rev.* E **67** 066115

[88] Baxter R J 2008 *Exactly Solved Models in Statistical Mechanics* 1st edn (New York: Dover)

[89] Sutherland B 2004 *Beautiful Models: 70 Years of Exactly Solved Quantum Many-Body Problem* 1st edn (Singapore: World Scientific)

[90] Krug J 1991 Boundary-induced phase transitions in driven diffusive systems *Phys. Rev. Lett.* **67** 1882

[91] Harris T E 1965 Diffusion with 'collisions' between particles *J. Appl. Prob.* **2** 323

[92] Liggett T M 1985 *Interacting Particle Systems* 1st edn (New York: Springer)

[93] Evans M R and Blythe R A 2002 Non-equilibrium dynamics in low dimensional systems *Physica* A **313** 110

[94] Karzig T and von Oppen F 2010 Signatures of critical full counting statistics in a quantum-dot chain *Phys. Rev.* B **81** 045317

[95] Evans M R 1996 Bose–Einstein condensation in disordered exclusion models and relation to traffic flow *Europhys. Lett.* **36** 13

[96] Derrida B 1998 An exactly soluble non-equilibrium system: the asymmetric simple exclusion process *Phys. Rep.* **301** 65

[97] Krapivsky P L, Redner S and Ben-Naim E 2010 *A Kinetic View of Statistical Physics* 1st edn (Cambridge: Cambridge University Press)

[98] Barma M 1992 Dynamics of field-driven interfaces in the two-dimensional Ising model *J. Phys. A: Math. Gen.* **25** L693

[99] Barma M 2006 Driven diffusive systems with disorder *Physica* A **372** 22

[100] Chatterjee S and Barma M 2006 Dynamics of fluctuation-dominated phase ordering: hard-core passive sliders on a fluctuating surface *Phys. Rev.* E **73** 011107

[101] Chatterjee S and Barma M 2008 Shock probes in a one-dimensional Katz–Lebowitz–Spohn model *Phys. Rev.* E **77** 061124

[102] Harris R J and Stinchcombe R B 2004 Disordered asymmetric simple exclusion process: mean-field treatment *Phys. Rev.* E **70** 016108

[103] Shaw L B, Sethna J P and Lee K H 2004 Mean-field approaches to the totally asymmetric exclusion process with quenched disorder and large particles *Phys. Rev.* E **70** 021901

[104] Shaw L B, Kolomeisky A B and Lee K H 2004 Local inhomogeneity in asymmetric simple exclusion processes with extended objects *J. Phys. A: Math. Gen.* **37** 2105

[105] Zia R K P, Dong J J and Schmittmann B 2011 Modeling translation in protein synthesis with TASEP: a tutorial and recent developments *J. Stat. Phys.* **144** 405

[106] Derrida B, Janowski S A, Lebowitz J L and Speer E R 1993 Exact solution of the totally asymmetric exclusion process: shock profiles *J. Stat. Phys.* **73** 813

[107] Mallick K 1996 Shocks in the asymmetric exclusion model with an impurity *J. Phys. A: Math. Gen.* **29** 5375

[108] Speer E R 1994 The two species totally asymmetric exclusion process *On Three Levels: The Micro-, Meso-, and Macroscopic Approaches in Physics* ed M Fannes, C Maes and A Verbeure (New York: Plenum)

[109] Mallick K, Mallick S and Rajewsky N 1999 Exact solution of an exclusion process with three classes of particles and vacancies *J. Phys. A: Math. Gen.* **32** 8399

[110] Ferrari P A and Martin J B 2007 Stationary distributions of multi-type totally asymmetric exclusion processes *Ann. Prob.* **35** 807

[111] Evans M R, Ferrari P A and Mallick K 2009 Matrix representation of the stationary measure for the multispecies TASEP *J. Stat. Phys.* **135** 217

[112] Mallick K 2011 Some exact results for the exclusion process *J. Stat. Mech.* **2011** P01024

[113] Gantmacher F R 1964 *Matrix Theory* 1st edn (New York: Chelsea)

[114] Jain K, Marathe R, Chaudhuri A and Dhar A 2007 Driving particle current through narrow channels using classical pump *Phys. Rev. Lett.* **99** 190601

[115] Born M and Green H S 1946 A general kinetic theory of liquids: I. The molecular distribution functions *Proc. R. Soc. Lond.* A **188** 10

[116] Kirkwood J G 1946 The statistical mechanical theory of transport processes: I. General theory *J. Chem. Phys.* **14** 180

[117] Kirkwood J G 1947 The statistical mechanical theory of transport processes: II. Transport in gases *J. Chem. Phys.* **15** 72

[118] Derrida B, Domany E and Mukamel D 1992 An exact solution of a one dimensional asymmetric exclusion model with open boundaries *J. Stat. Phys.* **69** 667

[119] Janowski S A and Lebowitz J L 1992 Finite size effects and shock fluctuations in the asymmetric exclusion process *Phys. Rev.* A **45** 618

[120] Derrida B, Evans M R, Hakim V and Pasquier V 1993 Exact solution of a 1D asymmetric exclusion model using a matrix formulation *J. Phys. A: Math. Gen.* **26** 1493

[121] Schütz G M and Domany E 1993 Phase transitions in an exactly soluble one-dimensional exclusion process *J. Stat. Phys.* **72** 277

[122] Schütz G M 2001 *Exactly Solvable Models for Many-Body Systems Far from Equilibrium* (*Phase Transitions and Critical Phenomena* vol 19) ed C Domb and J L Lebowitz (San Diego, CA: Academic)

[123] Blythe R A and Evans M R 2007 Nonequilibrium steady states of matrix-product form: a solver's guide *J. Phys. A: Math. Theor.* **40** R333

[124] Lakatos G, O'Brien J and Chou T 2006 Hydrodynamic mean-field solutions of 1D exclusion processes with spatially varying hopping rates *J. Phys. A: Math. Gen.* **39** 2253

[125] Alcaraz F C and Rittenberg V 2007 Different facets of the raise and peel model *J. Stat. Mech.* **2007** P07009

[126] Sasamoto T 1999 One-dimensional partially asymmetric exclusion process with open boundaries: orthogonal polynomial approach *J. Phys. A: Math. Gen.* **32** 7109

[127] Sasamoto T 2000 Density profile of the one-dimensional partially asymmetric simple exclusion process with open boundaries *J. Phys. Soc. Japan* **69** 1055

[128] Ferrari P A 1992 Shock fluctuations in the asymmetric simple exclusion *Prob. Theor. Relat. Fields* **91** 81

[129] Ferrari P A and Fontes L R G 1994 Current fluctuations for the asymmetric exclusion process *Ann. Prob.* **22** 820–32

[130] Ferrari P A, Fontes L R G and Kohayakawa Y 1994 Invariant measures for a two-species asymmetric process *J. Stat. Phys.* **76** 1153

[131] Derrida B 2011 Microscopic versus macroscopic approaches to non-equilibrium systems *J. Stat. Mech.* **2011** P01030

[132] Dhar D 1987 An exactly solved model for interfacial growth *Phase Transit.* **9** 51

[133] Kandel D, Domany E and Nienhuis B 1990 A six-vertex model as a diffusion problem: derivation of correlation functions *J. Phys. A: Math. Gen.* **23** L755

[134] Rajesh R and Dhar D 1998 An exactly solvable anisotropic directed percolation model in three dimensions *Phys. Rev. Lett.* **81** 1646

[135] Gwa L H and Spohn H 1992 Bethe solution for the dynamical-scaling exponent of the noisy Burgers equation *Phys. Rev.* A **46** 844

[136] Kim D 1995 Bethe ansatz solution for crossover scaling functions of the asymmetric xxz chain and the Kardar–Parisi–Zhang-type growth model *Phys. Rev.* E **52** 3512

[137] Kim D 1997 Asymmetric xxz chain at the antiferromagnetic transition: spectra and partition functions *J. Phys. A: Math. Gen.* **30** 3817

[138] Golinelli O and Mallick K 2005 Spectral gap of the totally asymmetric exclusion process at arbitrary filling *J. Phys. A: Math. Gen.* **38** 1419

[139] Golinelli O and Mallick K 2006 The asymmetric simple exclusion process: an integrable model for non-equilibrium statistical mechanics *J. Phys. A: Math. Gen.* **39** 12679

[140] Derrida B and Lebowitz J L 1998 Exact large deviation function in the asymmetric exclusion process *Phys. Rev. Lett.* **80** 209

[141] Derrida B and Evans M R 1999 Bethe ansatz solution for a defect particle in the asymmetric exclusion process *J. Phys. A: Math. Gen.* **32** 4833

[142] Bethe H 1931 Zur theory der metalle: I. Eigenwerte und eigenfunctionen atomkette *Z. Phys.* **71** 205

[143] Gaudin M 1983 *La fonction d'onde de Bethe* 1st edn (Paris: Masson)

[144] Langlands R P and Saint-Aubin Y 1995 *Algebro-Geometric Aspects of the Bethe Equations: 'Strings and Symmetries'* (*Lecture Notes in Physics* vol 447) (Berlin: Springer)

[145] Golinelli O and Mallick K 2005 Spectral degeneracies in the totally asymmetric exclusion process *J. Stat. Phys.* **120** 779

[146] Bogoliubov N M 2009 Determinantal representation of correlation functions in the totally asymmetric exclusion model *SIGMA* **5** 052 (arXiv:0904.3680)

[147] Schütz G M 1997 Exact solution of the master equation of the asymmetric exclusion process *J. Stat. Phys.* **88** 427

[148] Priezzhev V B 2003 Exact nonstationary probabilities in the asymmetric exclusion process on a ring *Phys. Rev. Lett.* **91** 050601

[149] Priezzhev V B 2005 Non-stationary probabilities for the asymmetric exclusion process on a ring *Pramana J. Phys.* **64** 915

[150] van Beijeren H, Kutner R and Spohn H 1985 Excess noise for driven diffusive systems *Phys. Rev. Lett.* **54** 2026

[151] Halpin-Healy T and Zhang Y C 1995 Kinetic roughening phenomena, stochastic growth, directed polymers and all that *Phys. Rep.* **254** 215

[152] Majumdar S N and Barma M 1991 Tag diffusion in driven systems, growing interfaces and anomalous fluctuations *Phys. Rev.* B **44** 5306

[153] de Gier J and Essler F H L 2006 Exact spectral gaps of the asymmetric exclusion process with open boundaries *J. Stat. Mech.* **2006** P12011

[154] de Masi A and Ferrari P A 1984 Self-diffusion in one-dimensional lattice gases in the presence of an external field *J. Stat. Phys.* **38** 603–13

[155] Proeme A and Blythe R A and Evans M R 2011 Dynamical transition in the open-boundary totally asymmetric exclusion process *J. Phys. A: Math. Theor.* **44** 035003

[156] Gorissen M and Vanderzande C 2011 Finite size scaling of current fluctuations in the totally asymmetric exclusion process *J. Phys. A: Math. Theor.* **44** 115005

[157] Mitsudo T and Takesue S 2011 The numerical estimation of the current large deviation function in the asymmetric exclusion process with open boundary conditions arXiv:1012.1387

[158] Flindt C, Novotný T and Jauho A-P 2004 Current noise in a vibrating quantum dot array *Phys. Rev.* B **70** 205334

[159] Jiang D Q, Qian M and Qian M P 2004 *Mathematical Theory of Nonequilibrium Steady-States* (*Lecture Notes in Mathematics*) (Berlin: Springer)

[160] Shargel B H 2009 The measure-theoretic identity underlying transient fluctuation theorems *J. Phys. A: Math. Theor.* **42** 135002

[161] Prolhac S and Mallick K 2008 Current fluctuations in the exclusion process and Bethe ansatz *J. Phys. A: Math. Theor.* **41** 175002

[162] Prolhac S 2008 Fluctuations and skewness of the current in the partially asymmetric exclusion process *J. Phys. A: Math. Theor.* **41** 365003

[163] Derrida B and Mallick K 1997 Exact diffusion constant for the one-dimensional partially asymmetric exclusion process *J. Phys. A: Math. Gen.* **30** 1031

[164] Prolhac S 2010 Tree structures for the current fluctuations in the exclusion process *J. Phys. A: Math. Theor.* **43** 105002

[165] Prolhac S and Mallick K 2009 Cumulants of the current in a weakly asymmetric exclusion process *J. Phys. A: Math. Theor.* **42** 175001

[166] Appert-Rolland C, Derrida B, Lecomte V and Van Wijland F 2008 Universal cumulants of the current in diffusive systems on a ring *Phys. Rev.* E **78** 021122

[167] Bodineau T and Derrida B 2004 Current fluctuations in nonequilibrium diffusive systems: an additivity principle *Phys. Rev. Lett.* **92** 180601

[168] Bodineau T and Derrida B 2005 Distribution of currents in non-equilibrium diffusive systems and phase transitions *Phys. Rev.* E **72** 066110

[169] Bodineau T and Derrida B 2007 Cumulants and large deviations of the current through non-equilibrium steady states *C. R. Phys.* **8** 540

[170] de Gier J and Essler F H L 2005 Bethe ansatz solution of the asymmetric exclusion process with open boundaries *Phys. Rev. Lett.* **95** 240601

[171] de Gier J and Essler F H L 2008 Slowest relaxation mode of the partially asymmetric exclusion process with open boundaries *J. Phys. A: Math. Theor.* **41** 485002

[172] Alcaraz F C and Lazo M J 2004 The Bethe ansatz as a matrix product ansatz *J. Phys. A: Math. Gen.* **37** L1

[173] Cantini L 2008 Algebraic Bethe ansatz for the two-species ASEP with different hopping rates *J. Phys. A: Math. Theor.* **41** 095001

[174] Arita C, Kuniba A, Sakai K and Sawabe T 2009 Spectrum of a multi-species asymmetric simple exclusion process on a ring *J. Phys. A: Math. Theor.* **42** 345002

[175] Povolotsky A M 2004 Bethe ansatz solution of zero-range process with non-uniform stationary state *Phys. Rev.* E **69** 061109

[176] Dorlas T, Povolotsky A and Priezzhev V 2009 From vicious walkers to TASEP *J. Stat. Phys.* **135** 483

[177] Majumdar S N, Mallick K and Nechaev S 2008 Bethe ansatz in the Bernoulli matching model of random sequence alignment *Phys. Rev.* E **77** 011110

[178] Priezzhev V B and Schütz G M 2008 Exact solution of the Bernoulli matching model of sequence alignment *J. Stat. Mech.* **2008** P09007

[179] Tracy C A and Widom H 2008 Integral formulas for the asymmetric simple exclusion process *Commun. Math. Phys.* **279** 815

[180] Rakos A and Schütz G M 2005 Current distribution and random matrix ensembles for an integrable asymmetric fragmentation process *J. Stat. Phys.* **118** 511

[181] Tracy C A and Widom H 1994 Level-spacing distributions and Airy kernel *Commun. Math. Phys.* **159** 151

[182] Kriecherbauer T and Krug J 2010 A pedestrian's view on interacting particle systems, KPZ universality and random matrices *J. Phys. A: Math. Theor.* **43** 403001

[183] Johansson K 2000 Shape fluctuation and random matrices *Commun. Math. Phys.* **209** 437

[184] Spohn H 2005 Kardas–Parisi–Zhang equation in one dimension and line ensembles *Pramana J. Phys.* **64** 847

[185] Spohn H 2006 Exact solutions for KPZ-type growth processes, random matrices, and equilibrium shapes of crystals *Physica* A **369** 71

[186] Ferrari P L 2011 From interacting particle systems to random matrices *J. Stat. Mech.* **2011** P10016

[187] Baik J, Deift P and Johansson K 1999 On the distribution of the length of the longest increasing subsequence of random permutations *J. Am. Math. Soc.* **12** 1119

[188] Tracy C A and Widom H 2008 A Fredholm determinant representation in ASEP *J. Stat. Phys.* **132** 291

[189] Tracy C A and Widom H 2009 Asymptotics in ASEP with step initial condition *Commun. Math. Phys.* **290** 129

[190] Tracy C A and Widom H 2009 Total current fluctuation in ASEP *J. Math. Phys.* **50** 095204

[191] Tracy C A and Widom H 2010 Formulas for joint probabilities for the asymmetric simple exclusion process *J. Math. Phys.* **51** 063302

[192] Sasamoto T and Spohn H 2010 The 1 + 1 dimensional Kardar–Parisi–Zhang equation and its universality class *J. Stat. Mech.* **2010** P11013

[193] Sasamato T and Spohn H 2010 One-dimensional KPZ equation: an exact solution and its universality *Phys. Rev. Lett.* **104** 230602

[194] Amir G, Corwin I and Quastel J 2011 Probability distribution of the free energy of the continuum directed random polymer in 1 + 1 dimensions *Commun. Pure Appl. Math.* **64** 466–537

[195] Calabrese P, LeDoussal P and Rosso A 2010 Free-energy distribution of the directed polymer at high temperature *Europhys. Lett.* **90** 20002

[196] Dotsenko V 2010 Bethe ansatz derivation of the Tracy–Widom distribution for one-dimensional directed polymers *Europhys. Lett.* **90** 20003

[197] Prolhac S and Spohn H 2011 The height distribution of the KPZ equation with sharp wedge initial condition: numerical evaluations *Phys. Rev.* E **84** 011119

[198] Calabrese P and LeDoussal P 2011 An exact solution for the KPZ equation with flat initial conditions *Phys. Rev. Lett.* **106** 250603

[199] Imamura T and Sasamoto T 2011 Exact analysis of the KPZ equation with half Brownian motion initial condition arXiv:1105.4659

[200] Prolhac S and Spohn H 2011 Two-point generating function of the free energy for a directed polymer in a random medium *J. Stat. Mech.* **2011** P01031

[201] Prolhac S and Spohn H 2011 The one-dimensional KPZ equation and the Airy process *J. Stat. Mech.* **2011** P03020

[202] Aldous D and Diaconis P 1999 Longest increasing subsequences: from patience sorting to the Baik–Deft–Johansson theorem *Bull. Am. Math. Soc.* **36** 413–32

[203] Corwin I 2011 The Kardar–Parisi–Zhang equation and universality class arXiv:1106.1596

[204] Stinchcombe R B and de Queiroz S L A 2011 Smoothly-varying hopping rates in driven flow with exclusion *Phys. Rev.* E **83** 061113

[205] Shaw L B, Zia R K P and Lee K H 2003 Modeling, simulations, and analyses of protein synthesis: driven lattice gas with extended objects *Phys. Rev.* E **68** 021910

[206] Schönherr G and Schütz G M 2004 Exclusion process for particles of arbitrary extension: hydrodynamic limit and algebraic properties *J. Phys. A: Math. Gen.* **37** 8215

[207] Schönherr G 2005 Hard rod gas with long-range interactions: exact predictions for hydrodynamic properties of continuum systems from discrete models *Phys. Rev.* E **71** 026122

[208] de Dominicis C, Brézin E and Zinn-Justin J 1975 Field-theoretic techniques and critical dynamics: I. Ginzburg–Landau stochastic models without energy conservation *Phys. Rev.* B **12** 4945

[209] Halperin B I, Hohenberg P C and Ma S-k 1974 Renormalization-group methods for critical dynamics: I. Recursion relations and effects of energy conservation *Phys. Rev.* B **10** 139

[210] Halperin B I, Hohenberg P C and Ma S-k 1976 Renormalization-group methods for critical dynamics: II. Detailed analysis of the relaxational models *Phys. Rev.* B **13** 4119

[211] Bausch R, Janssen H K and Wagner H 1976 Renormalized field theory of critical dynamics *Z. Phys.* B **24** 113

[212] Janssen H K and Schmittmann B 1986 Field theory of long-time behaviour in driven diffusive systems *Z. Phys.* B **63** 517

[213] Janssen H K and Schmittmann B 1986 Field theory of critical behaviour in driven diffusive systems *Z. Phys.* B **64** 503

[214] Leung K T and Cardy J L 1986 Field theory of critical behaviour in a driven diffusive system *J. Stat. Phys.* **44** 567

[215] Janssen H K and Oerding K 1996 Renormalized field theory and particle density profile in driven diffusive systems with open boundaries *Phys. Rev.* E **53** 4544

[216] Oerding K and Janssen H K 1998 Surface critical behavior of driven diffusive systems with open boundaries *Phys. Rev.* E **58** 1446

[217] Becker V and Janssen H K 1999 Field theory of critical behavior in driven diffusive systems with quenched disorder *J. Stat. Phys.* **96** 817

[218] Parmeggiani A, Franosch T and Frey E 2003 Phase coexistence in driven one-dimensional transport *Phys. Rev. Lett.* **90** 086601

[219] Parmeggiani A, Franosch T and Frey E 2004 Totally asymmetric simple exclusion process with Langmuir kinetics *Phys. Rev.* E **70** 046101

[220] Pierobon P, Frey E and Franosch T 2006 Driven lattice gas of dimers coupled to a bulk reservoir *Phys. Rev.* E **74** 031920

[221] Frey E, Parmeggiani A and Franosch T 2004 Collective phenomena in intracellular processes *Genome Inform.* **15** 46

[222] Wood A J 2009 A totally asymmetric exclusion process with stochastically mediated entrance and exit *J. Phys. A: Math. Theor.* **42** 445002

[223] Muhuri S and Pagonabarraga I 2008 Collective vesicle transport on biofilaments carried by competing molecular motors *Europhys. Lett.* **84** 58009

[224] Pronina E and Kolomeisky A B 2006 Asymmetric coupling in two-channel simple exclusion processes *Physica* A **372** 12

[225] Reichenbach T, Franosch T and Frey E 2006 Exclusion processes with internal states *Phys. Rev. Lett.* **97** 050603

[226] Garai A, Chowdhury D, Chowdhury D and Ramakrishnan T V 2009 Stochastic kinetics of ribosomes: single motor properties and collective behavior *Phys. Rev.* E **80** 011908

[227] Papoulis A 1984 *Probability, Random Variables, and Stochastic Processes* (New York: McGraw-Hill)

[228] Evans M R and Sugden K E P 2007 An exclusion process for modelling fungal hyphal growth *Physica* A **384** 53

[229] Sugden K E P, Evans M R, Poon W C K and Read N D 2007 Model of hyphal tip growth involving microtubule-based transport *Phys. Rev.* E **75** 031909

[230] Sugden K E P and Evans M R 2007 A dynamically extending exclusion process *J. Stat. Mech.* **2007** P11013

[231] Hough L E, Schwabe A, Glaser M A, McIntosh J R and Betterton M D 2009 Microtubule depolymerization by the kinesin-8 motor Kip3p: a mathematical model *Biophys. J.* **96** 3050

[232] Nowak S A, Fok P W and Chou T 2007 Dynamic boundaries in asymmetric exclusion processes *Phys. Rev.* E **76** 031135

[233] Fok P W and Chou T 2009 Interface growth driven by surface kinetics and convection *SIAM J. Appl. Math.* **70** 24

[234] Levitt D G 1973 Dynamics of a single-file pore: non-Fickian behavior *Phys. Rev.* A **8** 3050–4

[235] Alexander S and Pincus P 1978 Diffusion of labeled particles on one-dimensional chains *Phys. Rev.* B **18** 2011

[236] Karger J 1992 Straightforward derivation of the long-time limit of the mean-square displacement in one-dimensional diffusion *Phys. Rev.* A **45** 4173

[237] Barkai E and Silbey R 2010 Diffusion of tagged particle in an exclusion process *Phys. Rev.* E **81** 041129

[238] Sholl D S and Fichthorn K A 1997 Concerted diffusion of molecular clusters in a molecular sieve *Phys. Rev. Lett.* **79** 3569

[239] Sholl D S and Lee C K 2000 Influences of concerted cluster diffusion on single-file diffusion of Cf_4 in $ALPO_4$-5 and Xe in $ALPO_4$-31. *J. Chem. Phys.* **112** 817

[240] Khantha M, Cordero N A, Alonso J A, Cawkwell M and Girifalco L A 2008 Interaction and concerted diffusion of lithium in a (5, 5) carbon nanotube *Phys. Rev.* B **78** 115430

[241] Gabel A, Krapivsky P L and Redner S 2010 Facilitated asymmetric exclusion *Phys. Rev. Lett.* **105** 210603

[242] Chou T 1998 How fast do fluids squeeze through microscopic single-file pores? *Phys. Rev. Lett.* **80** 85

[243] Kolomeisky A B 2007 Channel-facilitated molecular transport across membranes: attraction, repulsion and asymmetry *Phys. Rev. Lett.* **98** 048105

[244] Derrida B, Douçot B and Roche P E 2004 Current fluctuations in the one dimensional symmetric exclusion process with open boundaries *J. Stat. Phys.* **115** 717

[245] Santos J E and Schütz G M 2001 Exact time-dependent correlation functions for the symmetric exclusion process with open boundary *Phys. Rev.* E **64** 036107

[246] Jovanovic-Talisman T *et al* 2009 Artificial nanopores that mimic the selectivity of the nuclear pore complex *Nature* **457** 1023

[247] Zilman A, Di Talia S, Chait B I, Rout M P and Magnasco M O 2007 Efficiency, selectivity, and robustness of nucleocytoplasmic transport *PLoS Comput. Biol.* **3** e125

[248] Chou T 1999 Kinetics and thermodynamics across single-file pores: solute permeability and rectified osmosis *J. Chem. Phys.* **110** 606

[249] Doyle D A *et al* 1998 The structure of the potassium channel: molecular basis of K^+ conduction and selectivity *Science* **280** 69

[250] Zilman A 2009 Effects of multiple occupancy and interparticle interactions on selective transport through narrow channels: theory versus experiment *Biophys. J.* **96** 1235

[251] Gwan J F and Baumgaertner A 2007 Cooperative transport in a potassium ion channel *J. Chem. Phys.* **127** 045103

[252] Hodgkin L and Keynes R D 1955 The potassium permeability of a giant nerve fibre *J. Physiol.* **128** 61

[253] Bernéche S and Roux B 2001 Energetics of ion conduction through the K^+ channel *Nature* **414** 73

[254] Khalili-Araghi F, Tajkhorshid E and Schulten K 2006 Dynamics of K^+ ion conduction through Kv1.2. *Biophys. J.* **91** L72

[255] Yesylevskyy S O and Kharkyanen V N 2005 Barrier-less knock-on conduction in ion channels: peculiarity or general mechanism? *Chem. Phys.* **312** 127

[256] Zilman A, Talia S Di, Jovanovic-Talisman T, Chait B T, Roux M P and Magnasco M O 2010 Enhancement of transport selectivity through nano-channels by non-specific competition *PLoS Comput Biol.* **6** e1000804

[257] Chou T and Lohse D 1999 Entropy-driven pumping in zeolites and biological channels *Phys. Rev. Lett.* **82** 3552

[258] Ilan B, Tajkhorshid E, Schulten K and Voth G A 2004 The mechanism of proton exclusion in aquaporin channels *Proteins* **55** 223

[259] de Grotthuss C J T 1806 Sur la décomposition de l'eau et des corps qu'elle tient en dissolution l'aide de l'lectricité galvanique *Ann. Chim.* **58** 54

[260] Noam A 1995 The Grotthuss mechanism *Chem. Phys. Lett.* **244** 456

[261] Pomes R and Roux B 1996 Structure and dynamics of a proton wire: a theoretical study of H+ translocation along the single-file water chain in the gramicidin A channel *Biophys. J.* **71** 19

[262] Voth G A 2006 Computer simulation of proton solvation and transport in aqueous and biomolecular systems *Acc. Chem. Res.* **39** 143

[263] Cui Q and Karplus M 2003 Is 'proton wire' concerted or step-wise? A model study of proton transfers in carbonic anhydrase *J. Phys. Chem.* **107** 1071

[264] Scott R I, Mokrab Y, Carvacho I, Sands Z A, Samson M P and Clapham D E 2010 An aqueous H^+ permeation pathway in the voltage-gated proton channel Hv1 *Nature Struct. Mol. Biol.* **17** 869

[265] de Grioot B L, Frigato T, Helms V and Grubmuller H 2003 The mechanism of proton exclusion in the aquaporin-1 water channel *J. Mol. Biol.* **333** 279

[266] Jensen M Ø, Röthlisberger U and Rovira C 2005 Hydroxide and proton migration in aquaporins *Biophys. J.* **89** 1744

[267] Dellago C, Naor M M and Hummer G 2003 Proton transport through water-filled carbon nanotubes *Phys. Rev. Lett.* **90** 105902

[268] Chou T 2002 An interacting spin–flip model for one-dimensional proton conduction *J. Phys. A: Math. Gen.* **35** 4515

[269] Chou T 2004 Water alignment, dipolar interactions, and multiple proton occupancy during water-wire proton transport *Biophys. J.* **86** 2827

[270] Schumaker M F 2003 Numerical framework models of single proton conduction through gramicidin *Front. Biosci.* **8** s982

[271] Omer M and Noam A 2007 Structure and energetics of the hydronium hydration shells *J. Phys. Chem.* A **111** 2253

[272] Chowdhury D, Schadschneider A and Nishinari K 2005 Physics of transport and traffic phenomena in biology: from molecular motors and cells to organisms *Phys. Life Rev.* **2** 318

[273] Chowdhury D *et al* 2008 Intra-cellular traffic: bio-molecular motors on filamentary tracks *Eur. Phys. J.* B **64** 593

[274] Lau A W C, Lacoste D and Mallick K 2007 Nonequilibrium fluctuations and mechanochemical couplings of a molecular motor *Phys. Rev. Lett.* **99** 158102

[275] Lacoste D, Lau A W and Mallick K 2008 Fluctuation theorem and large deviation function for a solvable model of a molecular motor *Phys. Rev.* E **78** 011915

[276] Lacoste D and Mallick K 2009 Fluctuation theorem for the flashing ratchet model of molecular motors *Phys. Rev.* E **80** 021923

[277] Wang H and Oster G 2002 Ratchets, power strokes, and molecular motors *Appl. Phys.* A **75** 315

[278] Astumian R D 2010 Thermodynamics and kinetics of molecular motors *Biophys. J.* **98** 2401

[279] Aghababaeie Y, Menon G I and Plischke M 1999 Universal properties of interacting Brownian Motors *Phys. Rev.* E **59** 2578

[280] Cooper G M and Hausman R E 2007 *The Cell: A Molecular Approach* (Sunderland, MA: Sinauer Associates)

[281] Jülicher F and Prost J 1995 Cooperative molecular motors *Phys. Rev. Lett.* **75** 2618

[282] Jülicher F, Ajdari A and Prost J 1997 Modeling molecular motors *Rev. Mod. Phys.* **69** 1269

[283] Vilfan A, Frey E and Schwabl F 1998 Elastically coupled molecular motors *Euro. Phys. J.* B **3** 535

[284] Badoual M, Jülicher F and Prost J 2002 Bidirectional cooperative motion of molecular motors *Proc. Natl Acad. Sci. USA* **99** 6696–701

[285] Stukalin E B, Phillips H III and Kolomeisky A B 2005 Coupling of two motor proteins: a new motor can move faster *Phys. Rev. Lett.* **94** 238101

[286] Kolomeisky A B and Fisher M E 2007 Molecular motors: a theorist's perspective *Annu. Rev. Phys. Chem.* **58** 675–95

[287] Brugués J and Casademunt J 2009 Self-organization and cooperativity of weakly coupled molecular motors under unequal loading *Phys. Rev. Lett.* **102** 118104

[288] Evans M R, Juhász R and Santen L 2003 Shock formation in an exclusion process with creation and annihilation *Phys. Rev.* E **68** 026117

[289] Juhász R and Santen L 2004 Dynamics of an exclusion process with creation and annihilation *J. Phys. A: Math. Gen.* **37** 3933

[290] Mirin N and Kolomeisky A B 2003 The effect of detachments in asymmetric simple exclusion processes *J. Stat. Phys.* **110** 811

[291] Greulich P and Schadschneider A 2009 Disordered driven lattice gases with boundary reservoirs and Langmuir kinetics *Phys. Rev.* E **79** 031107

[292] Adamson A W and Gast A P 1997 *Physical Chemistry of Surface* (New York: Wiley)

[293] Pierobon P, Mobilia M, Kouyos R and Frey E 2006 Bottleneck-induced transitions in a minimal model for intracellular transport *Phys. Rev.* E **74** 031906

[294] Klumpp S and Lipowsky R 2003 Traffic of molecular motors through tube-like compartments *J. Stat. Phys.* **113** 233

[295] Alberts B *et al* 1994 *Molecular Biology of the Cell* (New York: Garland Science)

[296] Lipowsky R, Chai Y, Klumpp S, Liepelt S and Müller M J I 2006 Molecular motor traffic: from biological nanomachines to macroscopic transport *Physica* A **372** 34

[297] Kolomeisky A B 1997 Exact solutions for a partially asymmetric exclusion model with two species *Physica* A **245** 523

[298] Pronina E and Kolomeisky A B 2007 Spontaneous symmetry breaking in two-channel asymmetric exclusion processes with narrow entrances *J. Phys. A: Math. Theor.* **40** 2275

[299] Tsekouras K and Kolomeisky A B 2008 Inhomogeneous coupling in two-channel asymmetric exclusion processes *J. Phys. A: Math. Theor.* **41** 465001

[300] Du H F, Yuan Y M, Hu M B, Wang R, Jiang R and Wu Q S 2010 Totally asymmetric exclusion processes on two intersected lattices with open and periodic boundaries *J. Stat. Mech.* **2010** P03014

[301] Kim K H and den Nijs M 2007 Dynamic screening in a two-species asymmetric exclusion process *Phys. Rev.* E **76** 021107

[302] Jakob N and Poul N 2005 Elongation factors on the ribosome *Curr. Opin. Struct. Biol.* **15** 349

[303] Alcaraz F C and Bariev R Z 1999 Exact solution of the asymmetric exclusion model with particles of arbitrary size *Phys. Rev.* E **60** 79

[304] Gupta S, Barma M, Basu U and Mohant P K 2011 Driven k-mers: correlations in space and time arXiv:1106.3910

[305] Zia R K P, Dong J J and Schmittmann B 2011 unpublished

[306] Lakatos G and Chou T 2003 Totally asymmetric exclusion processes with particles of arbitrary size *J. Phys. A: Math. Gen.* **36** 2027

[307] Kolomeisky A B 1998 Asymmetric simple exclusion model with local inhomogeneity *J. Phys. A: Math. Gen.* **31** 1153

[308] Chou T and Lakatos G 2004 Clustered bottlenecks in mRNA translation and protein synthesis *Phys. Rev. Lett.* **93** 198101

[309] Dong J J, Schmittmann B and Zia R K P 2007 Inhomogeneous exclusion processes with extended objects: the effects of defect locations *Phys. Rev.* E **76** 051113

[310] Dong J J, Schmittmann B and Zia R K P 2007 Towards a model for protein production rates *J. Stat. Phys.* **128** 21

[311] Chen C *et al* 2011 Single-molecule fluorescence measurements of ribosomal translocation dynamics *Mol. Cell* **42** 367

[312] Basu A and Chowdhury D 2007 Traffic of interacting ribosomes: effects of single-machine mechanochemistry on protein synthesis *Phys. Rev.* E **75** 021902

[313] Garai A, Chowdhury D and Ramakrishnan T V 2009 Fluctuations in protein synthesis from a single RNA template: stochastic kinetics of ribosomes *Phys. Rev.* E **79** 011916

[314] Pierobon P 2009 *Traffic of Molecular Motors: From Theory to Experiments* (Berlin: Springer)

[315] Ciandrini L, Stansfield I and Romano M C 2010 Role of the particle's stepping cycle in an asymmetric exclusion

process: a model of mRNA translation *Phys. Rev.* E **81** 051904
[316] Sachs A B 1990 The role of poly(A) in the translation and stability of mRNA *Curr. Opin. Cell. Biol.* **2** 1092
[317] Wells S E, Hillner P E, Vale R D and Sachs A B 1998 Circularization of mRNA by eukaryotic translation initiation factors *Mol. Cell* **2** 135
[318] Kahvejian A, Svitkin Y V, Sukarieh R, M'Boutchou M N and Sonenberg N 2005 Mammalian poly(A)-binding protein is a eukaryotic translation initiation factor, which acts via multiple mechanisms *Genes Dev.* **19** 104
[319] Chou T 2003 Ribosome recycling, diffusion, and mRNA loop formation in translational regulation *Biophys. J.* **85** 755
[320] Willett M, Pollard H J, Vlasak M and Morley S J 2010 Localization of ribosomes and translation initiation factors to talin/β3-integrin-enriched adhesion complexes in spreading and migrating mammalian cells *Biol. Cell.* **102** 265
[321] Lerner R S and Nicchitta C V 2006 mRNA translation is compartmentalized to the endoplasmic reticulum following physiological inhibition of cap-dependent translation *RNA* **12** 775
[322] Cook L J, Zia R K P and Schmittmann B 2009 Competition between many totally asymmetric simple exclusion processes for a finite pool of resources *Phys. Rev.* E **80** 031142
[323] Cook L J and Zia R K P 2009 Feedback and fluctuations in a totally asymmetric simple exclusion process with finite resources *J. Stat. Mech.* **2009** P02012
[324] Carslaw H S and Jaeger J C 2004 *Conduction of Heat in Solids* (Oxford: Oxford University Press)
[325] Betterton M D and Jülicher F 2005 Opening of nucleic-acid double strands by helicases: active versus passive opening *Phys. Rev.* E **71** 011904
[326] Betterton M D and Jülicher F 2005 Velocity and processivity of helicase unwinding of double-stranded nucleic acids *J. Phys.: Condens. Matter* **17** S3851
[327] Garai A, Chowdhury D and Betterton M D 2008 Two-state model for helicase translocation and unwinding of nucleic acids *Phys. Rev.* E **77** 061910
[328] Manosas M, Xi X G, Bensimon D and Croquette V 2010 Active and passive mechanisms of helicases *Nucl. Acids Res.* **38** 5518
[329] Kim M, Santen L and Noh J D 2011 Asymmetric simple exclusion process in one-dimensional chains with long-range links *J. Stat. Mech.* **2011** P04003
[330] Adams D A, Zia R K P and Schmittmann B 2007 Power spectra of the total occupancy in the totally asymmetric simple exclusion process *Phys. Rev. Lett.* **99** 020601
[331] Cook L J and Zia R K P 2010 Power spectra of a constrained totally asymmetric simple exclusion process *J. Stat. Mech.* **2010** P07014
[332] Evans M R and Hanney T 2005 Nonequilibrium statistical mechanics of the zero-range process and related models *J. Phys. A: Math. Gen.* **38** R195
[333] Rácz Z and Zia R K P 1994 Two-temperature kinetic Ising model in one dimension: steady-state correlations in terms of energy and energy flux *Phys. Rev.* E **49** 139
[334] Schmittmann B and Schmüser F 2002 Stationary correlations for a far-from-equilibrium spin chain *Phys. Rev.* E **66** 046130
[335] Mobilia M, Schmittmann B and Zia R K P 2005 Exact dynamics of a reaction-diffusion model with spatially alternating rates *Phys. Rev.* E **71** 056129
[336] Aliev M A 2009 Generating function of spin correlation functions for kinetic Glauber–Ising model with time-dependent transition rates *J. Math. Phys.* **50** 083302
[337] Lavrentovich M O and Zia R K P 2010 Energy flux near the junction of two Ising chains at different temperatures *Europhys. Lett.* **91** 50003
[338] Farago J and Pitard E 2007 Injected power fluctuations in 1D dissipative systems *J. Stat. Phys.* **128** 1365
[339] Farago J and Pitard E 2008 Injected power fluctuations in one-dimensional dissipative systems: role of ballistic transport *Phys. Rev.* E **78** 051114
[340] Wei Q H, Bechinger C and Leiderer P 2000 Single-file diffusion of colloids in one-dimensional channels *Science* **287** 625
[341] Champagne N, Vasseur R, Montourcy A and Bartolo D 2010 Traffic jams and intermittent flows in microfluidic networks *Phys. Rev. Lett.* **105** 044502
[342] Rost H 1981 Non-equilibrium behaviour of a many particle process: density profile and local equilibria *Prob. Theory Relat. Fields* **58** 41
[343] Sopasakis A and Katsoulakis M A 2006 Stochastic modeling and simulation of traffic flow: asymmetric single exclusion process with Arrhenius look-ahead dynamics *SIAM J. Appl. Math.* **66** 921
[344] Schreckenberg M, Schadschneider A, Nagel K and Ito N 1995 Discrete stochastic models for traffic flow *Phys. Rev.* E **51** 2939–49
[345] Karimipour V 1999 Multispecies asymmetric simple exclusion process and its relation to traffic flow *Phys. Rev.* E **59** 205
[346] Srinivasan R 1993 Queues in series via interacting particle systems *Math. Oper. Res.* **18** 39